THESIS APPROVAL

GRADUATE SCHOOL, KASETSART UNIVERSITY

Doctor of Philosophy (Genetic Engineering)

DEGREE

Genetic Engineering | Interdisciplinary Graduate Program

FIELD | **PROGRAM**

TITLE: Recombinant HIV-1 Reverse Transcriptase and Its Mutants Study; Cloning, Expression, Purification and Preliminary Crystallization for X-Ray Crystallography

NAME: Mr. Kun Silprasit

THIS THESIS HAS BEEN ACCEPTED BY

THESIS ADVISOR

(Assistant Professor Kiattawee Choowongkomon, Ph.D.)

THESIS CO-ADVISOR

(Associate Professor Supa Hannongbua, Dr.rer.nat.)

THESIS CO-ADVISOR

(Mrs. Buabarn Kuaprasert, Ph.D.)

GRADUATE COMMITTEE CHAIRMAN

(Associate Professor Siriwan Silapacharanan, Ph.D.)

APPROVED BY THE GRADUATE SCHOOL ON _____

DEAN

(Associate Professor Gunjana Theeragool, D.Agr.)

THESIS

RECOMBINANT HIV-1 REVERSE TRANSCRIPTASE AND ITS MUTANTS STUDY; CLONING, EXPRESSION, PURIFICATION AND PRELIMINARY CRYSTALLIZATION FOR X-RAY CRYSTALLOGRAPHY

KUN SILPRASIT

A Thesis Submitted in Partial Fulfillment of
the Requirements for the Degree of
Doctor of Philosophy (Genetic Engineering)
Graduate School, Kasetsart University
2010

Kun Silprasit 2010: Recombinant HIV-1 Reverse Transcriptase and Its Mutants Study; Cloning, Expression, Purification and Preliminary Crystallization for X-Ray Crystallography. Doctor of Philosophy (Genetic Engineering), Major Field: Genetic Engineering, Interdisciplinary Graduate Program. Thesis Advisor: Assistant Professor Kiattawee Choowongkomon, Ph.D. 138 pages.

The serious epidemic disease, HIV can resistance to these drug substances in some patients and transmission of drug resistant HIV has been described for many years. We propose to test novel NNRTIs form computational drugs design, dipyridodiazepinone derivatives. Therefore, we cloned, expressed and purified recombinant HIV-1 RT. The protocol was developed to get highly recovery of heterodimeric enzyme. We developed simple and fast method for determine RT activity, PicoGreen-fluorometric assay. PicoGreen dye interact with HIV-RT reaction products like, RNA/DNA heteroduplex, the highly sensitive dye can detect even a small amount of the reaction product. We report the efficiency of the fluorometric method using PicoGreen dye to measure enzyme activity and anti-HIV. A small amount of PicoGreen dye is enough to test a minimal quantity of substrate to rapidly determine the enzyme kinetic properties Km and Vmax. The enzyme kinetic study and kinetic parameters, K_m and V_{max}, were rapidly determined. In addition, we applied this method to screen HIV-RT inhibitors. The five inhibitors showed higher inhibition activity than the commercial drug nevirapine. The fifty percent inhibitions were determined by using inhibitor dose response curve. Two inhibitors showed higher inhibition efficiency with their IC_{50} values. Our purposed fluorometric method using PicoGreen dye showed easy, rapid, and sensitive detection protocol to determine HIV-RT activity and enzyme kinetic study. Moreover, this PicoGreen-fluorometric assay can be used for high-throughput inhibitor screening application. In addition, we crystallized HIV-1 RT/novel complex. The single crystal can be grown from our condition and molecular structure will be further studied.

_____ _____ ___ / ____ / ____

Student's signature Thesis Advisor's signature

ACKNOWLEDGEMENTS

I would like to thank Assistant Professor Kiattawee Chuwongkomon, Associate Professor Supa Harnnhongbua and Dr. Buabarn Kuaprasert for excellent graduate advisor and committees. I also thank for their patience, understanding and encouragement though the years. Without their kindness and understanding, this work could not be accomplished.

My gratitude is also to Assistant Professor Kanoktip Packdibamrung and Assistant Professor Pattana Srifah Huehne for serving as the members of thesis committees, for their valuable comments and also for useful suggestion. I am graceful to Associate Professor Supanna Techasakul and Dr. Patchreenart Saparpakorn, Chemistry Department for her kindness in providing HIV-1 RT inhibitors and many chemical compounds.

I also wish to thank to all members in Biochemistry Department for their help and discussion. I also thank them for their sincerity and friendships. Special thanks are also extend to all members of KC 7403 laboratory; pee Ple, pee Toom, Aoy, Su, Kade, Noi, Pam, Na, Peach, Ae, Toy, Nui, Bade, Nin, Noom, Not, Keang, Jar, Khim and Phoo for their kind suggestion and help.

This research was supported by the Graduate Scholarship (GS50-D02), Research Scholarship (2550/08), Synchrotron Light Research Institute, and supported in part by the Thailand Research Fund (RTA5080005).

Finally, the greatest indebtedness is expressed to my father, my mother, my bother and Lah for their unlimited love, understanding and encouragement.

Kun Silprasit

May, 2010

TABLE OF CONTENTS

Page

LIST OF TABLES

LIST OF FIGURES

LIST OF FIGURES (Continued)

LIST OF FIGURES (Continued)

LIST OF FIGURES (Continued)

LIST OF FIGURES (Continued)

LIST OF ABBREVIATIONS

µl	=	microliter
µM	=	micromolar
µmol	=	micromole
DTT	=	dithiothreitol
EDTA	=	ethylenediamine tetraacetic acid
h	=	hour
HIV-1RT	=	human immunodeficiency virus-1 reverse transcriptase
FPLC	=	flast performance liquid chromatography
kDa	=	kilo Dalton
Km	=	Michaelis–Menten constants
M	=	molar
mg	=	milligram
min	=	minute
ml	=	milliliter
mM	=	millimolar
ng	=	nanogram
nm	=	nanometer
NNRTI	=	non nucleotide reverse transcriptase inhibitor
NRTI	=	nucleotide reverse transcriptase inhibitor
PAGE	=	polyacrylamide gel electrophoresis
PEG	=	polyethylene glycol
SDS	=	Sodium dodecyl sulfate
UV	=	ultraviolet
Vmax	=	maximum velocity

RECOMBINANT HIV-1 REVERSE TRANSCRIPTASE AND ITS MUTANTS STUDY; CLONING, EXPRESSION, PURIFICATION AND PRELIMINARY CRYSTALLIZATION FOR X-RAY CRYSTALLOGRAPHY

INTRODUCTION

Acquired Immuno Deficiency Syndrome (AIDS) is the serious epidemic disease, it causes people died and carrier of disease germs around the world. In Thailand, spreading of Human Immunodeficiency Virus (HIV-1) infection is still serious epidemic, especially from mother to child which causes the children die youngly. To cure this problem, Thai government offers antiretroviral treatment regimens. The anti-HIV drugs such as nonnucleotide analogue and nucleotide analogue compounds were used to inhibit HIV reverse transcriptase (RT) enzymes. However, it shows that HIV can resistance to these drug substances in some patients and transmission of drug resistant HIV has been described for many years. Two type of anti HIV-1 virus drugs, Non-nucleotide Reverse transcriptase inhibitors (NNRTI) and Nucleotide Reverse transcriptase inhibitors (NRTI). The NNRTI drugs are specific to HIV -1 RT and low toxicity than NRTI. Nevirapine, a NNRTI drug, is a commercial drug and was used for cue AIDS patient for long time. However, some mutant HIV-1 virus such as K103N in HIV-1 RT protein was drug resistant strains, it resists to nevirapine inhibiting causes virus can propagate in patients. The X-ray crystal structure of mutant K103N HIV-1 RT complexes with nevirapine showed asparagines 103 resist binding of functional group in Nevirapine. Next generation drug, Efavirenz, was developed by change some functional group for favorable binding to mutant K103N and cause it can inhibit this mutant and wildtype HIV-1 RT. However, the usage of this molecule for a long time, drug resistant strains was also observed, a double mutant K103N/Y181C. The high efficiency inhibitor has to continuing develop for curing this problem. The screening of synthetic and natural substances are very useful method to find inhibitor, the developed assays to rapid and simple screen for HIV-1 RT inhibitory activity were relatively interesting.

Several biochemical assays have been reported with the aim of measuring the enzymatic activity of RT, which can be classified into 2 categories; radioactive and non-radioactive methods. There are many limitations for this method including permission for laboratory place, time consuming procedure and disposal of large quantity of scintillation material.

This research, we proposed to biochemically characterize HIV-1 RT with novel NNRTIs. We cloned, expressed the enzyme by using bacterial system and purified RT was used for inhibition kinetic study, the simple and fast protocol, PicoGreen-fluorescence method, was developed for enzyme and inhibition kinetic study. Then, the HIV-RT/inhibitor complexes were co-crystallized, the molecular structure will be investigated and understand by x-ray crystallography technique. By x -ray crystallography experiment and structure model can understand inhibitor/enzyme interaction and molecular mechanism of novel HIV-1 RT inhibitors will be understood.

OBJECTIVES

1. To clone, express and purify recombinant HIV-1 RT from bacterial expression system.

2. To develop simple and rapid method to study enzymatic properties of recombinant HIV-1 RT with novel inhibitors.

3. To determine enzyme and inhibitor kinetic properties.

4. To crystallize recombinant HIV-1 RT/inhibitors complex, for x-ray diffraction analysis.

LITERATURE REVIEW

1. HIV-1 RT

1.1 Structure and Function

The HIV-1 virion contains, in addition to the viral proteins, two copies of a single-stranded RNA genome. HIV-1 RT has two enzymatic activities; a DNA polymerase that can copy either a DNA or an RNA template, and an RNase H that cleaves RNA only if the RNA is part of an RNA/DNA duplex. The two enzymatic functions of RT, polymerase and RNase H, co-operate to convert the RNA into a double stranded linear DNA. This conversion takes place in the cytoplasm of the infected cell. After DNA synthesis has been completed, the resulting linear double-stranded viral DNA is translocated to the nucleus where the viral DNA is inserted into the host genome by HIV-1 Integrase. This inserted DNA copy, called a provirus, is the source of both viral genomic and viral messenger RNAs, which are generated by the host DNA-dependent RNA polymerase. Although other viral proteins (notably the nucleic acid chaperone nucleocapsid, and perhaps IN), and probably some cellular factors, help RT carry out the reactions that convert the viral RNA into DNA, HIV-1 RT contains all the necessary enzymatic activities for the conversion.

The HIV-1 RT is encoded by the pol gene that is translated as part of the Gag-Pol polyprotein precursor during the late stage of virus replication and translated enzyme maturation is mediated by the viral protease, which is released by autocatalytic cleavage. This cleavage occurs between amino acids F440 and Y441 of the 66 kDa subunit (p66) to yield the 51 kDa (p51) subunit (Michael *et al*., 2005). Both subunits contain an identical amino-terminal sequence and form an asymmetric heterodimer. The polymerase domain is associated with the amino terminus of both the RT subunits, while the RNase H activity is associated with the carboxyl-terminal domain of the p66 subunit (Molna *et al.,*1993). The catalytic function located in p66 subunits, that composed of 4 domains; finger, palm, thumb and RNase H domain. However, the polymerase site is only active in the open RT conformation, which is

present in the p66 subunit alone (Palaniappan *et al.*, 1997). The native p66/p51 heterodimer is the most stable form and the dimeric form of the enzyme possesses significant RT activity. The overall folding in the p51 subunit is similar to the folding in the p66 subunit but the spatial arrangement of subdomains is different and it lacks the RNase H subdomain. HIV-1 RT is a flexible enzyme, especially the fingers sub domain of p66 subunit has the opportunity of large scale motions while the p51 subunit is essential lly rigid. Binding of RT to dsDNA increases the flexibility and the ability of the p66 fingers to close down after binding of a dNTP molecule (Sluis-Cremer *et al.*, 2003).

1.2 The polymerase active site

The polymerase active site is composed of three catalytic carboxylates in the palm subdomain of p66 (D110, D185, and D186) that bind two divalent ions (Mg2+ appears to be the divalent cation used in vivo; Mn2+ can support polymerization in vitro) that are required for catalysis (Wakefield *et al.*, 1992, and Ding *et al.,* 1998). D185 and D186 are part of the YXDD motif that is highly conserved in retroviral RTs (X is Met residue in HIV RT and Val, Leu, or Ala in other retroviruses), residues 19-21.

1.3 The dNTP binding site

Prior to nucleotide incorporation, RT must select the appropriate dNTP. Besides the constraints imposed by Watson-Crick base pairing, also the structure of the polymerase active site is involved in the selection of the proper base. The most residues in the fingers domain and the palm subdomain are involved. Y183 and M184, two amino acids from the highly conserved YMDD are in close proximity to the 3'OH primer terminus and the bound dNTP. Other important amino acids lining the dNTP-pocket are K65, R72, D113, F116, F160 and especially Y115 and Q151 (Ding *et al.*, 1998)

1.4 Template/primer binding site

The majority of the RT-template/primer contacts involve the residues of the fingers, palm and thumb subdomains that form a hand shaped clamp, which mediate the positioning of the template/primer relative to the polymerase active site. The numerous interactions between the template/primer and RT are Van Der Waals contacts and hydrogen bonds that are not sequence-dependent and primarily involve the sugar- phosphate backbone of the nucleic acid and structural elements of the palm, thumb and RNaseH of p66. This is consistent with the fact that RT can copy a wide variety of different templates. In addition, hydrophobic interactions make a major contribution to the stability of the polymerase-DNA complex. In an RT/dsDNA complex, the bound DNA has a hybrid structure. RT has numerous interactions with 2'-OH groups of the RNA template that include residues 280 and 284 of the p66 thumb, residues of the template grip including 89 and 91 of the p66 palm and RNase H residues .

1.5 RNase H

The active site of the RNase H domain comprises four important residues that are required to interact with the divalent cations in the catalytic reaction: D443, E478, D498 and D549 in p66 subunit. The RNase H active site is also capable of binding other bivalent cations than Mg^{2+}, like Mn^{2+}. The RNase H domain makes significant contact with the thumb domain of the p51 subunit that affects the level of the RNase H activity of RT. The importance of the p51 thumb in obtaining the optimal RNase H structure is clearly shown when replacement of the p54 thumb in HIV-2 RT which exhibits a ten-fold lower RNase activity - by the p51 thumb domain of HIV-1 RT was found to restore the RNase H activity level as high as that of HIV-1 RT (Sarafianos *et al.*, 2001).

2. HIV-1 RT mechanism

The polymerase activity of RT requires both a primer and a template. The

principle of RT mechanism was begun by, binding of RT to heteroduplex of template/primer cause conformational change in the position of the p66 thumb, from a closed to an open conformation. The 3′ end of the primer strand is bound at the priming site (P site), adjacent to the polymerase active site. The initial step in nucleotide incorporation is the binding of the incoming dNTP at the nucleotide binding site (N site) to form a ternary complex. The rate-limiting step in the polymerization reaction is a conformational change in which a portion of the p66 fingers subdomain closes down on the incoming dNTP, which helps to align the 3′-OH of the primer, the α-phosphate of the dNTP, and the polymerase active site. And then, forming of the phosphodiester bond between the newly incorporated nucleoside and the primer were performed. The conformation of fingers domain was opened to allow the pyrophosphate to leave the active site. In DNA synthesis, the nucleic acid substrate must translocate relative to RT to free the nucleotide-binding site so that RT can bind the next incoming dNTP. The chemical step requires two divalent metal ions and there is good reason to believe that the normal in vivo metals are both Mg^{2+}. The metals coordinate the oxygens of all three phosphates of the incoming dNTP and the side chains of the three catalytic Asp residues. (D110, D185 and D186) Metal coordination at the polymerase site facilitates the attack of the 3′-OH on the α-phosphate of the incoming nucleotide by activating the hydroxyl group. The two metal ions also stabilize the charge of the reaction intermediates. In the details for reverse transcription mechanism of the HIV-1 genome was explained by nine steps processing. Each retroviral particle contains two copies of the RNA genome and minus-strand DNA synthesis starts near the 5′ end of the plus-stand RNA genome using a host tRNAlys3 that anneals at the primer-binding site (PBS) as a primer. The first step, synthesis proceeds to the 5′ end of the RNA genome through the U5 region, ending at the R region at the 5′end, forming the minus-strand strong stop DNA. The second, DNA synthesis is accompanied by RNaseH digestion of the RNA portion of the RNA/DNA hybrid product, thus exposing the single-stranded DNA product.

The third step, this exposure facilitates hybridization with the R region at the 3′ end of the same, or the second, RNA genome, a strand-transfer reaction known as the first jump. The forth step, when minus-strand elongation passes a polypurine-rich

region called the polypurine tract (PPT) region, a unique plus-strand RNA primer is formed by RNase H cleavage at its borders. Plus-strand synthesis then continues back to the U5 region using the minus-strand DNA as a template. The fifth step, meanwhile, minus-strand synthesis continues through the genome using the plus-strand RNA as a template, and removing the RNA template in its wake via RNase H activity. The sixth step, the RNase H digestion products formed are presumed to provide additional primers for plus-strand synthesis at a number of internal locations along the minus-strand DNA. Seventh step, PPT-initiated plus-strand DNA synthesis stops after copying the annealed portion of the tRNA to generate the plus-strand DNA form of the PBS, forming the plus-strand strong stop product. The tRNA is then removed by the RNase H activity of RT. Eighth step, this may facilitate annealing to the PBS complement on the minus-strand DNA, providing the complementarily for the second jump. DNA synthesis then continues. The ninth step, strand displacement synthesis by RT to the PBS and PPT ends, and/or repair and ligation of a circular intermediate, produces a linear duplex with long terminal repeats (LTRs) at both ends.

3. HIV-1 RT inhibitors

Since, HIV RT is the essential molecule for viral life cycle, the most of inhibitors has been created and established to stop the enzyme activity. Because of dNTP is used as substrate for reverse transcription , the inhibitors was designed like nucleotide structure, called nucleotide RT inhibitors (NRTIs), that can competitive incorporated with cellular dNTP into RNA or DNA polymer. Besides, heterodimer is active form for enzyme activity, some inhibitors was design to inhibit heterodimer forming, such as, group of non-nucleoside RT inhibitors (NNRTIs). The NNRTIs molecular structure is different from the nucleoside structure, therefore it is not involve to dNTP incorporate. All these NNRTIs bind to the NNRTI binding pocket that is an allosteric hydrophobic site close to, but distinct from, the catalytic active site of the RT (Crespan *et al.*, 2005). The inhibitory effect of NNRTIs does not require intracellular metabolic activation. NNRT are non-competitive (or mixed-type) inhibitors with respect to the substrates or template/primer. Whereas inhibitory of NNRT can be by binding specific binding pocket, the NNRTIs are highly specific for

HIV-1 RT and do not recognize other lentiviral RTs or any other DNA or RNA polymerases from viral or cellular origin. This explains the highly selective anti-HIV-1 activity of the NNRTIs. NNRTIs that are approved for clinical use by the FDA are nevirapine, delavirdine and efavirenz, whereas etravirine, dapivirine and rilpivirine are currently subject of clinical phase I/II studies, either for potential microbicide use (dapivirine) or for systemic (oral) therapy of HIV-1 (Boyle *et al.*, 2002). Crystal structures of RT with bound NNRTIs generally have the p66 thumb subdomain in an extended position. For unliganded RT the thumb subdomain can either be folded down into the DNA–RNA binding cleft (Rodgers *et al.*, 1995) or can adopt a more extended position. Examination of various crystal forms of RT with different NNRTIs bound showed significant variations in relative domain positioning. Thus, there is no clear evidence that NNRTI binding induces a single positioning of the p66 thumb subdomain.

Comparing the NNRTI bound and free forms of RT indicated a significant and consistent movement of strands beta 2-bata 3 containing the critical Asp110, Asp185 and Asp186 active site triad. Such a distortion of the key catalytic residues can explain the inhibition of RT by NNRTIs. Parallel rapid reaction kinetic experiments showed that the rate limiting step inhibited was the chemical bond formation, in line with the proposed structural mechanism. A variant of this active site displacement mechanism has been recently proposed in which the NNRTI distorts the catalytic triad position such that it is in a conformation incompatible with the binding of divalent cations Mn^{2+} /Mg^{2+}. This suggestion was based on an RT crystal structure determined in the absence of NNRTI and with ATP bound but in a mode significantly different to dNTP binding in the catalytic complex (Huang *et al.*, 1998).

4. HIV-1 RTdrugs resistant strains

To day, the HIV-1 infected patients can preserve their life by anti HIV-1 drugs treatment. However, inconsistency drugs uptake causes virus can escape and then it can propagate again, virus propagation in this stage will increase mutation rate. In addition, these mutants become to drugs resistant. HIV drugs resistant strain is

dramatically problem, patient has to increase a mount of drugs or alter kind of drugs, it increase cost and cytotoxic effect.

4.1 NNRTI resistance

Since, many NNRTIs has been developed and some was approved to be comercial drugs, example nevirapine, delavirdine (first generation), efavirenz (second generation), and etravirine (third generation). In addition, several other potent that inhibit HIV-1 at nanomolar concentrations (EC_{50}) are in clinical trials. However, there are mutations in RT that can cause resistance to all of the approved NNRTIs. Most of the NNRTI resistance mutations are found in and around the NNRTIs binding pocket, especially, the drugs resistance mutant K103N and Y181C are the most frequently observed in patients treated with the approved NNRTIs. Moreover, L100I, K101E, V106A, V179D, Y188L, G190A, and P236L were observed in patients. The NNRTI resistance mutations can occur singly, or in combinations. The molecular modeling and biochemical studies have contributed to understand NNRTI drug resistance and develop the better NNRTIs. The current information suggests that there are at least three classes of NNRTI-resistance mechanisms.

4.1.1 Loss/change of key hydrophobic interactions

The molecular structure studies shown that the aromatic ring of the first generation NNRTIs specifically interact with 3 amino acid residues, Y181, Y188, and F227 in the hydrophobic core of the NNRTI binding pocket. The mutations in these key residues (Y181C, Y188L, and F227L) cause significant resistance through the loss of the rigid-aromatic ring interactions with NNRTIs (Olivares *et al.*, 2004). To cure this mechanism, the strategic flexibility inhibitor was design. This intrinsic flexibility makes it possible for the newer drugs to have compensatory interactions with RTs that have mutations causing resistance to the first-generation NNRTIs. This flexibility in the binding has been called wiggling and jiggling (Das *et al.*, 2004), and its structural basis has been described in recent structural studies of wild-type,

K103N/Y181C, and L100I/K103N HIV-1 RT complexes with TMC278/rilpivirine (Das *et al.*, 2000) . The rigid aromatic rings were changed to be the flexibility, allow NNRTIs adapt to interact with key residue for resistance mutations.

4.1.2 Steric hindrance

The central region of the NNRTI binding pocket contain key residue, L100 and G190. Although some flexible inhibitor can inhibit drugs resistance RT with Y181, Y188, and F227 mutation, the mutations in L100 and G190 cause high levels of resistance to many NNRTIs. For example, HBY 097, which effectively inhibits viruses carrying the Y181C mutation, cannot inhibit viruses that carry the G190A mutation. the G190A mutation would cause the C_β atom of A190 to have a steric lash with the quinoxaline moiety and reduce the binding of HBY 097 (Stefan *et al.,* 2009*)*. While, G190A introduces a bulge, the L100I mutation confers resistance by changing the shape of the pocket (the amino acid is β-branched instead of γ-branched.

4.1.3 Pocket entrance mutations

The entry of NNTIs into the binding pocket is the key step to inhibit the HIV-1 RT. The mutation in the rim of this pocket is the problem for inhibitor function. The rim of the entrance to the NNRTI binding pocket contains two key amino acid residues K101 and K103. The mutations in these residues cause resistance by interfering with the entry of NNRTIs into the pocket. For example the K103N and K101E mutations, these mutations cause resistance to first generation NNRTIs. To overcome this problem, the second generation NNRTIs was designed to interact with the side chain of the mutated N103 residue, such as DAPY. Although, we known the three main mechanism of these drugs resistance mutation, many new drugs were improved to overcome the resistance virus strains, the using of inhibitor still causes new drugs resistance HIV-1 RT. Recently, it has been reported that a number of mutations in the connection, or RNase H subdomains of RT, can enhance

resistance to both NRTI and NNRTI inhibitors of RT. The mutation in RNase H subdomains cause reduction in RNase H activity, which allows more time for the excision mechanism to occur, therefore, increasing resistance to AZT.

5. HIV-1 RT activity measurement

5.1 Radio isotropic method

Assay for RNA-Dependent DNA Polymerase Activity was performed by using poly(rA).oligo(dT) and ^{32}P-dTTP, The polymerase function cause ^{32}P-dTTP incorporated into oligo(dT) primer. The amount of polymerized deoxynucleotide triphosphates was assayed by precipitating the ^{32}P-dTTP labeled hetero duplex DNA/RNA. The precipitation was occurred by adding salmon sperm DNA in 0.2 M sodium pyrophosphate and precipitating the labeled polymer with cold 10% (wt/vol) trichloroacetic acid. The precipitates were collected on Whatman GF/C fiberglass filters by suction filtration. The incorporated triphosphate was measured by assaying for ^{32}P in a liquid scintillation counter.

5.2 Non Radio Isotropic method

Non-radioactive methods, such as electrochemiluminescence (Munshi *et al.,* 2008), chemiluminascence (Odawara *et al.,* 2002), recombinant *E. coli* cell based screening (Kim and Loeb, 1995), and real time measurements of elongation by a RTusing surface plasmon resonance (Buckle *et al.,* 1996). Many laboratories developed RT-PCR strategies to detect and quantify virion-associated retrovirus genomes rely on sequence-specific primer design and require RNA isolation procedures which make it expensive and labor intensive. In contrast, biochemical assays which estimate the amount of virion-associated RT (RT-assays) can universally detect and quantify retrovirus particles. The enzymatic activity of RT, present in all retroviruses, is measured using an RNA template which is reverse transcribed *in vitro* by the retroviral enzyme. The resulting DNA product (cDNA) is then quantified as a measure of the amount of virions present.

Since fluorescence dyes are sensitive to detect small amount of polynucleotide, the fluorometric method have been developed to detect HIV-1 RT activity. The binding modes of dye molecules bound with DNA are major or minor groove-binding and intercalation. Type of minor-groove binders are Hoechst 33342, Hoechst 33258 and 4',6'-diamidino-2-phenylindole (DAPI). Classes of dyes which intercalate into dsDNA are divided such as acridines, anthraquinones, cyanine dyes (PicoGreen, YOYO-1 iodide, SYBR Green I and SYBR GOLD) and phenanthridinium ions (ethidium bromide and propidium iodide) (Ihmels *et al*., 2005).

The fluorescence dye 4', 6-diamidino-2-phenylindole (DAPI) has been reported for this propose. Although, DAPI can be used for detect HIV-1 RT activity and kinetic study by using 359 nm excitation and 460 nm emission (Seville *et al*., 1996), large amount of poly (A) and oligo (dT) were needed for activity assay and large reaction volume was required. Moreover, DAPI is sensitive to pyro-phosphate, an intermediate of polymerase reaction, the spectral overlap in the emission spectra of DAPI and DAPI-DNA with DAPI-poly-P at 360 nm is also a limitation of using DAPI for polynucleotide detection (Sobbi *et al*., 2008)

PicoGreen is a fluorophore which was shown intercalation to DNA (Cosa *et al.*, 2001). It has similar character to SYBR Green I for affinity which there is high affinity for DNA and a large fluorescence enhancement upon DNA binding. PicoGreen was developed and patented by Molecular Probes (*Molecular Probes,* E-22064). This dye shows a sensitivity of detecting DNA down to 250 pg/ml and strongly increasing in fluorescence signal (>1000 times) in the presence of dsDNA or DNA: RNA duplex, but does not show a significant increasing in fluorescence in the presence of proteins, carbohydrates, ssDNA, RNA, or free nucleotides (Blotta *et al.*, 2005).

6. Protein x-ray crystallography

In order to initiate crystallization, the protein solution has to be brought to a thermodynamically unstable state of supersaturation. The solution can be brought

back to the stable equilibrium state through precipitation of the protein, which is the most frequent process, or through crystallization. The supersaturated state can be achieved by several techniques: evaporation of solvent molecules, change of ionic strength, change of pH, change of temperature or change of some other parameter (Bergfors *et al.*, 1999). Nucleation requires a greater protein concentration than growth. The solution needs to be supersaturated. Supersaturation might, however, lead to formation of too many nucleation points. Seeding is a way of limiting the number of nucleation points. Growth rate and crystal size depend on the degree of super-saturation. Cessation of growth may be caused by depletion of a particular component, which actually is building up the crystal, growth defects or the flow of molecules around the crystal. The crystal-packing interactions involve salt bridges, hydrogen bonds, van der Waals-, dipole-dipole and stacking interactions.

6.1 Protein crystallization methods

6.1.1 Vapor diffusion

The most frequently used crystallization method is the vapor diffusion technique. In this technique a small droplet of typically 2-10 µl of the protein is mixed with an equal or similar volume of the crystallizing solution (usually buffer, salt, and precipitant) and placed in a reservoir containing 500 – 1000 µl of the crystallizing solution in a closed system. The difference in concentration between the drop and the reservoir drives the system toward equilibrium by diffusion, usually of water molecules, through the vapor phase. The protein becomes supersaturated and crystals start to form when drop and reservoir are at or close to equilibrium. Vapor diffusion method can be prepared in several ways including hanging drops, sitting drops, sandwich drops, reverse vapor diffusion, and pH gradient vapor diffusion

6.1.2 Dialysis

Dialysis offers a way of manipulating the ionic strength that is not possible with vapor diffusion. The dialysis can be set up in various ways, e.g., in

dialysis bags or collodion thimbles (also called ultra thimbles), Zeppezauer cells, or buttons. In the button the protein is placed inside the button which then covered by a dialysis membrane. Dialysis membranes are semi-permeable: They allow small molecular weight substances to diffuse in while preventing the protein from diffusing out. Dialysis is the most effective technique for crystallization by decreasing the ionic strength. If a protein is less soluble at low ionic strength, it is often possible to crystallize it simply by dialyzing it against a weak buffer or even water. In this case, no precipitant is necessary. Unlike vapor diffusion, the protein concentration remains constant during the dialysis experiment.

6.1.3 Microbatch technique

In the batch technique, the precipitant and the target molecule solution are simply mixed. Supersaturation is achieved by mixing rather than by diffusion. It can be also be used as a rapid micro-scale screening under microscope for the purpose of determining the solubility conditions. Batch technique can also be performed under oil. The oil prevents evaporation and extremely small drops (< 2 μl) can be made, hence it is termed “microbatch”.

In this study, we propose to crystallize complex of HIV-1 RT with some NNRTIs such as nevirapine and efavirenz which have been used in anti-AIDS chemotherapy. Moreover, there are some novel compounds designed by using computer-aided molecular design and synthesized at Department of Chemistry, Kasetsart University. These compounds which have been tested based on virucidal and virustatic testing as well as HIV-1 RT assay will be complexed with HIV-1 RT both wild type and mutant enzymes. The obtained results are expected to get structural information for the new and potent HIV-1 RT.

METERIALS AND METHODS

Materials

1. General instruments

1.1 Autopipette: Gilson, Germany

1.2 Balance (4 digits): Denver balance, USA

1.3 Centrifuge: Hermle refrigerate centrifuge model Z383K, Hermle Labortechnik GmbH, Germany

1.4 Heat Box: D1100, Labnet, USA

1.5 Microplate reader: Sunrise, TECAN, Austria

1.6 Peristaltic pump: ECONO pump, Bio-Rad, USA

1.7 pH meter: Seven Easy pH meter, Mettler toledo, USA

1.8 Power supply: AE 8750, ATTO, Japan

1.9 Recorder: PowerChrom 280 system, EDAQ

1.10 Slab gel electrophoresis: AE 6530, ATTO, Japan

1.11 UV detector: ECONO UV monitor, Bio-Rad, USA

1.12 UV Spectrophotometer: Cary 50 Conc, Varian, Australia

1.13 Water bath: Memmert, Germany

1.14 Vivaspin-10 ultrafiltration membrane concentrators : Vivascience AG, Hanover, Germany

2. Protein purification and analysis Instruments

2.1 Chromatographic prepacked column: Amersham Biosciences, Piscataway, NJ, USA

2.2 DEAE cellulose: Whatman, England

2.3 EnzChek® Reverse Transcriptase Assay Kit : Molecµlar Probe, OR, USA .Composed of PicoGreen reagent 400Xdye stock in DMSO, 350 bases Poly(A) ribonucleotide 1 mg/ml template in 100 mM Tris.HCl, 0.5 mM EDTA pH 8.1, Oligo d(T)16 primer 50 µg/ml in 100 mM Tris.HCl, 0.5 mM EDTA pH 8.1

2.4 Fast protein liquid chromatography (FPLC): AKTAprime plus, GE Healthcare, Sweden

2.5 FLWIN lab software analysis: Perkin Elmer, Norwalk,. Conn

2.6 Fraction collector: Biologic BioFrac Fraction collector, Bio-Rad, USA

2.7 Perkin Elmer Luminescence Spectrometer LS50B: USA

2.8 Phosphor cellμlose P11: Whatman, England

2.9 Ni-nitrilotriacetic acid (Ni-NTA) agarose resin : Qiagen, CA, USA

3. Crystallizations Instruments

3.1. Cell cμlture plate 24 well: Corning, NY, USA

3.2. Crystal cap magnetic vial: Hampton Research, CA, USA

3.3. Crystal wand: Hampton Research, CA, USA

3.4. MicroBatch 60 well: Nunc, Roskilde, Denmark

3.5. Mounted Cryoloop loop: Hampton Research, CA, USA

3.6. Siliconised Circle Cover slip 18 mm : Hampton Research, CA, USA

3.7. Sitting drop plate 96 well: Corning, NY, USA

3.8. Stereo Microscope: Bausch & Lomb, NY, USA

4. Bacterial strains and plasmid vector

Esherichia coli strains DH5α were used for routine cloning and plasmid preparations, strains BL21 (DE3) were used for protein expression. The plasmids pGEX3X and pET33B expression vector were used to construct high-level expression of recombinant HIV-1 RT.

5. Source of material

Eleven Dipyridodiazepinone derivatives were provided from Dr Supanna Techasakul Department of Chemistry, Faculty of Science, Kasetsart University. HIV-1 RT genome library DNA was kindly provided by the Department of Medical Sciences, Ministry of Public Health, Thailand (HIVHXB2CG, Accession

number K03455). Crystal screening solutions (Hampton Research) were kindly provided from Dr. Buabarn Kuaprasert (Synchrotron Light Research Institute, Nakornrachasema, Thailand).

Methods

1. Construction of recombinant HIV RT plasmid with pGEX system

The HIV RT gene was amplified from cDNA of the HIV genome by the Polymerase Chain Reaction (PCR) using a forward primer, p66F containing *Eco*N I restriction site, for both hetero subunits coding sequences,

p66F 5'GTCCCCATACTAGGTCCCATTAGCCCTATTGAGACTGTA'3 Tm = 56 ^{o}C
p66R 5'CGGGGATCCTTATAGTACTTTCCTGATTCCAGCACTGA'3 Tm = 57 ^{o}C
p51R 5'CACGAATTCTTAGAAGGTTTCTGCTCCTACTATGGGTTCTTT'3 Tm = 59 ^{o}C

And two reverse primers, p66R with *Bam*H I site and p51R with *Eco*R I site, to amplify RT66 and RT51 open reading frames (ORF), respectively. The primers were designed from a sequence of HIV RT gene in the database (Gene Bank, Accession number K03455) and restriction enzyme sites were added into the sequences. To instead GST with RT gene, *Eco*N I site was added into a 5 prime end of forward primer, the gene was started by existing ATG codon on the plasmid while *Bam*H I and *Eco*R I and a termination, TAA, codon was added into 5 prime end of the reverse primers for cloning RT66 and RT51 ORFs, respectively. The PCR reaction was preheated 94 ^{o}C 5 minutes and reaction proceed by 30 cycles of denaturing at 94 ^{o}C 30 seconds, annealing with 55^{o}C 30s and extension with 72 ^{o}C 1 minutes, and then last extension with 72^{o}C 10 minutes, Both PCR products, RT66 and RT51 DNA fragments, were purified by an ethanol precipitation. The expression plasmid, pGEX3X, and the DNA fragments cut by using appropriate restriction enzyme. The GST encoding region in the pGEX3X was also removed. The excised DNA fragments were ligated into the expression vector. The recombinant plasmid harboring HIV RT genes were called pGXRT66 or pGXRT51, which were under control of *tac* (T7/Lac)

promoter and carried an ampicillin resistant gene. Each plasmid was individually transformed into *Escherichia coli* strain BL21. The plasmids DNA containing RT66 and RT51 were isolated from the recombinant *E. coli*, and the RT sequences were confirmed by DNA sequencing (Macrogen, Korea).

2. Site direct mutagenesis create mutant RT.

The recombinant plasmid harboring HIV RT wild type gene were used as template for mutant recombinant plasmid creation, site direct mutagenesis -PCR based method is used as describe, the recombinant plasmids, pGX66 , was used as template in PCR experiment by using mutagenesis primers to produce mutant recombinant plasmid. The mutagenic oligonucleotides primers used for the kit were specifically designed using the criteria of the manual to have lengths of 25-45 bases with *T*m ≥ 78°C. The *T*m was calcμlated from following formμla:

$$T_m = 81.5 + 0.41\,(\%GC) - 675/N - \%mismatch$$

• N is the primer length in bases
• %GC and % mismatch are whole numbers

The primers RTK103NF and RTK103NR were used for mutant K103N mutagenesis, RTY181CF and RTY181CR were used for mutant Y181C mutagenesis, wildtype nucleotides were replaced with mutant nucleotide, showed as underline alphabet. The PCR reaction was preheated 94 ^{o}C 5 minutes and reaction proceeded by 20 cycles of denaturing at 94 ^{o}C 30 seconds, annealing with 60^{o}C 1 minute and extension with 68 ^{o}C 12 minutes, and then last extension with 68^{o}C 10 minutes, the newly circular PCR product was synthesized. The mutagenesis primers were shown as below.

K103N = AAC primer

RTK103NF 5'-CA GGG TTA AAA AAG AA**C** AAA TCA GTA ACA GTA C-3'

RTK103NR 5 –GT ACT GTT ACT GAT TT**G** TTC TTT TTT AAC CCT G-3
N = 33 bp, Tm = 77.57 ^{o}C, GC= 33 % and mismatch = 3%

Y181C = TGT primer

RTY181CF 5-CCA GAC ATA GTT ATC T**G**T CAA TAC ATG GAT GAT-3
RTY181CR 5-ATC ATC CAT GTA TTG A**C**A GAT AAC TAT GTC TGG-3
N = 33 bp, Tm = 79.88 ^{o}C, GC = 36.4% and mismatch = 3%

The parental plasmid pGX66 which was used as DNA template, were purified from *Escherichia coli* DH5α, these plasmid were methylated by host cells, while newly circular PCR product was not. Therefore, plasmid template were destroyed any by using methylated – digestion enzyme, Dpn I. The both PCR products were purified by ethanol precipitation and Dpn I restriction enzyme was added into purified solution to complete digest methylated plasmid. Finally, the digested solution remains only newly circular PCR product, mutant plasmids. These solutions were transformed into Escherichia coli DH5α and screen on amplicilin selection LB agar plate, The plasmid was detected for mutant DNA by using PCR with detection primer, forward primer Check K103NF and Check Y181CF, each forward primers were used with reverse primer 66R and the wildtype plasmid was used as control reaction. The PCR reaction was preheated 94 ^{o}C 5 minutes and reaction proceed by 30 cycles of denaturing at 94 ^{o}C 30 seconds, annealing with 60^{o}C 30s and extension with 72 ^{o}C 1 minutes, and then last extension with 72^{o}C 10 minutes. The mutant RT plasmids were confirmed by DNA sequencing. The mutated plasmid determining primers were shown as below.

Check K103NF 5’ CCCGCAGGGTTAAAAAAG**AAC**‘3 Tm = 56 ^{o}C

Check Y181CF 5’ AAATCCAGACATAGTTATC**TG** ‘3 Tm = 48.4 ^{o}C

The pGEX Plasmid construction for HIV-1 RT expression, protein expression was controlled by *tac* promoter (tac pro).

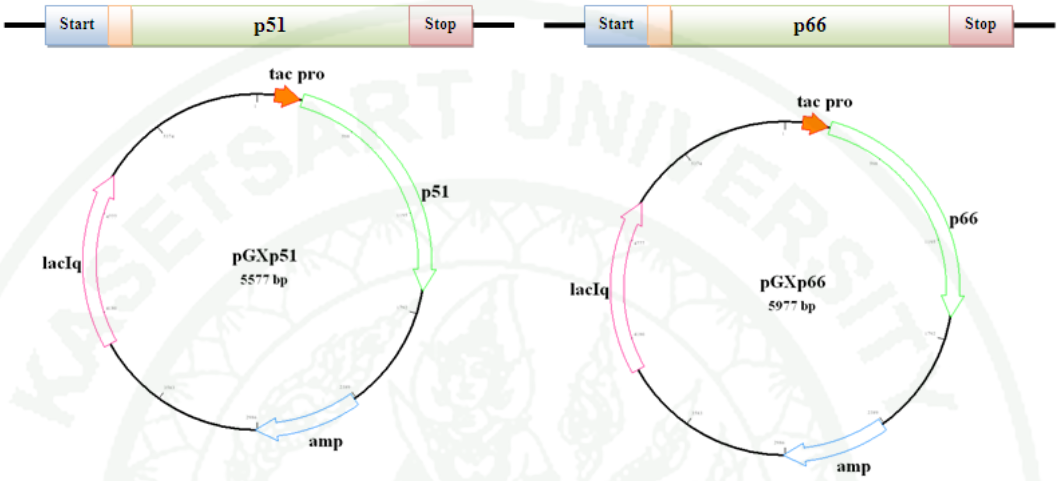

3. Construction of recombinant HIV-1 RT p51 6xhistag plasmid pET system

To minimize purification step, we used fusion 6X histag plasmid with pET system. HIV-1 RT p51 coding gene was subcloned into expression plasmid pET33B by using new designed primer for PCR technique, forward and reverse primer were 66F-NcoI and 51R-XhoI, the primer sequence were shown.

66F-NcoI 5'ATACCATGGTGCCCATTAGCCCTATTGAGACTGTA'3 Tm=55 °C
51R-XhoI 5'CCACTCGAGGAAGGTTTCTGCTCCTACTATGGGTTCTTT'3 Tm=60 °C

The *Nco* I site was added into a 5 prime end of forward primer, while Xho I was added into 5 prime end of the reverse primers for cloning RT51 ORFs. The PCR reaction was preheated 94 °C 5 minutes and reaction proceed by 30 cycles of denaturing at 94 °C 30s, annealing with 58 °C 30s and extension with 72 °C 1 minutes, and then last extension with 72 °C 10 minutes. The PCR product was purified, restriction cut and subclone to plasmid pET33B. The recombinant plasmid harboring HIV RT p51 genes were called pETRT51his, which were under control of T7 promoter and carried a Kanamycin resistant gene. The plasmid was transformed

into Escherichia coli strain BL21. The plasmids DNA containing RT51 were isolated from the recombinant *E. coli*, and the RT sequences were confirmed by DNA sequencing (Macrogen, Korea).

4. Protein expression of HIV-1 RT

4.1. Protein expression of untag HIV-1 RT

The cells containing plasmid pGXRT66 or pGXRT51 were cultured in 5 ml Luria-Bertani (LB) containing ampicillin (100 µg/ml) with shaking at 220 rpm at 37 ^{o}C, overnight. Then, 5 ml of cell were inoculated into a flask containing 500 ml LB with ampicillin and cultured with shaking at 220 rpm at 37 ^{o}C until $O.D._{600}$ equal to 0.4. The culture was placed at 16 ^{o}C with shaking at 220 rpm and the gene expression was induced by adding isopropyl-beta-d-thiogalactopyranoside (IPTG) into the culture with a final concentration of 0.4 mM.

HIV-1 RT amplified-PCR condition for pGEX expression system

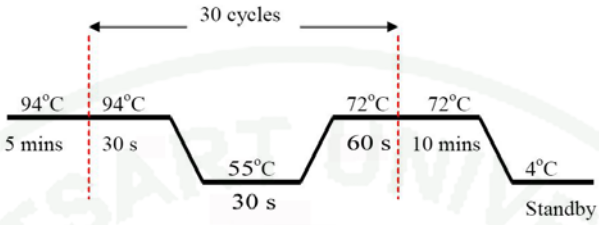

HIV-1 RT site direct mutagenesis-PCR condition for pGEX expression system

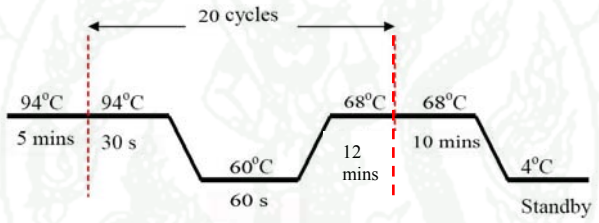

PCR condition for mutant plasmid screening

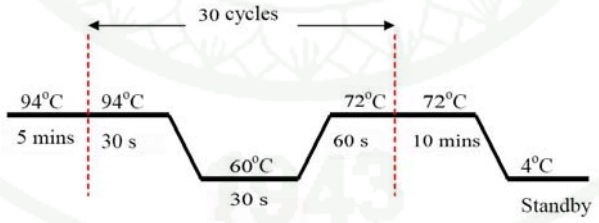

HIV-1RT amplified-PCR condition for pET expression system

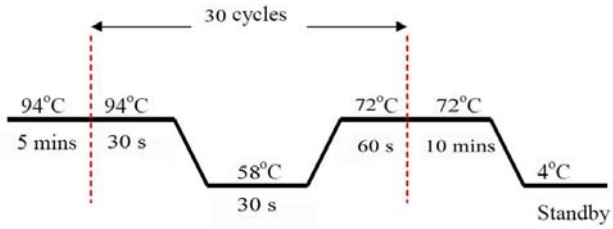

The pETp51H plasmid construction for HIV-1 RT expression, protein expression was controlled by *T7* promoter (T7).

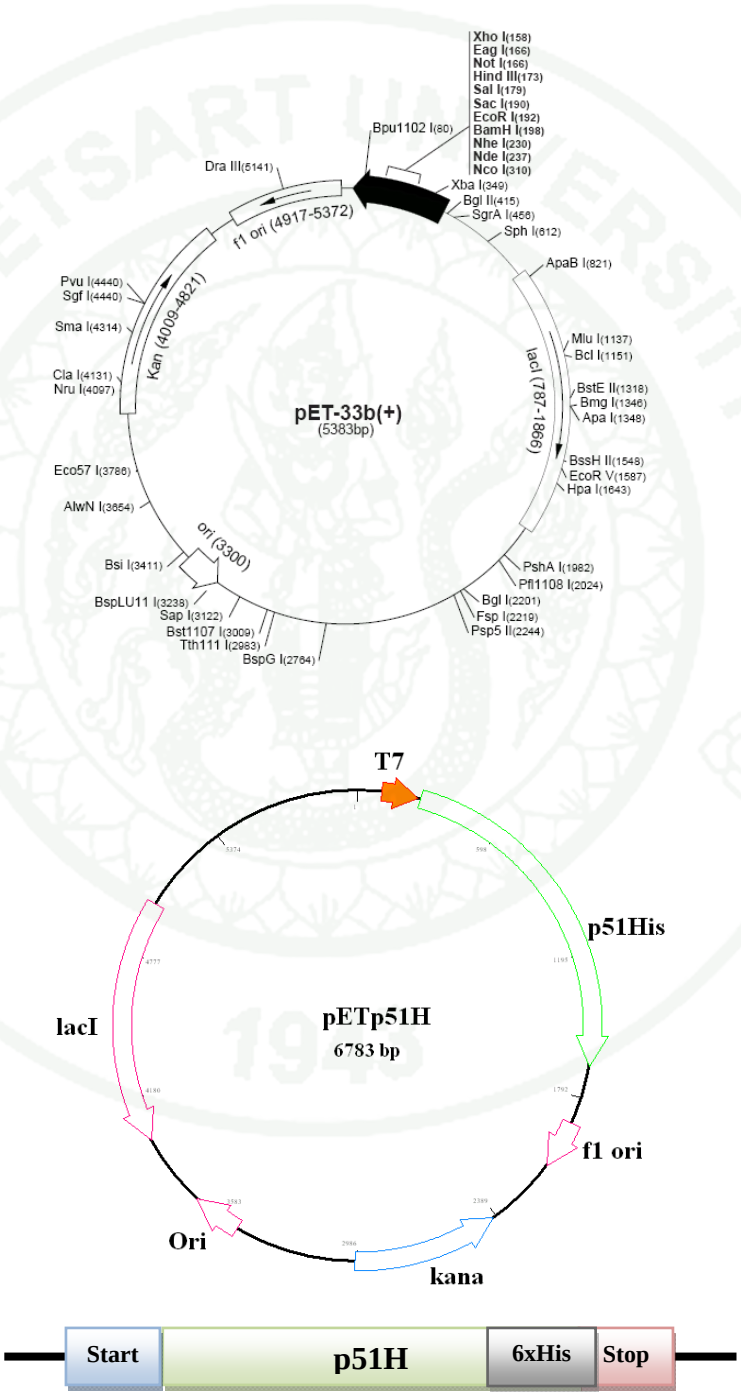

After 12 h of induction, the induced cells were harvested by centrifugation at 4,000 g for 10 minutes and the expressed protein was detected by using SDS-PAGE technique.

4.2 Protein expression of 6xhistag HIV-1 RT

The cells containing plasmid pGXRT66 or pETRT51his were cultured in 5 ml Luria-Bertani (LB) containing ampicillin (100 µg/ml) and Kanamycin (50 µg/ml) for plasmid pGXRT66 or pETRT51his , respectively, with shaking at 220 rpm at 37 ^{o}C, overnight. Then, 5 ml of cell were inoculated into a flask containing 500 ml LB with ampicillin or Kanamycin for cells containing plasmid pGXRT66 or pETRT51his, respectively. The cultured with shaking at 220 rpm at 37 ^{o}C until O.D.$_{600}$ equal to 0.4. and placed at 16 ^{o}C with shaking at 220 rpm, 1 h and the gene expression was induced by adding isopropyl-beta-d-thiogalactopyranoside (IPTG) into the cultures with a final concentration of 0.4 mM. After 12 h of induction, the induced cells were harvested by centrifugation at 4,000 g for 10 minutes and the expressed protein was detected by using SDS-PAGE technique.

5. Recombinant HIV RT protein preparation and purification

5.1 Purification protocol 1: untag HIV-1 RT purification using ion-exchange Chromatography

The purification steps were adapted from North *et al*., 1994. Both pGXRT66 and pGXRT51 expressed cells were suspended in a buffer A composing of 50 mM Tris-HCl, pH 7.5, 1 mM EDTA, 1 mM β-mercaptoethanol, 1 mM PMSF, 0.5 % and 5% glycerol and added Triton x-100 , and then lysed by sonication. Cell debris and inclusion bodies were removed by centrifugation at 10,000 g for 30 minutes, and then proteins in supernatant were precipitated in 35 % saturated ammonium sµlfate. After centrifugation at 10,000 g for 30 minutes, the pellet was dissolved in column buffer and dialyzed for 3 hrs against 1 liter of the column buffer A without Triton X-100. The protein solution was applied onto a DEAE-cellulose

column (Whatman) pre-equilibrated with the column buffer A, followed by elution with column buffer A containing 0.5 M NaCl at 4 ^{o}C. The fractions containing both 66 and 51 kDa subunits of RT were pooled and mixed together to get an active HIV-1 RT. The protein solution was dialyzed against column buffer, adjusted pH to 8.9 and then applied to a Phosphor cellulose P11 column (Whatman) equilibrated with the same column buffer A pH 8.9 at 4 ^{o}C. Heterodimeric RT was eluted by gradient elution with 0-0.3 M NaCl in column buffer pH 8.9. Then, the active RT was further purified by Q-sepharose anion-exchange column and gradient eluted with the gradient 0-0.5 M NaCl in the column buffer pH 8.9 at 4 ^{o}C. The enzyme purity was determined by SDS-PAGE.

5.2 Purification protocol 2 6xhistag HIV-1RT purification using Ni-NTA system

Both pGXRT66 and pETRT51 expressed cells were mixed and suspended in a buffer A (50 mM Tris HCl pH 7.5, 1 mM EDTA, 1 mM β-mercaptoethanol, 50 mM NaCl, 5% glycerol) containing 0.5% Triton X100 and 1 mM PMSF, Then, lysed by sonication. Cell debris and inclusion bodies were removed by centrifugation at 10,000 g for 30 minutes, and then the protein solution was applied onto a DEAE-cellulose column (Whatman) pre-equilibrated with the column buffer pH 7.5, followed by elution with 0.5 M NaCl in the same buffer at 4 ^{o}C. The Flow though fractions were applied to a Phosphor cellμlose P11 column (Whatman) equilibrated with the same column buffer pH 7.5 at 4 ^{o}C. The RT protein was eluted with buffer B (50 mM Phosphate pH 8.0, 300 mM NaCl, 30 mM Imidazole, 5% glycerol). Then, HIV-1 RT protein fraction was further purified to be heterodimeric form with Ni-NTA column, which was equilibrated with buffer B. HIV-1 RT was eluted by using gradient elution 30-250 mM imidazole in buffer B.

6. Fluorometric Assay of HIV-1 RT activity

All reagents were provided in EnzChek® Reverse Transcriptase Assay Kit. The mixture of 5 μl of 1 μg/μl the 350 bases-poly (rA) ribonucleotide templates and 5

µl of 50 ng/µl the oligo-dT primer in a nuclease-free microcentrifuge tube were incubated on ice for 1 h to allow the primer/template annealing. Then it was diluted to 200 fold with polymerization buffer, final concentration were 2.5 ng polyA and 0.125 ng dTTP/µl. The primer/template containing buffer was aliquoted and kept at -20 °C until used. For 10 stop-time points assay, 4 µl primer/template (contained 10 ng poly (rA) and 0.5 ng oligo-dT) was adequated into 10 wells, the reaction was started by adding 2 µl of 30 ng/µl purified enzyme into primer/template containing buffer. The reaction was incubated at 37°C before adding 5 µl 0.2 M EDTA to stop every 30 s, stopped at 30s for first well, 60 s for second well until 5 min for tenth wells. The complete terminated plate was gentle shaken and kept on ice for 30 minutes to allow forming of stable a heteroduplex RNA: DNA complex. The polymerizing activity of the enzyme was measured using a fluorometric assay by adding 200 µl of chilled 1/2,000 PicoGreen in TE buffer (10 mM Tris-HCl, pH 7.5 and 1 mM EDTA) into the reactions mixture and incubating on ice, in the dark for 10 minutes. The dye-EDTA terminated reactions mixture was pipetted to a 10 mm fluorometric micro cuvette and the fluorescence intensity was measured with the fluorospectrometer Perkin LS 50B by using excitation of 502 nm and emission of 523 nm. Time drive mode analysis by FLWIN software V.4 (PerkinElmer, USA) was used to analyze a fluorescence signal.

7. HIV-1 RT enzyme kinetic assay

7.1 Determine enzyme amount and time-dependent activity of HIV-1 RT

A stop time assay was performed to follow time-dependent HIV-1 RT activity and all assays were performed in 96 well plates. For the measurement HIV-1RT activity with varying RT amount, four master mixtures contained varying amount of RT amount were prepared. Six microliters of each stock purified HIV-1 RT was added into microcentrifuge tube containing 12 µl of primer/template buffer. Four master mixtures contained RT amount which final amount were 12, 25, 50 and 100 ng. Six microliters of each varying HIV-1 RT master mixture were adequated into 3 wells in 96 well plates on ice. The reaction was incubated at 37°C before adding 5 µl 0.2 M EDTA to stop at 40s for first well, 60 s for second well and 120 for third

wells. The completely terminated plate was incubated on ice for 30 minutes before adding 1/2,000 diluted dye solution then dye-EDTA terminated reactions mixture was pipetted to a fluorometric micro cuvette for fluorometric measurement.

7.2 Determination of the dTTP substrate dependent activity of HIV-1 RT

For determination of dTTP substrate dependent activity by using Lineweaver-Burk plotting, different the dTTP substrate concentration were used for assay. To prepared five concentrations of dTTP master mixtures, 14 µl of each stock dTTP was added into microcentrifuge tube containing 28 µl of primer/template buffer without dTTP. The five master mixtures contained dTTP which final concentrations were 6.25, 12.5, 25, 50 and 100 µM dTTP. Six microliters of each dTTP master mixture were adequate into 7 wells in 96 well plates before adding 2 µl of 30 ng/µl purified HIV-1 RT. The reaction was incubated at 37°C before adding 5 µl 0.2 M EDTA to stop at 30s for second well, 1 min for second well and 2 min for third wells until 5 min for last wells. For zero time point, reaction in the first well was stopped before incubation. The completely terminated plate was incubated on ice for 30 minutes before adding 1/2000 diluted dye solution. The dye-EDTA terminated reactions mixture was pipetted to a fluorometric micro cuvette for fluorometric measurement. The reaction rate (V) related to dTTP concentration (S) were plotted to determine K_m. The K_m of dTTP was obtained by Lineweaver-Burk plot *(*1/V versus 1/S, Y axis and X axis, respectively) and X co-ordinate showed $-1/K_m$, while Y co-ordinate showed $1/V_{max}$

8. Inhibition of HIV-1 reverse transcriptase activity

8.1 Inhibitors stock solution preparation

The dipyridodiazepinone derivatives stock preparation, the dipyridodiazepinone derivatives were dissolved in dimethyl sµlfoxide (DMSO), final concentrations were 20-30 mM. The stock solution was diluted as 100 fold by 10 mM

Tris-HCl, pH 7.4 containing 50% DMSO, final concentration was 0.3 mM stock solution.

8.2 PicoGreen-fluorometric assay HIV-1 RT activity with inhibitors

For the measurement HIV-1RT activity with inhibitors, The assay were performed by preparing master mixture of varying nevirapine, 20 µl of stock nevirapine (nevirapine in 10 mM Tris-HCl pH7.4 containing 50% DMSO) was added into microcentrifuge tube containing 40 µl of primer/template buffer. Three master mixtures contained nevirapine which final concentrations were 6.125, 12.3 and 24.6 µM. Six microliters of each varying nevirapine master mixture were aliquoted into 10 wells in 96 well plates before adding 2 µl of 30 ng/ µl purified HIV-1 RT. The control reaction without inhibitors was performed by adding 2 µl of inhibitor dilution buffer (10 mM Tris-HCl, pH 7.4 containing 50% DMSO) instead inhibitors. The assay was performed following above description.

8.3 Screening of anti-HIV agents

All compounds were compared inhibition efficiency by using 1 µM concentration and the assay was performed in 96-well plates. Eleven dipyridodiazepinone derivatives were selected for determining anti-HIV-1 RT activity. For the 7 mM stock solution, the dipyridodiazepinone derivatives were dissolved in DMSO. The stock solution was diluted by 10 mM Tris-HCl, pH 7.4 containing 50% DMSO until the diluted NNRIs concentration was 7 µM NNRTI. Two microliters of each diluted NNRTIs was added to the well. Then, 4 µl of the template/primer containing reaction were added and mixed into NNRTI in each well. After that, 2 µl of 30 ng/µl purified HIV-1 RT were added and mixed on ice. The mixtures were incubated at 37°C for 10 minutes. The reaction was stopped by 5 µl of 200 mM EDTA and incubated on ice for 30 minutes. Then, the fluorometric method was determined, percent inhibition and fold of relative inhibition compare to nevirapine were calculated following equation,

$$\text{Percent Inhibition} = \frac{(\text{Fluorescence RT activity without inhibitor} - \text{Fluorescence RT activity with inhibitor}) \times 100}{\text{Fluorescence RT activity without inhibitor}}$$

Fold of relative inhibition = Percent inhibition of compound / Percent inhibition of nevirapine

8.4 Fifty percent inhibition value determination of anti-HIV agents

Two microliters of each NNRTI were varied by two-fold serial dilution. Each well added 4 µl of the template/primer and mixed with NNRTI. 2 µl of 30 ng/µl purified HIV-1 RT were added and mixed on ice. The mixtures were incubated at 37°C for 10 minutes. The reaction was stopped by 5 µl of 200 mM EDTA and immediately incubated on ice for 30 minutes. The activity was determined by the fluorometric method. Nonlinear regression dose-response curves were plotted with percent inhibition and log inhibitor concentration.

8.5 Screening of Antiviral agent from Thai herb extract

Thai herbs were extracted by ethanol extraction and kept as ethanol extraction stock. For determine anti-HIV-1 RT activity, each ethanaol extracts were two fold-diluted with 10 mM Tris-HCl pH 7.4, 75 mM NaCl. The 2 µl of diluted solution was added to the well. Then, 4 µl of the template/primer containing reaction were added and mixed into NNRTI in each well. After that, 2 µl HIV-1 RT were added and mixed on ice. The mixtures were incubated at 37^{o}C for 10 minutes. The reaction was stopped by 5 µl of 200 mM EDTA and incubated on ice for 30 minutes. Control reaction was prepared by using 2 µl of buffer containing 50% ethanol instead of sample. The fluorometric method was determined. Percent inhibition and fold of relative inhibition were compared to nevirapine

9. Co-crystallization of HIV-1RT/inhibitors complexes

Pure recombinant HIV-1 RT was concentrated into 10 mM Tris-HCl pH 8.0, 75 mM NaCl by using Centricon C-100. The 10 mg/ml protein was used for crystallization experiment immediately, remaining protein solution were aliquoted

and kept at -20 °C for long term storage. Co-crystallization experiment was started by using 10 mg/ml protein solution that was mixed with inhibitor by 2:1 molar ratio inhibitor: protein solution. The complex solution was centrifuged 12,000 rpm for 10 minutes, clear solution was placed into new 1.5 ml centrifuged tube and was used for crystallization, The 19 solutions for crystallization experiment were selected from many previously publications, final prepared solution was filtrated by using 0.4 micron membrane filter.

9.1 Crystallization by the microbacth method

Ten microliters of 100% commercial baby oil was first pipetted into each well, then 1 µl of precipitant solution was added into the cone shaped depression well. 1 µl of protein/inhibitor mixture was pipetted into the well under an oil layer. To achieve a single drop of protein and precipitant, each well was carefully checked under a Zeiss Stemi 2000-C stereo microscope (Zeiss Corp, NJ, USA). If a single drop was not obtained, a cat whisker was used to push the separated drops together under oil. The crystallization plate was covered with the plate cover to prevent dust and debris from outside and incubated at 4°C. In these experiments, small aliquots of protein solution were taken out from 4°C and kept on ice while setting up crystallization at room temperature the plate were observed under stereo microscope every 3 days until a month.

9.2 Crystallization by the sitting drop method

The complexes solution composes of protein HIV-1 RT complexes with each inhibitor. Crystallization experiment was performed by pipette 100 µl crystallizing solution into 96 well sitting drop plate, and then pipetted 1 µl of crystallizing solution from well into sitting drop well. Following by adding 1 µl protein/inhibitor solution. Crystallizing plate was covered with clear plastic wrap and place into 4 °C incubator, the plates were observed under stereo microscope every 3 days until a month.

HIV-1 RT/Inhibitors complexes crystal screening solutions

A0 50 mM Bis tris Propane pH 6.8, 100 mM Ammonium sµlfate, 10%glycerol, 4% PEG8K

A1 50 mM Bis tris Propane pH 6.8, 100 mM Ammonium sµlfate, 10%glycerol, 8% PEG8K

A2 50 mM Bis tris Propane pH 6.8, 100 mM Ammonium sµlfate, 10%glycerol, 9% PEG8K

A3 50 mM Bis tris Propane pH 6.8, 100 mM Ammonium sµlfate, 10%glycerol, 10% PEG8K

A4 50 mM Bis tris Propane pH 6.8, 100 mM Ammonium sµlfate, 10%glycerol, 11% PEG8K

A5 50 mM Bis tris Propane pH 6.8, 100 mM Ammonium sµlfate, 10%glycerol, 12% PEG8K

A6 50 mM Bis tris Propane pH 6.4, 100 mM Ammonium sµlfate, 5%glycerol, 5% sucrose, 20 mM MgCl2, 10% PEG8K

B1 33% Ammonium sµlfate, 100 mM sodium phosphate pH 6.8

B2 34% Ammonium sµlfate, 100 mM sodium phosphate pH 6.8

B3 35% Ammonium sµlfate, 100 mM sodium phosphate pH 6.8

B4 50 mM HEPES pH7.2, 1.4 M Ammonium sµlfate, 5 mM MgCl2, 0.3 M KCl

C1 24.35 mM Citric acid, 51.5 mM Na_2HPO_4 pH5.0, PEG4K 6%

C2 24.35 mM Citric acid, 51.5 mM Na_2HPO_4 pH5.0, PEG4K 7%

C3 24.35 mM Citric acid, 51.5 mM Na_2HPO_4 pH5.0, PEG4K 8%

C4 24.35 mM Citric acid, 51.5 mM Na_2HPO_4 pH5.0, PEG4K 9%

C5 24.35 mM Citric acid, 51.5 mM Na_2HPO_4 pH5.0, PEG4K 10%

D1 50 mM Imidazole pH 6.4, 100 mM Ammonium sµlfate, 15 mM $MgSO_4$, 10% PEG8K

D2 50 mM Imidazole pH 6.4, 100 mM Ammonium sµlfate, 15 mM $MgSO_4$, 11% PEG8K

D3 50 mM Imidazole pH 6.4, 100 mM Ammonium sµlfate, 15 mM $MgSO_4$, 12% PEG8K

9.3 Crystallization by the hanging drop method

The complexes solution composed of protein HIV-1 RT complexes with each inhibitor. First, fill the grease from its tube into a 10- or 20-mL syringe. Crystallization experiment was performed by pipette 500 µl crystallizing solution into 24 well Libro plate, and then, use the syringe containing grease apply the grease

onto the elevated rim so that it will form a complete ring. To prepared crystallizing drops, pipetted 1 µl of crystallizing solution from well into 18 mm siliconized circle glass cover slips, and following with pipetted 1 µl protein/inhibitor solution into the solution drop. The cover slip containing drop was then turned so that the drop faces the reservoir and carefully pressed on the grease so that a tight seal will form and place into 4 ^{o}C incubator, the plate were observed under stereo microscope every 3 days until a month.

10. Optimization of crystal growth conditions

The solutions that appropriated for crystal growth were adjusted by varying of pH, salt concentration or percent PEG. Then, applied these solutions to crystallizing protocols.

RESULTS AND DISCUSSIONS

1. Construction of recombinant untag HIV RT plasmid with pGEX3X system

To express HIV-1 RT gene in *E. coli* under *Tac* promoter in bacterial expression plasmid, pGEX3X, The HIV-1 RT was amplified by using pairs of primers as showed in method section and HIV-1 genome cDNA library plasmid was used as DNA template. Because of HIV-1RT composing of 2 subunits, we separately cloned both DNA coding regions into bacterial vectors. There were two protocols for HIV-1 RT plasmid construction, one was co-expression of the two proteins on a single plasmid under same promoter (Hostomsky *et al*, 1992) or with its own promoter (Muller *et al.,* 1989 and 1991), and another was separately plasmid construction for two genes (Robrta *et al.,* 1993). Although, both protocols can produce heterdimeric RT, we decided to construct each gene into individual plasmid, because it was simple to manipulate and create mutant for each RT subunit. The 66F and 66R primers were used for amplify p66 subunit coding region and 66F and 51R primers were used for p51 subunit coding region. The figure 1A showed the PCR product size as 1.7 kb and 1.4 kb for HIV-1 RT p66 subunit and p51 subunit, respectively. Both PCR products were cut with appropriate restriction enzymes and purified by ethanol precipitations. To remove GST region from plasmid pGEX3X, the plasmid was cut by same enzymes and linear DNA fragment in sized 4.2 kb was separated by gel extraction from agarose gel electrophoresis. The figure 1B showed DNA fragment of 4.2 kb linear plasmid and 0.7 kb GST DNA. To ligation, both PCR product fragments were separately ligated into the plasmid instead of GST gene in pGEX3X plasmid. Each ligation mixture was individually transformed into *Escherichia coli* strain DH5α and cells harboring recombinant plasmid were selected on amplicilin-LB agar plate. Single colony was randomly picked into 3 ml amplicilin-LB media and cultured 37^{o}C over night. The plasmids DNA were extracted and detected for HIV-RT DNA by PCR using cloning primers. The figure 2 showed HIV-1 RT DNA detection for recombinant plasmid containing RT66 and RT51 gene. PCR products 1.7 kb or 1.4 kb for HIV-1 RTp66 and RTp51, respectively, were detected.

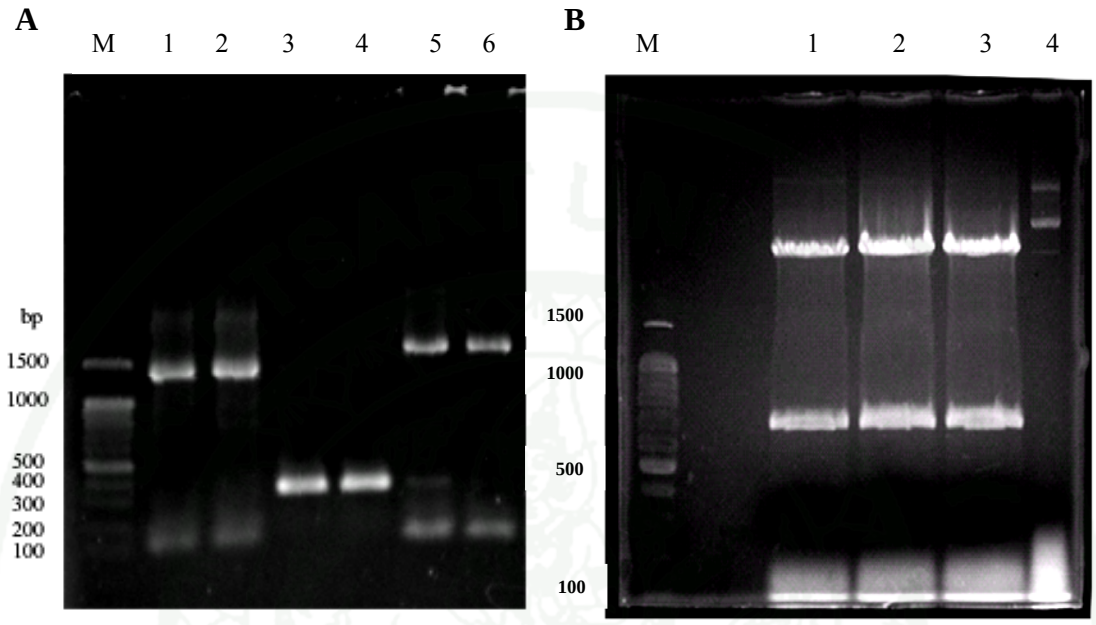

Figure 1 Gel electrophoresis of DNA fragment for recombinant plasmid construction. A, HIV-1RT DNA was amplified by PCR using specific primer, p51 DNA and p66 DNA showed 1400 bp (lane 1-2) and 1700 bp (lane 5-6), respectively. B, The pGEX3X plasmid fragment , 4200 bp (lane 1-3) was prepared by *Eco*N I and *Bam*H I, and then the GST DNA (700 bp) was removed. The digested pGEX3X plasmid was compared with undigested plasmid (Lane 4).

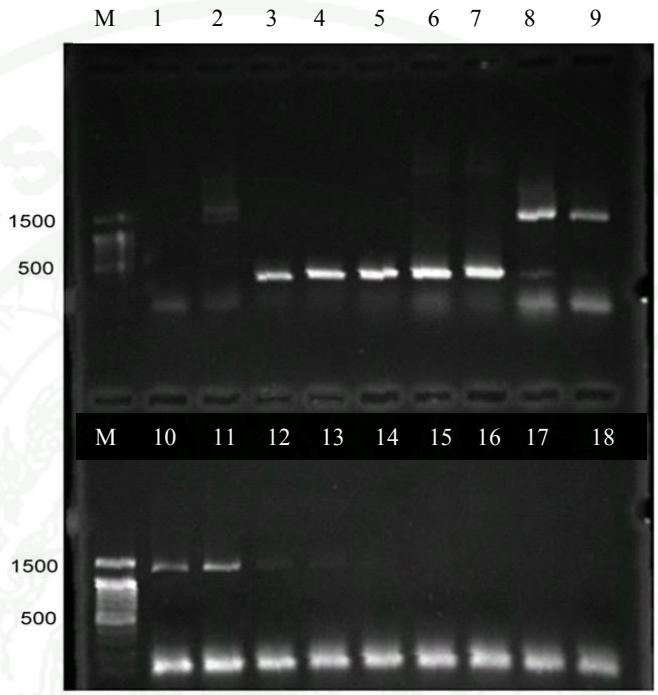

Figure 2 Gel electrophoresis of PCR products for screening the HIV-1 RT recombinant Plasmids, the PCR product shoed 1700 bp and 1400bp for positive clone of recombinant pGEXp66 (lane 8-9) and pGEXp51 plasmid (lane 10-11), respectively.

The plasmid containing RT gene was sequenced, as showed in Appendix. Because of we used own 66F primer for DNA sequencing, promoter and expression element did not show in sequencing. First 600 bp DNA peak were good enough for DNA analysis and DNA alignment showed the sequence similar to HIV-1 RT DNA template (HX2CG HIV-1RT) (figure 3). The recombinant plasmid harboring HIV-1 p66 gene and p51 gene were called, pGEXp66 and pGEXp51, respectively. Then, small scale expression was performed to confirm HIV-1RT expression plasmid (figure 4).

CLUSTAL W (1.81) multiple sequence alignment

```
HX2CGp66              CCCATTAGCCCTATTGAGACTGTACCAGTAAAATTAAAGCCAGGAATGGATGGCCCAAAA
66_1-66F.ab1_ABI      -------NNNNNNTACCCCCNNNCCCAGTAAATT--AAGCCAGGAATGGATGGCCCAAAA
51_1-66F.ab1_ABI      -NNNNCCCCNNNNNNCCCCCCNNCCCAGGTAATT--AAGCCAGGAATGGATGGCCCAAAA
                                       *    ****  ** *  ************************

HX2CGp66              GTTAAACAATGGCCATTGACAGAAGAAAAAATAAAAGCATTAGTAGAAATTTGTACAGAG
66_1-66F.ab1_ABI      GTTAAACAATGGCCATTGACAGAAGAAAAAATAAAAGCATTAGTAGAAATTTGTACAGAG
51_1-66F.ab1_ABI      GTTAAACAATGGCCATTGACAGAAGAAAAAATAAAAGCATTAGTAGAAATTTGTACAGAG
                      ************************************************************

HX2CGp66              ATGGAAAAGGAAGGGAAAATTTCAAAAATTGGGCCTGAAAATCCATACAATACTCCAGTA
66_1-66F.ab1_ABI      ATGGAAAAGGAAGGGAAAATTTCAAAAATTGGGCCTGAAAATCCATACAATACTCCAGTA
51_1-66F.ab1_ABI      ATGGAAAAGGAAGGGAAAATTTCAAAAATTGGGCCTGAAAATCCATACAATACTCCAGTA
                      ************************************************************

HX2CGp66              TTTGCCATAAAGAAAAAAGACAGTACTAAATGGAGAAAATTAGTAGATTTCAGAGAACTT
66_1-66F.ab1_ABI      TTTGCCATAAAGAAAAAAGACAGTACTAAATGGAGAAAATTAGTAGATTTCAGAGAACTT
51_1-66F.ab1_ABI      TTTGCCATAAAGAAAAAAGACAGTACTAAATGGAGAAAATTAGTAGATTTCAGAGAACTT
                      ************************************************************

HX2CGp66              AATAAGAGAACTCAAGACTTCTGGGAAGTTCAATTAGGAATACCACATCCCGCAGGGTTA
66_1-66F.ab1_ABI      AATAAGAGAACTCAAGACTTCTGGGAAGTTCAATTAGGAATACCACATCCCGCAGGGTTA
51_1-66F.ab1_ABI      AATAAGAGAACTCAAGACTTCTGGGAAGTTCAATTAGGAATACCACATCCCGCAGGGTTA
                      ************************************************************

HX2CGp66              AAAAAGAAAAAATCAGTAACAGTACTGGATGTGGGTGATGCATATTTTTCAGTTCCCTTA
66_1-66F.ab1_ABI      AAAAAGAAAAAATCAGTAACAGTACTGGATGTGGGTGATGCATATTTTTCAGTTCCCTTA
51_1-66F.ab1_ABI      AAAAAGAAAAAATCAGTAACAGTACTGGATGTGGGTGATGCATATTTTTCAGTTCCCTTA
                      ************************************************************

HX2CGp66              GATGAAGACTTCAGGAAGTATACTGCATTTACCATACCTAGTATAAACAATGAGACACCA
66_1-66F.ab1_ABI      GATGAAGACTTCAGGAAATATACTGCATTTACCATACCTTGTATAAACAATGAGACACCA
51_1-66F.ab1_ABI      GATGAAGACTTCAGGAAATATACTGCATTTACCATACCTAGTATAAACAATGAGACACCA
                      ***************** ********************* *********************

HX2CGp66              GGGATTAGATATCAGTACAATGTGCTTCCACAGGGATGGAAAGGATCACCAGCAATATTC
66_1-66F.ab1_ABI      GGGATTAGATATCAGTACAATGTGCTTCCACAGGGATGGAAAGGATCACCAGCAATATTC
51_1-66F.ab1_ABI      GGGATTAGATATCAGTACAATGTGCTTCCACAGGGATGGAAAGGATCACCAGCAATATTC
                      ************************************************************

HX2CGp66              CAAAGTAGCATGACAAAAATCTTAGAGCCTTTTAGAAAACAAAATCCAGACATAGTTATC
66_1-66F.ab1_ABI      CAAAGTAGCATGACAAAAATCTTAGAGCCTTTTAGAAAACAAAATCCAGACATAGTTATC
51_1-66F.ab1_ABI      CAAAGTAGCATGACAAAAATCTTAGAGCCTTTTAGAAAACAAAATCCAGACATAGTTATC
                      ************************************************************

HX2CGp66              TATCAATACATGGATGATTTGTATGTAGGATCTGACTTAGAAATAGGGCAGCATAGAACA
66_1-66F.ab1_ABI      TATCAATACATGGATGATTTGTATGTAGGATCTGACTTAGAAATAGGGCAGCATAGAACA
51_1-66F.ab1_ABI      TATCAATACATGGATGATTTGTATGTAGGATCTGACTTANAAATAGGGCAGCATAAAACA
                      ************************************ *************** ****

HX2CGp66              AAAATAGAGGAGCTGAGACAACATCTGTTGAGGTGGGGACTTACCACACCAGACAAAAAA
66_1-66F.ab1_ABI      AAAATAGAGGAGCTGAGACAACATCTGTTGAGGTGGGGACTTACCACACCAGACAAAAAG
51_1-66F.ab1_ABI      AAAATAGAGGAGCTGACACCACATCTGTTGAGGTGGGGACTTACCACACCAGACAAAAAA
                      *************** ** ***************************************
```

Figure 3 DNA alignment of recombinant plasmids, pGEXp66 and pGEXp51 DNA with HIV-1 RT DNA (HIVHXB2CG, accession No. K03455).

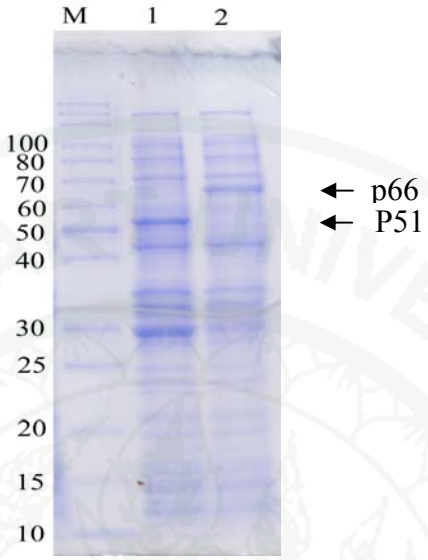

Figure 4 Recombinant HIV-1 RT p66 and p51 protein expression by *E. coli* BL21 (DE3) with 0.4 mM IPTG, 100 µl of induced cell culture was mixed with 20 µl 6X sample loading dye and then boiled for 10 min. Ten microliters of Induced cell harboring pGEXp51(lane 1) and pGEXp66 (lane 2) were loaded into SDS-PAGE.

2. Creation of RT mutant by using site-direct mutagenesis PCR based method

Since drugs resistance HIV-1 RT K103N, Y181C and double mutant K103N/Y181C cause dramatically problem for HIV-1 virus infected patient treatment. We interested in studying about these mutant enzymes. Site-direct mutagenesis PCR based method was used for create these mutant HIV-1 RT genes. Because of HIV-1 RT p66 subunit is multifunctional protein that contains polymerase and Rnase H activity, the mutation on these sites effect on RT activity. Therefore, we created mutation sites on p66 gene (pGEXp66). The plasmid pGEXp66 was used as template to create mutant HIV-1 RT gene by site-direct mutagenesis PCR based method. Each mutant primer, K103NF /K103NR and Y181CF/Y181CR, were used for PCR. Although, we can not detect mutagenesis PCR product by agarose gel, each PCR product solution was cut with *Dpn*I 37 ^{o}C 3 h and individually transformed into *E. coli* DH5α. The single colony on each amplicilin agar plate was picked into 3 ml

LB for overnight culture, and then plasmid was extracted and checked for mutant DNA by using PCR with detection primer pairs. For KNF/66R PCR products showed the expected sized of 1400 bp and YCF/66R showed about 1120 bp (figure 5). The mutant K103N and Y181C DNA were confirmed by DNA sequencing (Appendix A) and positions of mutated DNA were showed in figure 6. The mutant plasmids were called pGEXp66K103N and pGEXp66Y181C for HIV-1 RT K103N and Y181C, respectively.

To create double K103N/Y181C mutant, single mutant plasmid pGEXp66K was used as template and primers Y181CF/Y181CR was used to create double mutant by site-direct mutagenesis PCR based method. The mutant plasmid was screened by using PCR with YCF/66R primer pairs as shown in figure 7, the p66Y181C DNA was confirmed by DNA sequencing (Appendix A) and position of mutated DNA was shown in figure 8, the double mutant plasmid was called pGEXp66K103N/Y181C.

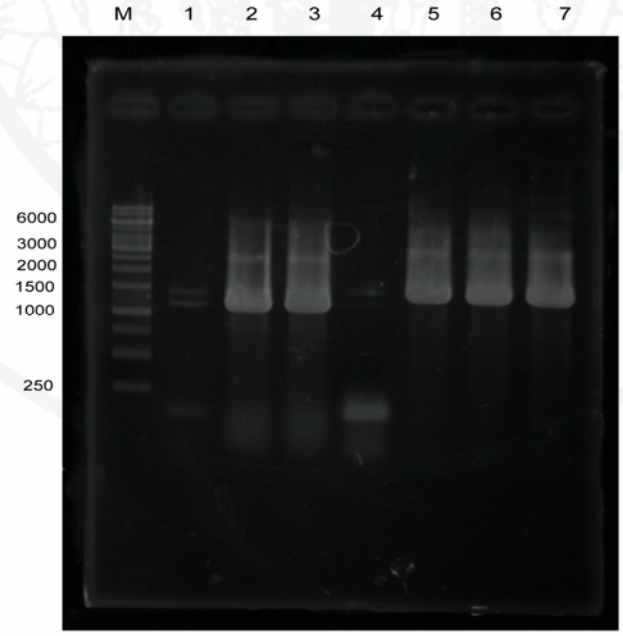

Figure 5 Gel electrophoresis of PCR screening of mutant p66K103N (lane 2 and 3) and Y181C (lane 5-7) HIV-1RT recombinant plasmid by using KNF/66R and YCF/66R primer pairs, respectively. The negative control reactions were performed by using wild-type plasmid as template for PCR with YCF/66R primer pairs (lane 1) and KNF/66R primer pairs (lane 4).

A. Wild type p66K103 (AAA)

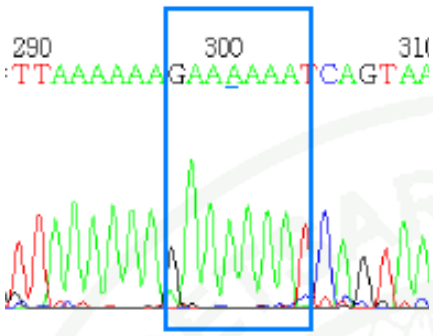

Wild type p66Y181 (TAT)

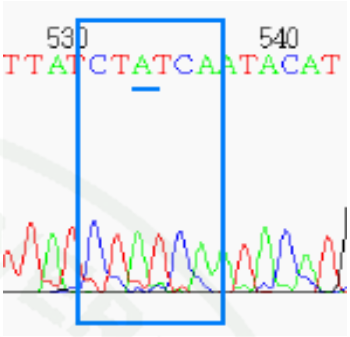

B. Mutant p66K103N (AA**C**)

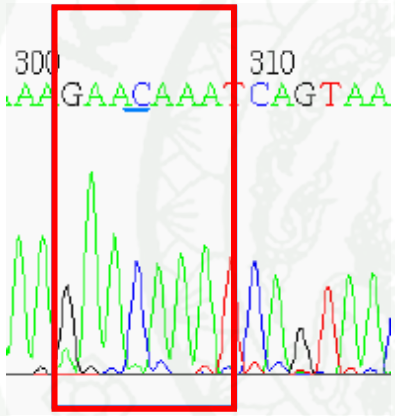

Y181 (TAT)

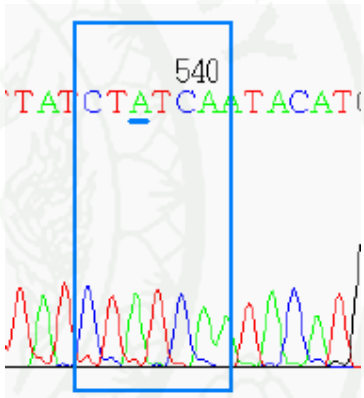

C. K103 (AAA)

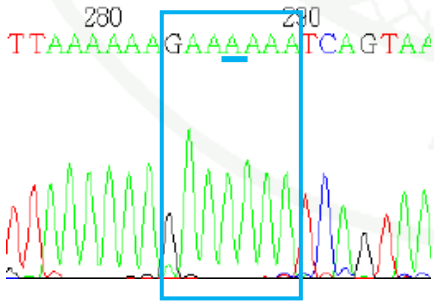

Mutant p66 Y181C **(**T**G**T**)**

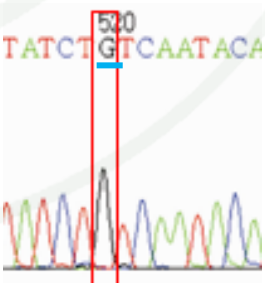

Figure 6 Position of mutant DNA showed p66K1013 N (B), p66Y181C (C) mutant compared with wild-type HIV-1RT DNA (A). The blue box indicated wild-type nucleotide, while red box indicated mutated nucleotide.

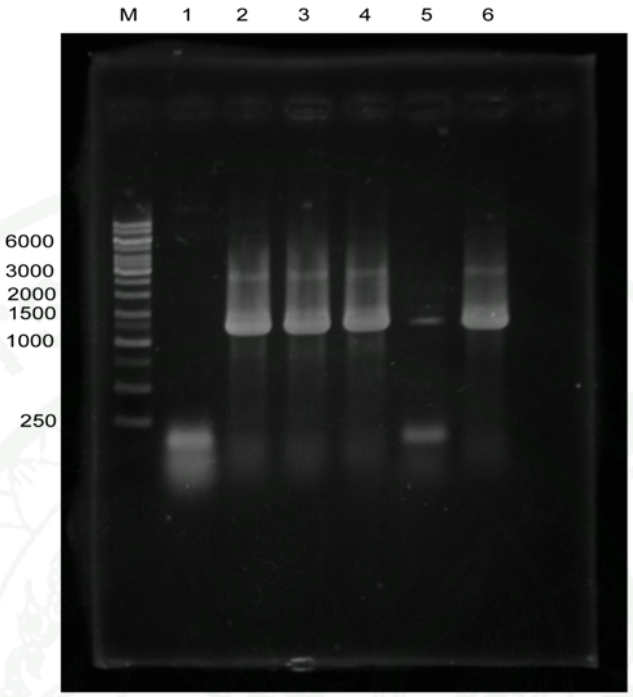

Figure 7 Gel electrophoresis of PCR screening of double mutant p66 K103N/Y181C HIV-1RT recombinant plasmid, the pGEX66KY mutant plasmid were detected the by PCR using YCF/66R primer pairs. The single colonies were randomly picked for colony PCR (lane 2-6), the wild-type plasmid was used as template for negative control reaction (lane 1).

A. Wild-type p66K103 (AAA) Wild-type p66Y181 (TAT)

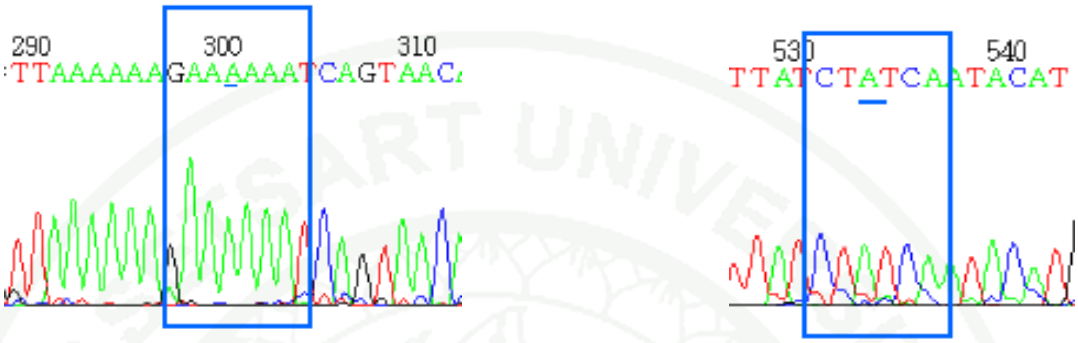

B. Mutant p66 K103N (AAC) Mutant p66Y181C (TGT)

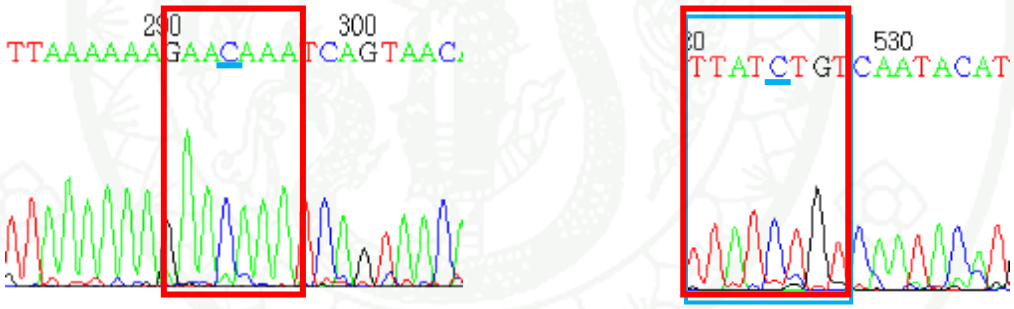

Figure 8 Position of mutant DNA showed p66 K1013 N /Y181C double mutant (B) compared with wild-type HIV-1RT DNA (A). The blue box indicated wild-type nucleotide, while red box indicated mutated nucleotide.

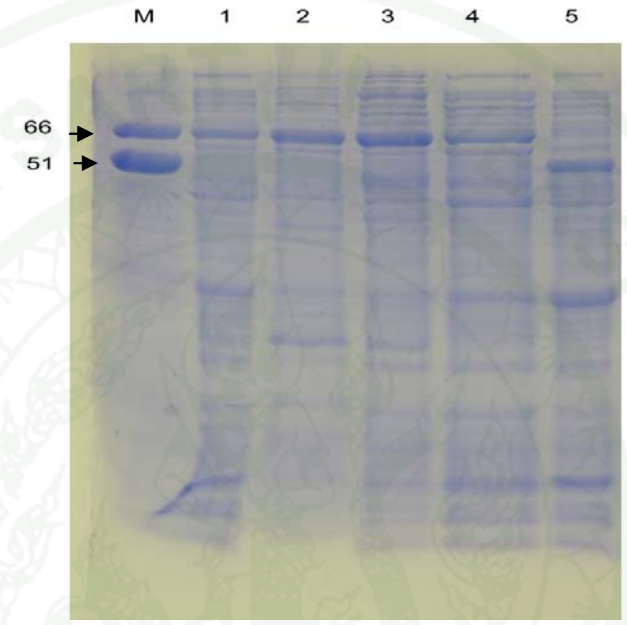

Figure 9 Expression pattern of *E. coli* BL21 (DE3) harboring mutant HIV-1 RT recombinant plasmid. The 20 µl of induced wild-type HIV-1RT pGEXp66 (lane 1), mutant K103N HIV-RT pGEXp66K (lane 2), mutant Y181C HIV-RT pGEXp66Y (lane 3), mutant K103N/Y181C HIV-RT pGEXp66KY (lane 4) and p51 subunit pGEXp51harboring cells (lane 5), were mixed with sample loading dye, then boiled and loaded into SDS-PAGE. The size of expressed protein band were compared with HIV-1RT protein marker (M).

The 3 ml overnight cell culture of mutant plasmid pGEX66K, pGEX66Y and pGEX66KY harboring cells were added with 0.4 mM IPTG for recombinant protein expression. By the small-scale expression from *E. coli* strains – BL21 (DE3), the expression of mutant plasmids was observed by using SDSP-AGE (figure 9). The major of expressed protein from mutant plasmid showed 66 kDa in size, that similar to wildtype RT p66 protein.

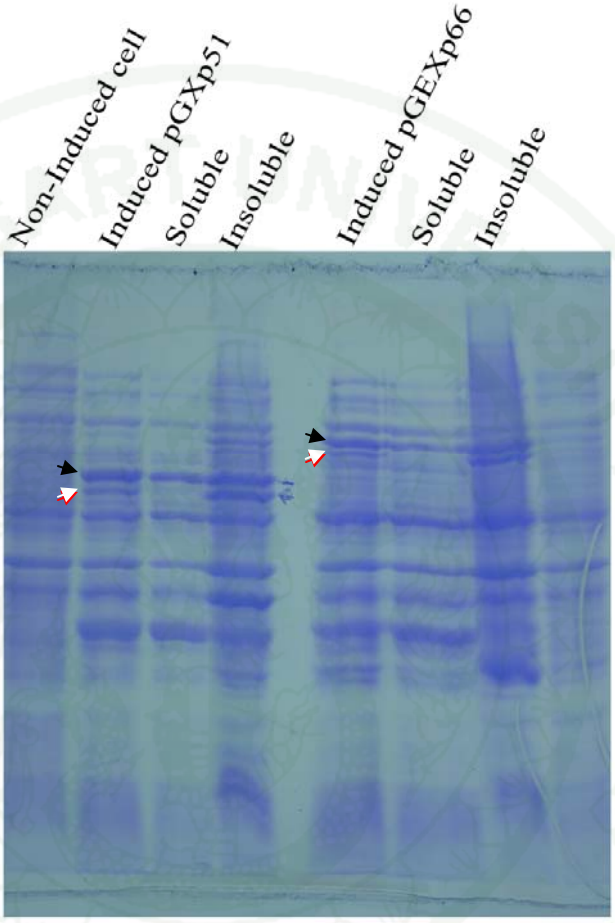

Figure 10 The recombinant HIV-1 RT plasmid expression by using 0.4 mM IPTG at 37 ^{o}C, 3 h shaking incubation. The back arrow indicated expressed protein and white arrow indicated degraded fragments.

We determined expression level of recombinant HIV-1 RT plasmid in BL21(DE3) by 0.4 mM IPTG induction at 37 ^{o}C for 3 h, the figure 10 showed that degraded protein fragment was observed for induced cell lysate both pGEXp66 and pGEXp51 cells. Although, target protein was still in soluble fraction, the results showed some p66 and p51 protein were in insoluble fraction, therefore we may some loss protein by inclusion bodies formation. For high protein recovery, we tried to reduce protein degradation and inclusion body formation by expression induction at low temperature.

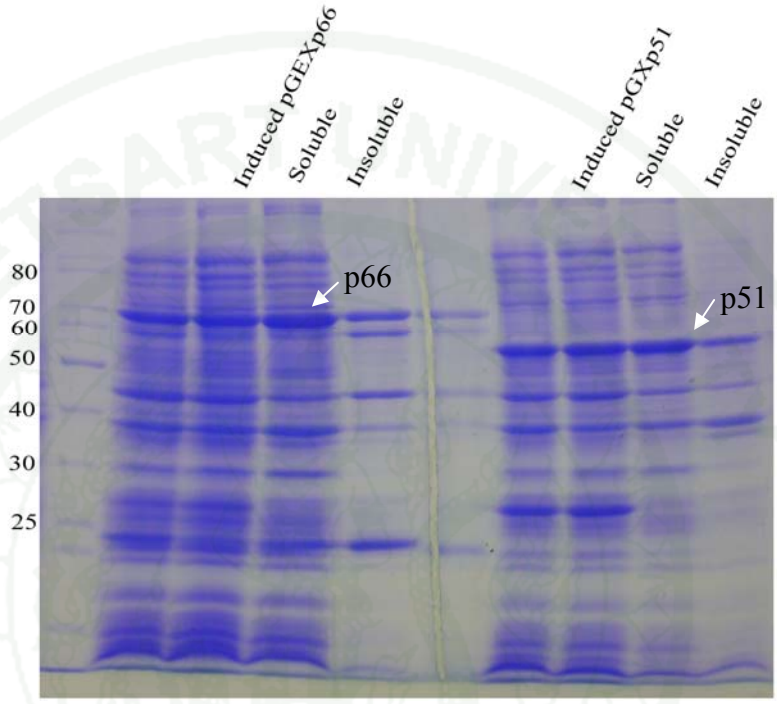

Figure 11 The recombinant HIV-1 RT expression by using 0.4mM IPTG at 20 ^{o}C, for 16 h shaking incubation. The dominant p66 and p51 protein were observed in soluble protein fractions (white arrows).

The low temperature expression of recombinant HIV-1 RT as showed in figure 11, the results that degraded fragment was decreased in induced cell lysate both pGEXp66 and pGEXp51, therefore, low temperature expression could reduce protein degradation. However, we still observed that target protein was located both soluble and insoluble fractions. Since, the inclusion bodies formation is common phenomenon for recombinant protein expression in *E. coli*, the cytoplasm where transcription and translation are tightly couple and one polypeptide was released from ribosome every 35 second this environment contain 300-400 mg/ml protein concentration (François *et al*., 2004). The small peptide can reach to native conformation by fast fold kinetic, whereas large multidomain protein often required the assistance folding modulators, therefore over expression of large multidomain recombinant often formed inclusion bodies. Since, the p66 and p51 were complex

structure and multidomain protein, over expression of these proteins in *E. coli* system might cause some protein population could not reach to native conformation. Although, we tried to decrease growth, transcription and translation rates by reducing of IPTG concentration and using low temperature induction, the inclusion bodies were still detected. However, expression at low temperature could reduce degraded protein. We used this condition for large scale expression.

3. Large scale protein expression and purification of recombinant untag wild-type HIV-1 RT

The large scale of 1 liter expression of recombinant p66/p51 was performed, the soluble protein detected by SDS-PAGE (figure 12). However, the major expression HIV-1RT was found in inclusion bodies fraction. Since, one phenomenon of the production of recombinant protein in microorganisms that often is encountered is the formation of inclusion bodies; that is, the recombinant protein aggregates in an insoluble form in the cytoplasm or periplasm. This formation of inclusion bodies can create both opportunities and problems. It has been suggested that inclusion bodies are formed from intermediates of the folding pathway, and increased growth temperature for the producing bacteria is one parameter that has been reported to promote the aggregation of recombinant protein as inclusion bodies (Strandberg *et al*., 1991). However, the mechanism behind inclusion body formation is not well understood. Early hypotheses included solubility limitations, protein size, type of promoter, and improper disulfide formation. Although, we tried to express protein at low temperature (20 ^{o}C), the inclusion bodies were still observed. However, the soluble fraction was further used for purification. The recombinant protein was purified with ammonium sulfate precipitation, anion exchange P11 and DEAE.

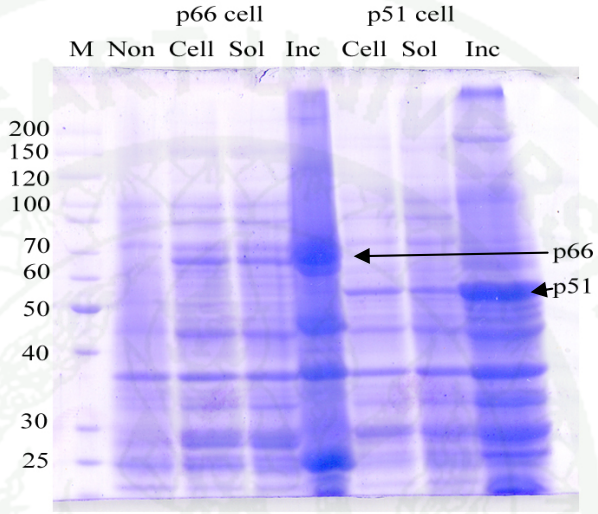

Figure 12 SDSPAGE showed xpression pattern of *E. coli* BL21 (DE3) harboring mutant HIV-1 RT recombinant plasmid, 1 L cells cultures (cells harboring pGEXp66, p66 cell and cells harboring pGEXp51, p51 cell) were induced with 0.4 mM IPTG at 20 ^{o}C for 16 h. The induced cells lysate (Cell), soluble protein fraction from cell lysate (Sol) and insoluble protein fraction from cell lysate (Inc) were compared with non-induced cells lysate (Non).

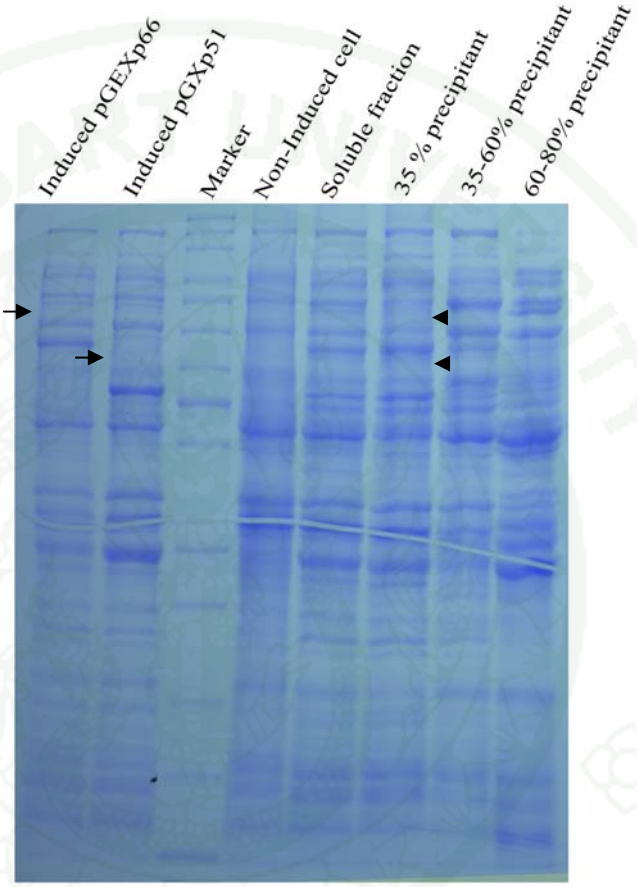

Figure 13 SDS-PAGE of ammonium sulfate precipitation fraction for untag protein HIV-1 RT (p66/p51). The soluble protein fraction from induced cells lysates were used for protein precipitation by using ammonium sulfate. The arrows indicated p66 and p51 protein, the dominant p66 and p51 protein were observed in 35% ammonium sulfate precipitate fraction.

The figure 13 showed initially purification recombinant HIV-1RT by ammonium sulfate precipitation, we used 0-35%, 35-60% and 60-80% saturated ammonium sulfate. The p66 and p51 protein band was found in 0-35% salts fraction. The ammonium sulfate precipitation is a method used to purify proteins by altering their solubility. It is a specific case of a more general technique known as salting out. Since proteins differ markedly in their solubilities at high ionic strength, salting-out is

a very useful procedure to assist in the purification of a given protein. The commonly used salt is ammonium sulfate, which has no adverse effects upon enzyme activity. In addition, pH of solution effect on protein- ammonium sulfate precipitation. Since, SO_4^{2-} ion interact with protein surface, the plus net charge protein cause good interact with SO_4^{2-} ion, therefore, the best precipitation pH must be lower than protein pI. The HIV-1RT pI approximated 8.5, therefore we used solution pH 7.5 for ammonium sulfate precipitation.

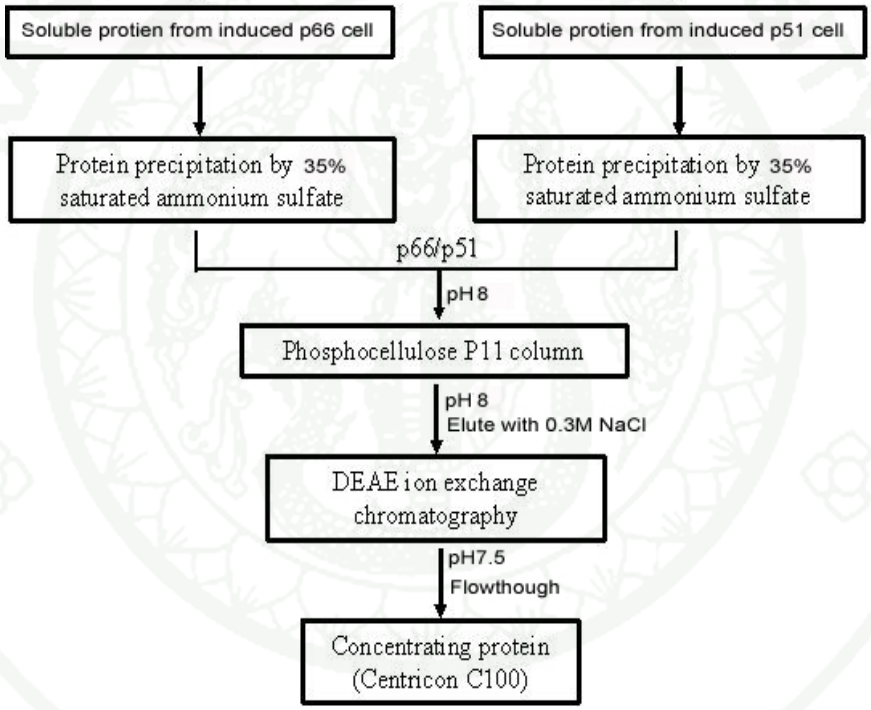

Figure 14 Purification protocol for untag protein HIV-1RT (p66/p51). The induced recombinant cells were lysed by sonication at pH7.5, and then protein was precipitated with ammonium sulfate. Final, protein fraction was dialyzed and further purified by ion exchange column.

Following our protocol (figure 14), the 35 % ammonium sulfate precipitate was dissolved, dialyzed and further purified by column chromatography. Since HIV-1 RT exhibited DNA/RNA binding property, many publications used ssDNA cellulose column for early step. The P11 cellulose phosphate contained the phosphate group as a ligand similar to DNA/RNA backbone. Therefore, DNA/RNA binding

protein could bind to this column resin. The subunit p66 and p51 HIV-1RT was detected from eluted fraction. Most contaminated proteins were removed from HIV-1 RT protein fraction but p51 protein band showed higher amount than p66 protein band and then the fraction was further purified with DEAE. Since, pI of HIV-1RT were 8.5, 8.5 and 8.8 for p51, p66 monomer and p66/p51 heterdimer, respectively. At this pH 7.5, the HIV-1 RT flowed through from the anion exchange DEAE column and the pure protein with equal band protein of p51 and p66 was observed in this fraction (figure 15). By using these purification protocols, we were able to prepare approximately 2 mg of the heterodimeric forms of RT from 1 liter of *E. coli* culture. The protein yield was lower than that from previously reported (6-10 mg) (Hou *et al*., 2004), which may be due to the multiple purification steps. However, the homogeneity and purity of the recombinant HIV-1 RT are the most important issue since the RT will be used for further kinetics study and X-ray crystallography.

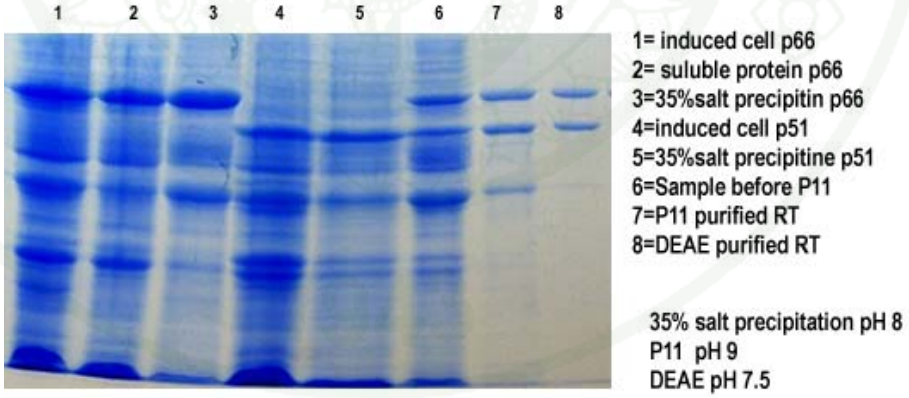

Figure 15 SDS-PAGE of recombinant wild-type HIV-1 RT in purification steps.

Table 1 Specific activity determination of HIV-1RT form purification

Fraction	Total protein (mg)	Fluorescence (Intensity)	Specific activity[1] (Intensity mg^{-1})	Purification[2] fold
Cell lysate	61.9	63.56	1.03	1.00
Soluble fraction	60.2	243.81	4.05	3.93
Ammonium sulfate precipitate	28.59	200.89	7.03	6.83
P11phosphate column	7.75	100.09	12.91	12.53
DEAE column	1.9	190.55	100.29	97.37

[1]Specific activity = Fluorescence Intensity/Total protein (mg)

[2]Purification fold = Specific activity of further purification/ Specific activity of cell lysate

We used EnzCheck assay kit (Molecular probe, E-22064) to determine recombinant HIV-1 RT activity, this assay based on fluorescence method using PicoGreen, a compounds specifically interacts with product of RT reaction. The previously report showed that fluorescence method using DAPI-fluorescence dye, can determine recombinant RT activity from bacterial crude extract (Chavan *et. al.,* 1995). These DAPI-fluorescence dye and PicoGreen are a member of cyanin dye that specific binds to the double strand polynucleotide, therefore, we can used PicoGreen to measure the activity of our recombinant HIV-1 RT for each purification step. Although, EnzCheck assay kit does not use for this propose, we can apply this method for our study. The RT specific activity increased related to RT purity (Table 1). However, the pure RT was recovered with 2 mg per 1 L cell culture, it may not enough for further experiment. The expression of HIV-1 RT using bacterial system had been first reported in 1987 (Larder *et al*., 1987), many purification protocols were improved, for example, single step purification using HPLC (Fletcher *et al*., 1996), two steps using metal-binding column with His-tag (Stuart *et al*., 1990 and Maier *et*

al., 1999), but the purification yield and the effect of fusion-tagRT on protein kinetic activity are not satisfactorily obtained. Although, our protocol can produce pure protein enough for activity and kinetic assay, but it was not enough for protein crystallization. In addition, heterdimeric form was not confirmed by size exclusion column chromatography. We tried to construct fusion his-tag p51/p66 protein.

4. Construction of recombinant 6x histag HIV RT plasmid with pET system

Highly expression with pET system was reported for a long time. Many publications used this system for recombinant HIV-1RT expression. The histidine tag orientation was discussed, fusion tag on C or N –terminal had an effect on protein folding and purification (Hammarström *et al*., 2006). Following Stuart 1989 (Stuart *et al*., 1989), the high protein yield and purity was performed by tagging C-terminal of p51 with six histidines. Heterdimeric form was indicated by two subunits (histag-p51/untag-p66) were eluted together with Ni^{2+}-NTA column. For high expression of HIV-1RT by pET system, the p51 gene was subcloned to pET33B. Using primers p51F and p51Rhis to amplify *p51* gene from pGEX51 plasmid, the PCR products of approximately 1.4 kb (figure 16) was purified with ethanol precipitation and restriction with *Nco* I and *Bam*H I, and then cloned into plasmid pET33B which was cut with same enzymes. The ligation mixture was transformed into *Escherichia coli* strain DH5α and cells harboring recombinant plasmid were selected on kanamycin-LB agar plate. Single colony was random picked into 3 ml LB media and cultured 37 ^{o}C over night.

The plasmids DNA were extracted and detected for HIV-1 RT DNA by PCR using cloning primers. The figure 17 showed HIV-1 RT p51 DNA detection for recombinant plasmid containing RT51 gene. PCR products, 1.4 kb (lane 6, 8 and 9), were detected and the RT sequences were confirmed by DNA sequencing (Appendix A). The recombinant pET33B-51his was used for expressed p51 protein with C-terminal 6xhis tag, under T7 promoter.

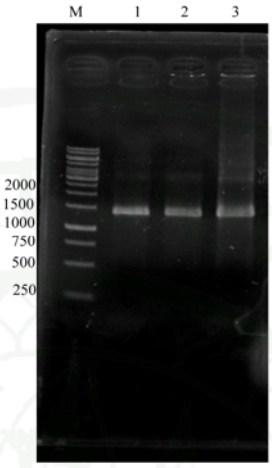

Figure 16 Gel electrophoresis of PCR product amplified HIV-1 RT p51 DNA by using p51F and p51Rhis primer pair, expected sizes of p51 (1.4 Kb) dominant appeared in agar gel electrophoresis (lane 1-3). The PCR product was used for recombinant pETp51 plasmid construction.

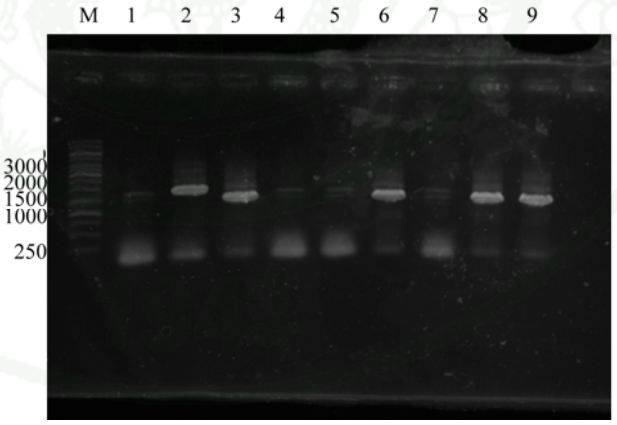

Figure 17 Gel electrophoresis of recombinant p51 histag plasmids screening by using PCR using p51F and p51Rhis primer pair. The negative control reaction was using of pET33B as DNA template (lane 1), while the size of p66 DNA (lane 2) and p51 DNA (lane3) were used for determining positive cloned. The Randomly picked colonies were screened by colony PCR (lane 4-9).

The pET system contains a high selectivity T7 RNA polymerase for its cognate promoter (Novagen, 2002). In the pET system, the protein coding sequence of interest is cloned to downstream of the T7 promoter and then transformed into *E. coli* strain BL21 DE3. Protein expression was achieved by IPTG induction of a chromosoally integrated cassette in which the T7 RNA polymerase was expressed from the lacUV5 promoter and then polymerase would be specific binding to T7 promoter in expression vector. Next, host RNA polymerase would be transcripted by the highly activity, together with high efficiency translation and target protein was the majority of the cellular protein after a few hours. We compared expression level form pGEX system and pET system.

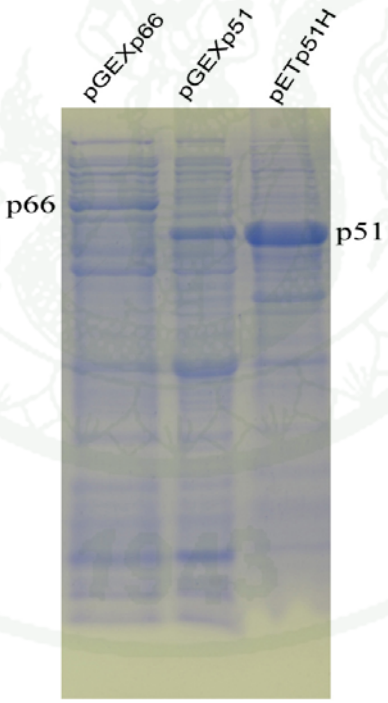

Figure 18 SDS-PAGE of expression of recombinant RT pGEXp66, RT pGEXp51 and pETp51H, 100 µl of induced cell culture was mixed with 20 µl 6X sample loading dye and then boiled for 10 min or until appearing of clear blue color solution. Ten microliters of sample was loaded into SDS-PAGE. The higher expression level of p51 protein was detected for pET system.

The recombinant plasmid pETp51H was transformed into *E coli* BL21 (DE3) and cultured 37 ^{o}C overnight in LB media containing 50 µg/ml kanamycin. Then, small scale RT expression was induced by adding 0.4 mM IPTG into recombinant *E coli* culture, 37 ^{o}C. 100 ul of 3 h-induced cell was used for expression pattern determination, the whole cell protein was determined by SDS-PAGE, and the higher expression of pET system was confirmed by SDS- PAGE compared with pGEXp51 (figure 18). Since, pET and pGEX system were different in promoter region, which effected to expression level of recombinant protein. The pGEX system under controlled with *Tac* promoter, this promoter is a hybrid *trp-lac* promoter that is regulated by *lac* repressor. Normally, two domains upstream of the start site of transcription have been identified for which a consensus sequence has been formulated. These domains are the -35 sequence (5'-TT- G-A-C-A) and the Pribnow box (5'-T-A-T-A-A-T) in the' -10 region. The *tac* promoter was created by replacing its -35 region of lac UV5 with the -35 region of the stronger trp promoter (Herman *et al*., 1993). This promoter is chemically induced by the addition of isopropylthio-β- D-galactosidase (IPTG) similar to pET system.

The pET system was controlled by *T7* promotor which suitably binding for T7 RNA polymerase. By using BL21 (DE3) for expression host, this host was modified by Novagen to produce large amount of recombinant protein by using T7 RNA polymerase and it specifically bind to T7 promoter in pET vector. Since, we used pET 33b for HIV-1 RT p51 protein expression, the expression was driven under T7 promoter, and therefore, the expression level of our target gene was more than pGEX system.

5. Large scale protein Expression and purification of recombinant 6Xhigtag HIV-1 RT

Due to high expression of pET vector, the 0.5 liter pET33B-p51 expressed cell culture was mixed to 1 liter pGEX66 expressed cell culture, the expressed recombinant His6-tagged p51/p66 wild type HIV-RT was purified by using DEAE, P11 and Ni-NTA column chromatography. The HIV-1 protein flowed though from

DEAE column at pH 7.5, and then the fraction was further purified with P11 cellulose phosphate column. By DNA/RNA binding protein property of HIV-1RT, the active fraction was detected from eluted fraction. The figure 19 showed that most of contaminated protein was removed from HIV-1 RT protein fraction. By optimized condition from wild type HIV-1 RT purification, the protocol was applied for all mutant protein purification (figure 20).

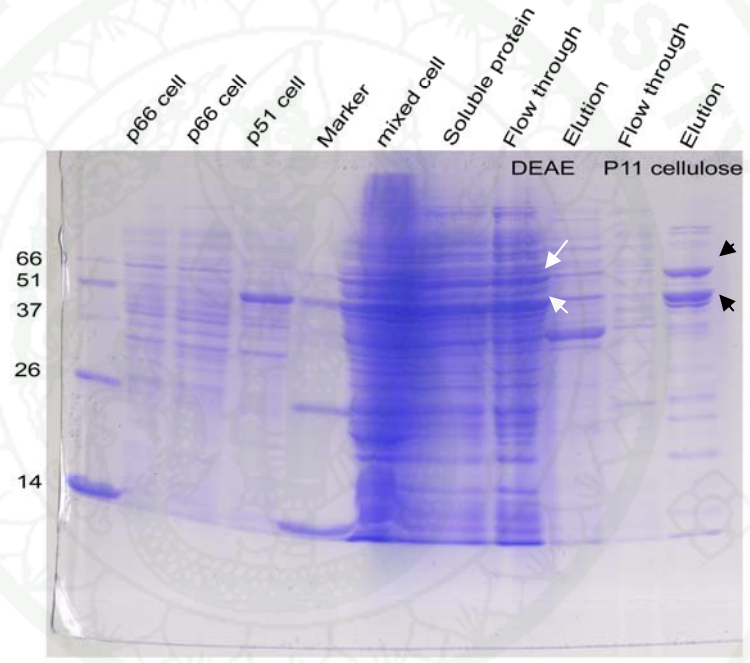

Figure 19 The wild type HIV-1RT purified by DEAE and P11 cellulose Phosphate column. The both induced cells (p66 cell and p51 cell) were mixed together (mixed cell) and lysed by sonication, the soluble protein fraction (soluble protein) was loaded into DEAE column. The HIV-1 p66 and p51 were detected from flow through (white arrow), then this fraction was loaded into phosphor cellulose P11 column. The p66 and p51 were observed from eluted fraction (black arrow).

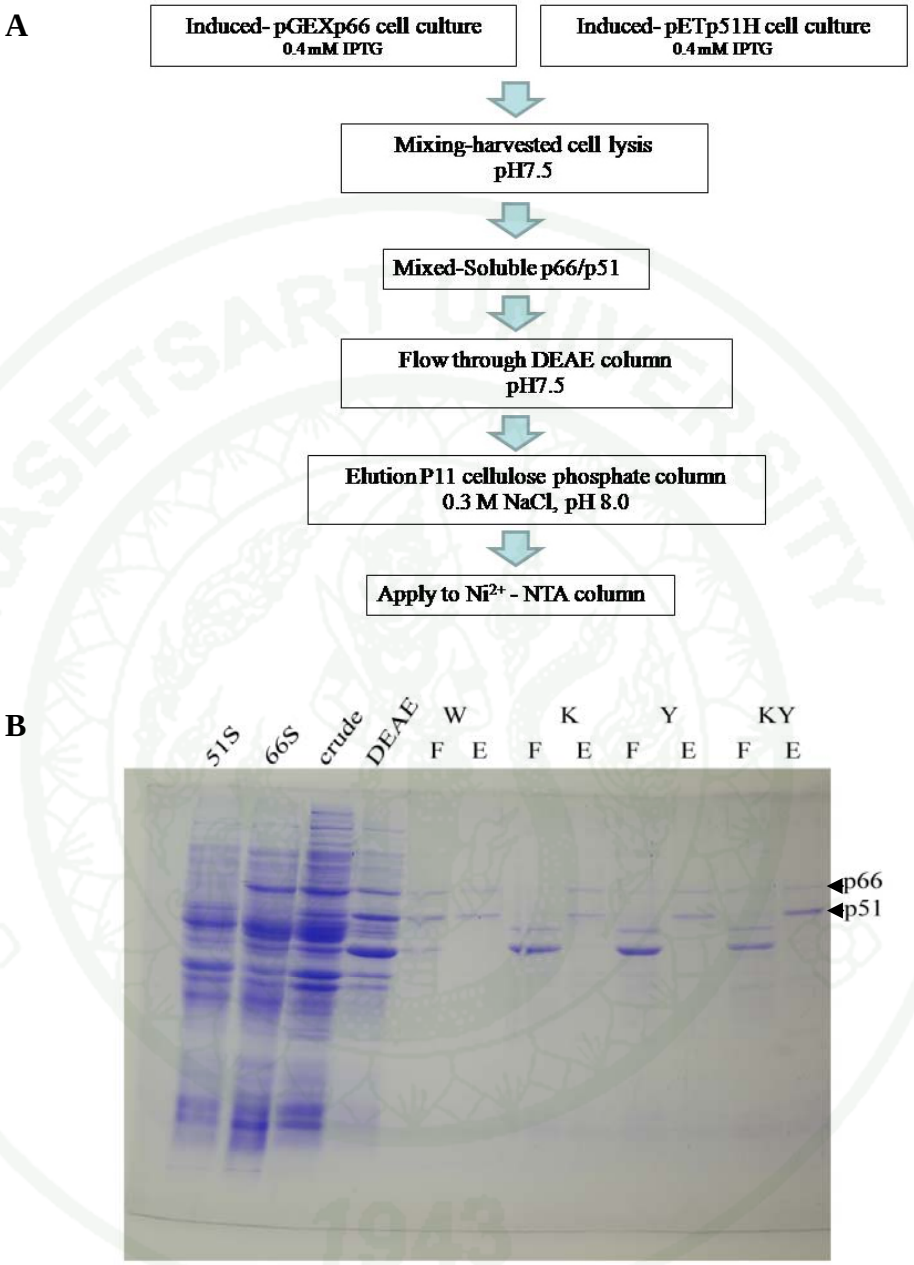

Figure 20 The SDS-PAGE of histag HIV-1 RT purification. (A) the purification protocol and (B) showed the wild type ($p66^{wt}/p51^{wt}$) and mutant HIV-1RT (K; $p66^{K103N}/p51^{wt}$, Y; $p66^{Y181C}/p51^{wt}$, KY; $p66^{K103N/Y181C}/p51^{wt}$)were purified by DEAE and P11 cellulose phosphate column before Ni^{2+} - NTA column (F; flow though fraction, E; eluted fraction).

Although, we got new plasmid construction, pET51H, that contained 6 x Histag fusion protein, p51-histag. We tried to use single step purify p66/p51histag RT by using Ni^{2+} - NTA affinity column. However, single step protocol could not purify our RT, there were many impurity protiens from host cell lysates. Therefore, we tried to remove other impurities protein by using ion exchange column chromatography in early purification step. The figure 30 showed that most *E. coli* proteins were removed by using DEAE and phosphor cellulose P11 column. Then, HIV-1 RT was purified by the AKTA Purification System which had Ni^{2+} -NTA column, the purification profile showed 2 elution peaks (figure 21). The highly pure protein with equal band protein of p51 and p66 was observed by using gradient elution of imidazole, while excess p51 was remove by 250 mM imidazole elution. Following this purification results, recombinant HIV-1RT compose of 6xhistag p51 and untag p66, therefore the equal protein band of pure HIV-1 RT indicated heterodimeric protein of HIV-1RT.

For mutant HIV-1RT purification, *E. coli* BL21 (DE3) harboring mutant plasmids were cultured and induced for protein production. Following wild type purification protocol, each mutant pGEXp66 expressed cell was mixed with pET33B-p51h expressed cell and further purified following untag purification protocol. The results were similar to wild type RT purification profile; there were two protein peaks as showed in figure 22 and 23. After concentrated by using centricon with 100 kDa filter membrane, the highly pure heterdimeric HIV-1 RT (>95% by coomasieblue stain, Appendix C) were observed with SDS-PAGE for both wild type and mutant HIV-1RT (figure 24).

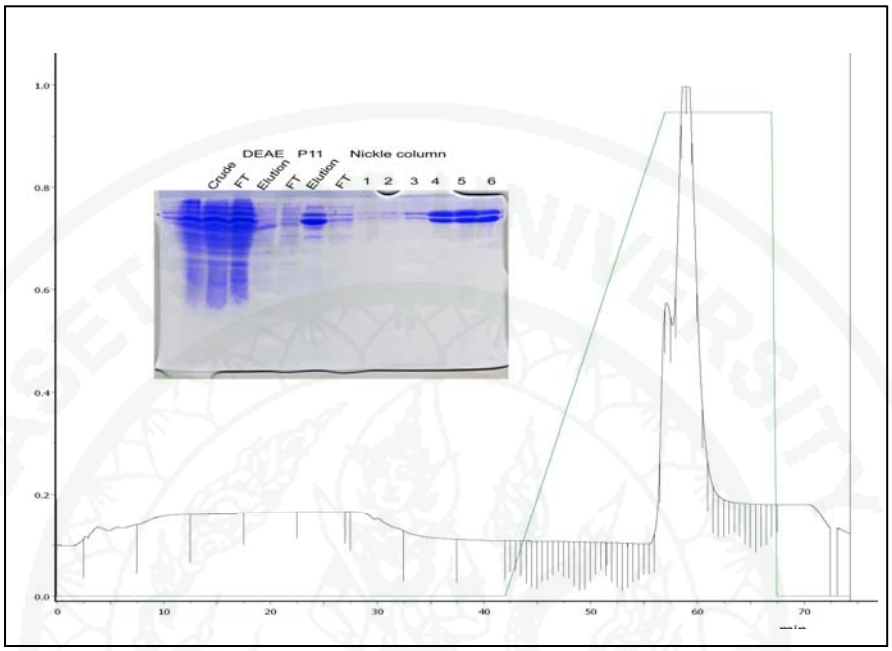

Figure 21 SDS-PAGE and chromatogram of Ni^{2+} -NTA column purification profiles for wild type HIV-1 RT ($p66^{wt}/p51^{wt}$).

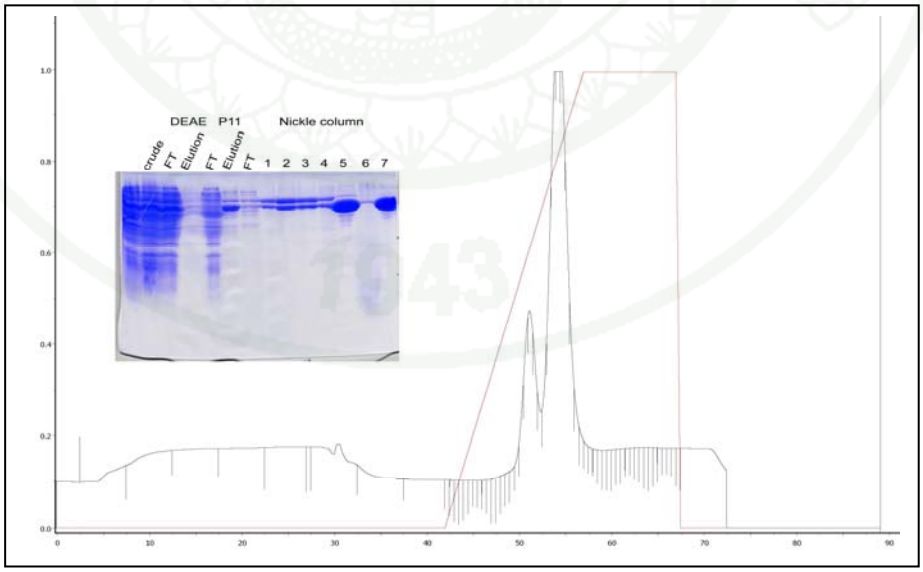

Figure 22 SDS-PAGE and chromatogram Ni^{2+} -NTA column purification profile for K103N HIV-1RT ($p66^{K103N}/p51^{wt}$).

A

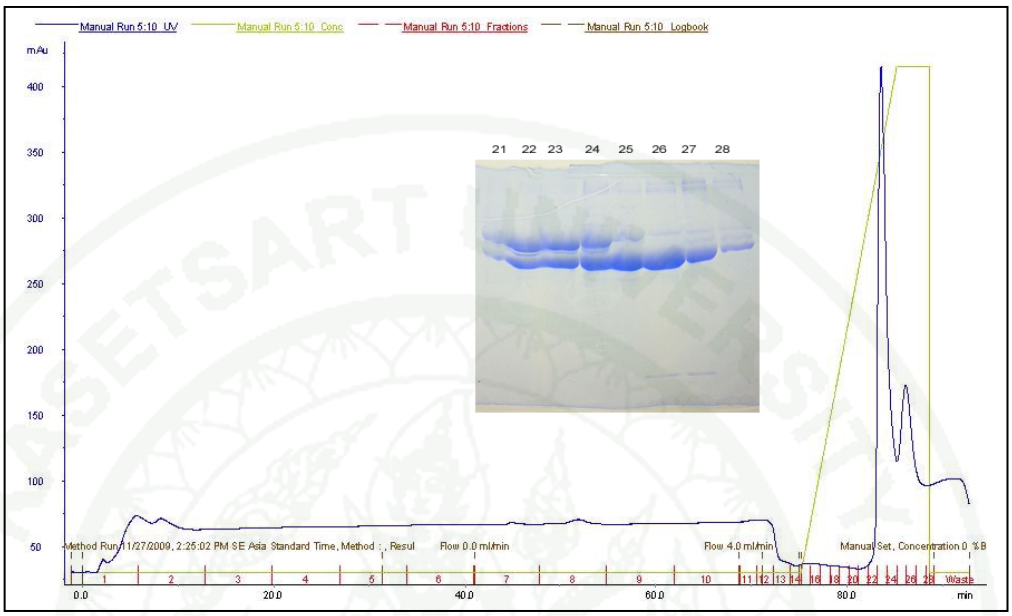

B

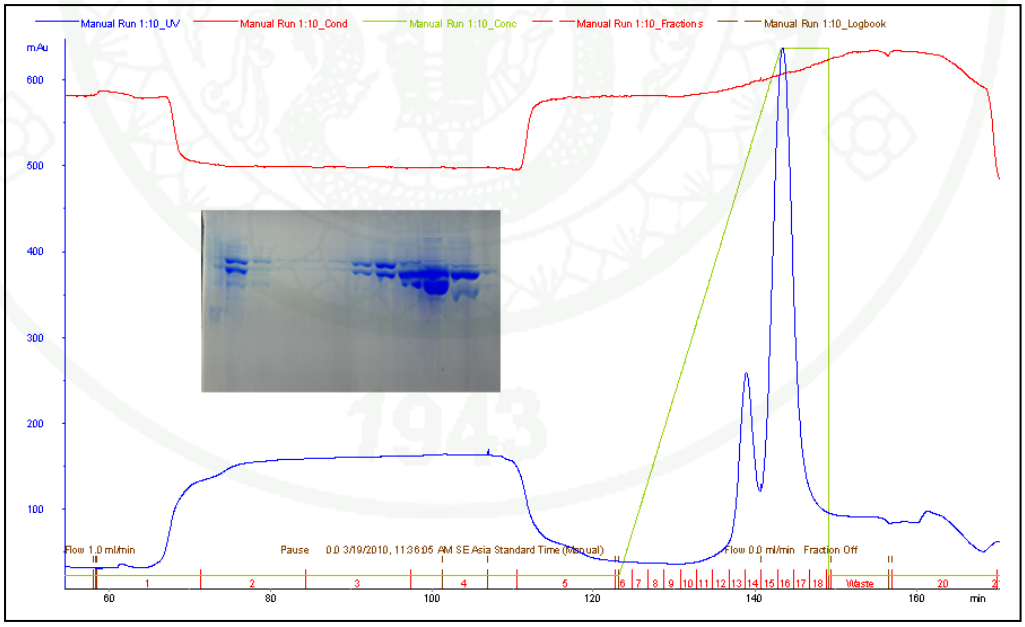

Figure 23 SDS-PAGE and chromatogram of Ni^{2+} -NTA column purification profile for HIV-1 RT. (A) Y181C ($p66^{Y18C1}/p51^{wt}$) and (B) double mutant K103N/Y181C ($p66^{K103N/Y181C}/p51^{wt}$).

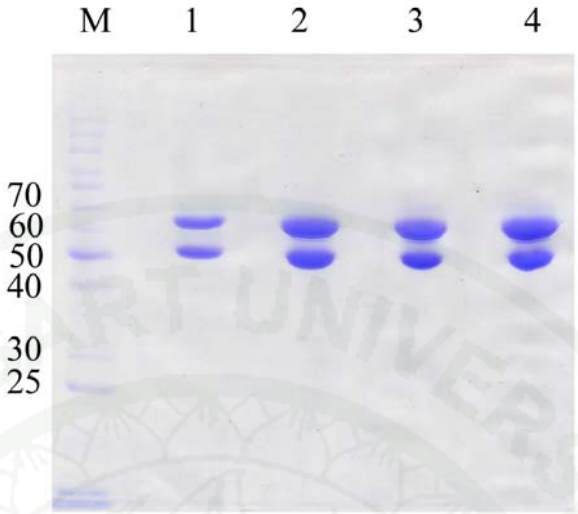

Figure 24 SDS-PAGE of final purified HIV-1 RT which concentrated by using Centricon -100. The comparing to protein marker (M), the heterodimeric protein of mutant Y181C HIV-1 RT (lane 1; $p66^{Y18C1}$/ $p51^{wt}$), mutant K103N HIV-1 RT (lane 2; $p66^{K103N}$/$p51^{wt}$) , mutant K103N/Y181C HIV-1 RT (lane 3; $p66^{K103N/Y181C}$/$p51^{wt}$) and wildtype HIV-1 RT (lane 4; $p66^{wt}$/ $p51^{wt}$) showed expected sizes of 66 and 51 kDa.

6. Fluorometric Assay of HIV-1 RT activity

6.1 Determine sensitivity of PicoGreen method

Although conventional isotropic method for HIV-1 RT activity determination is highly sensitivity, there are some significant disadvantages that limit their utility (Seville *et al*., 1996). The isotropic assay experiment have to be premised for radioactivity, this method is labor-intensive and time consuming procedures, disposal of large quantities of radioactive materials have to be good managed, and there are many error since the assay are complex that involved step wherein DNA/RNA precipitated or bound to filter wash free radioactive label substrates. To avoid the limitation of isotopic method, we applied a fluorescence dye, PicoGreen, for the determination of recombinant HIV-1 RT activity. PicoGreen can interact with

heteroduplex DNA/RNA with high sensitive activity as previously described (Singer *et al.,* 1997). Therefore, a little amount of double stand appearing in reaction can be detected with PicoGreen. Although, real-time assay with PicoGreen was reported for Polymerase III (Seville, *et al.,*1996) , the real-time assay of PicoGreen to RT activity could not be determined the increasing fluorometric signals as shown in figure 25A. This may due to the PicoGreen can competitively interact with RT causing the undetectable HIV-1 RT activity. Therefore we adopt the standard protocol to use the stop time point assay by stop the reaction at different times before adding the PicoGreen in the reaction mixtures. With this method, the fluorometric intensities could gain back the increasing of intensity making an accurate measure of kinetic properties of RT. However, with this method, it needed more PicoGreen for getting the rate of enzyme in each reaction. Therefore we checked the sensitivity of PicoGreen in the lower amount than recommendation in the assay kit instruction. The RT activity detection was performed with four dilutions, 1/400, 1/1000, 1/2000 and 1/4000 of stock PicoGreen dye in TE buffer and enzyme activity was detected at 0, 1, 3 and 5 minutes by using stop time point method. The similarity of RT activity detection with 1/400, 1/1000, 1/2000 diluted dye were shown in figure 25B, these results indicated the 1/2000 dilution appropriated to detect polymerizing products. The RT substrate amount and reaction volume we used in this paper were less than previous report with the fluorescence method.

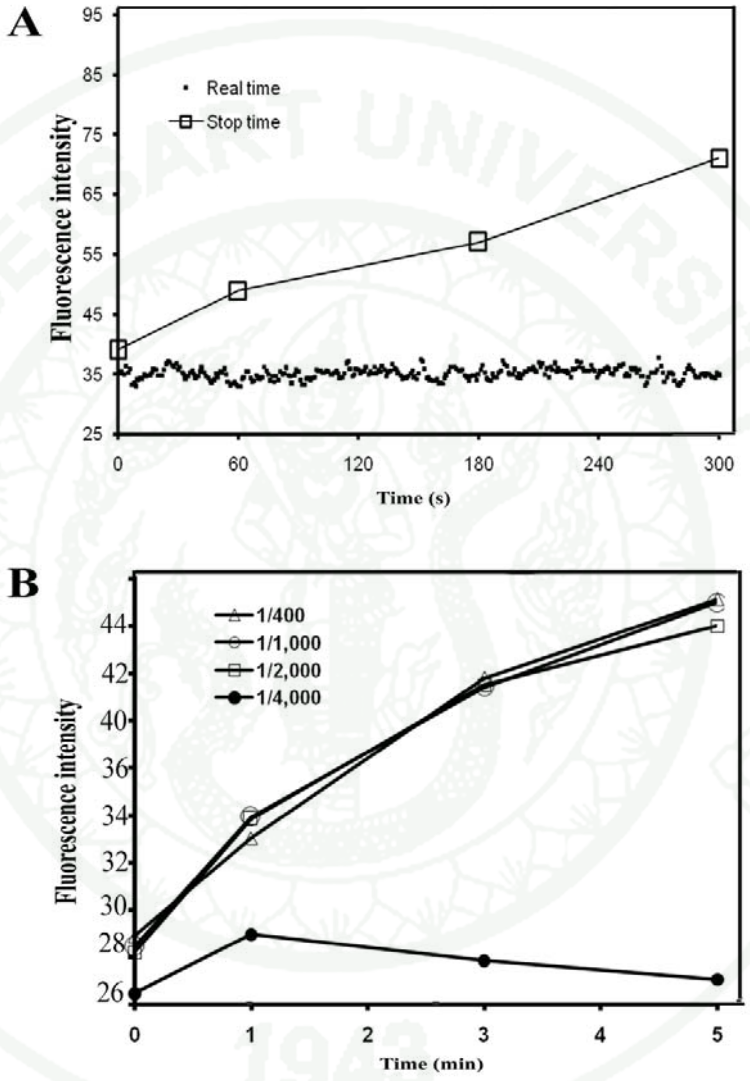

Figure 25 Sensitivity of Picogreenfluorescence methods. (A) comparation of Real-time(■) and stop-time point (□) assay by using PicoGreen-fluorometric method Determines HIV-1RT activity, the Real-time assay showed inhibitory effect on HIV-RT activity.PicoGreen-fluorometric method determines HIV-1RT activity.(B) the appropriated dye dilution determining for RT activity measurement.

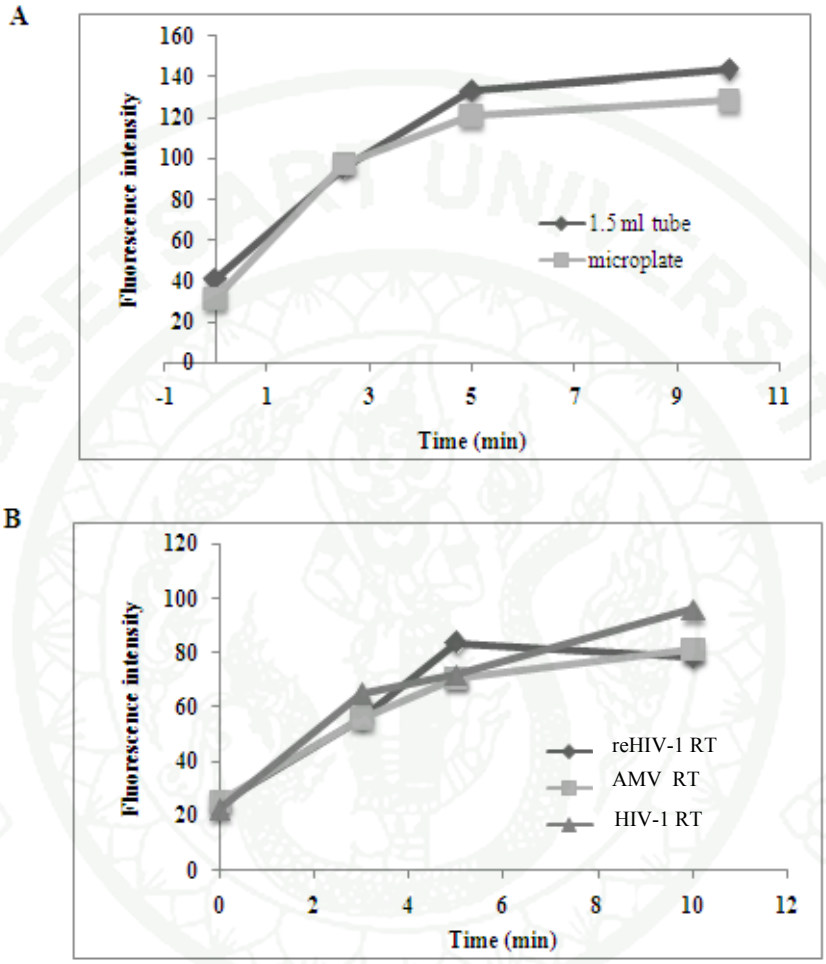

Figure 26 RT activity determinations by using PicoGreen-fluoroscopic method. (A) comparison of recombinant HIV-1RT activity between 1.5 ml tube assay and microplate assay. (B) comparison of microplate assay activity between recombinant HIV-1 RT (reHIV-1 RT) and commercial RT (AMV-RT and HIV-1 RT).

The early assay experiment, the reaction were performed in 1.5 ml micro centrifuge tube with 20-25 µl reaction volume, that consisted of 5 µl RT and 20-25 µl reaction buffer. We tried to extend amount of assay reaction by decreasing reaction

volume, 5 µl in 1.5 ml micro centrifuge tube or micro plate that composed of 1-2 µl RT and 4-5 µl reaction buffer. The 1/2000 diluted PicoGreen solution was used for measure RT reaction product, the fluorescence intensity was determined with excitation of 502 and emission of 523 nm. The figure 26A showed that RT activity increased as incubation time increasing; the activity assay by using micro plate was similar to activity assay by 1.5 ml micro centrifuge tube assay. Therefore, small volume reaction can be used for RT activity determination in micro plate.

Then, we used small volume reaction assay and compared recombinant RT activity with commercial enzyme including HIV-1 RT and AMV RT. The figure 26B showed fluorescence intensity increasing related to longer incubation time, this results indicated that recombinant HIV-1 RT contain RT activities similar to other RT. Therefore, our purification protocol can be used for recombinant HIV-1 RT.

Since, fluorescence dye can be used for detect small amount of DNA or RNA, many publication used PicoGreen to detect amount of dsDNA or PCR product, based upon these properties, several cyanines have been successfully used in a range of applications, including DNA detection and quantification, DNA fragment sizing, DNA damage detection, real-time polymerase chain reaction, detection of hybridization of single strands, and detection or measurement of biological activity. In addition they tried to apply fluorescence dye to measure enzyme activity, especially polynucleotide polymerizing and hydrolyzing enzyme. The PicoGreen-fluorescence dye was applied to measure DNase I activity, this enzyme hydrolyzed DNA caused decreasing of fluorescence intensity whth longer incubation time (Tolun *et al.,* 2003). The previously report showed highly sensitivity of PicoGreen. This sensitivity is 400 fold greater than that achieved with Hoechst 33258 (10 ng/ml), 20-fold greater than that achieved with YOYO-1 (0.5 ng/ml), and 100-fold greater than that achieved with YO-PRO (2.5 ng/ml) (singer *et al.,* 1997). Although, our method used 1/2000 PicoGreen dilution, the final dye concentration can not calculated since no reporting in PicoGreen instruction (stock 400x). However, previously publications reported that the dye greatest sensitivity and widest dynamic range were obtained when the PicoGreen agent was present at a final concentration of 0.8 mM in the assay mixture.

Because of highly selectivity of PicoGreen to double strand polynucleotides, many publications tried to expand dye-polynucleotide interaction mechanism. The mode of binding of PicoGreen reagent is not known, no one report for PicoGreen mechanism. However, Victoria L 1997 reported PicoGreen properties ; (a) its fluorescence is not very base-selective but shows some conformation dependence, (b) its fluorescence is sensitive to salt (particularly divalent cations) and ionic detergents, and (c) it binds heparin with some fluorescence enhancement PicoGreen dye may intercalate and may have surface or groove interactions as well.

By simulation experiment showed that the preference for association involving the quinoline ring is also consistent with the limited restriction of the rotation around the B–D double bond (figure 27) (Mikelsons *et al.,* 2005). Although, PicoGreen effectively intercalates into both ssDNA and dsDNA, the effects of high dye concentrations indicate that the dimers observed in CD spectra are responsible for the energy transfer or self-quenching decay observed in fluorescence time-resolved studies.

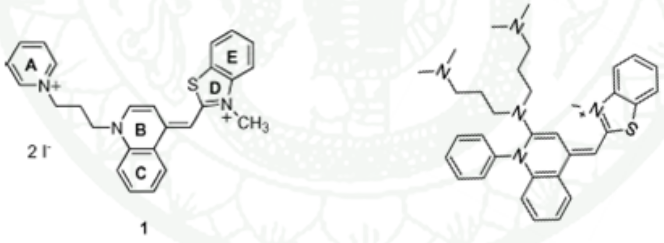

Figure 27 Conformation structure of cyanin dye. (**A**) the basic molecular structure of cyanin dye and (**B**) the PicoGreen molecular structure.

Source: Mikelsons *et al.,* 2005

The highly fluorescence signal in dsDNA interaction may involved in dye dimer formation. The formation of dimers is higher in ssDNA than dsDNA and therefore dye–ssDNA complexes are more prone to undergo energy transfer deactivation than complexes formed with dsDNA (Cosa *et al.,* 2001). It caused highly fluorescence signal in dsDNA interaction.

6.2 PicoGreen-Fluorescence determine enzyme amount and time-dependent activity of HIV-1 RT

To test whether the used concentration of the dye molecule was enough to interact with all DNA/RNA duplex production, the higher enzyme amount was used. The fluorescence signals were linearly increased by longer reaction time with 12, 25, 50 and 100 ng of RT (figure 28). This indicated that the used condition was enough for the DNA/RNA duplex production of at least 50 ng of RT/ 6 µl reactions (0.071 µM). We also further tested the period of time that can measure as an initial rate with different amount of RT (12-100 ng). The results showed fluorescent intensities of the first two minutes reactions were linear (figure 28A). Furthermore, the initial reaction rates were shown to be proportional with amounts of RT (figure 28B). Together, this developed fluorometric method could measure amount and time dependent RT activity.

Using the above conditions, we also compared enzyme activities between wild type and three mutant RT, K103N, Y181C and K103N/Y181C. The RT activities of all mutant RTs were also linearly increased by the longer reaction time and reached maximum after 5 min (figure 29) except for K103N that seem to be reached maximum after 3 min. Nevertheless, all mutant RTs were linearly increased in first two minutes which were enough for determination of the initial rates. These the results showed that we could apply this fluorometric method for determining enzyme kinetics in both wild type and mutant RTs.

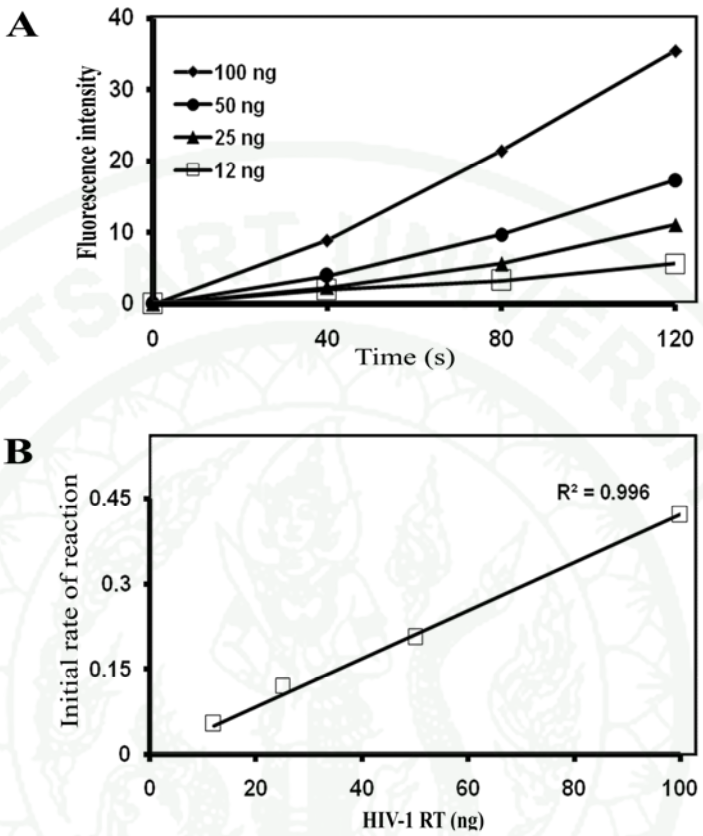

Figure 28 The PicoGreen-fluorometric method measure time-dependent of HIV-1 RT activity, (A) enzyme amount -dependent of wild type HIV-1 RT activity. (B) Showed the enzyme amount–reaction rate was a linear relation.

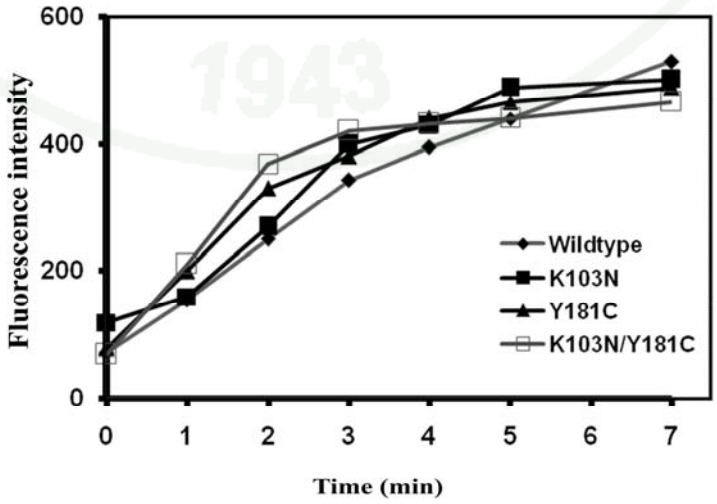

Figure 29 Time-dependent of wild type and mutant RT activity was determined by PicoGreen-fluorometric method.

7. PicoGreen-Fluorescence Determine the dTTP substrate dependent activity of HIV-1 RT

Since, kinetic parameters can determine enzyme properties and inhibitor function, the easy and fast method is very useful for conventional assay. To examine whether the increasing of dTTP is able to accelerate the reverse transcriptase reaction rate, the relationship between dTTP and reaction rate was determined by varying concentration of dTTP (figure 30). The Lineweaver-Burk plot indicated the increasing of reaction rate (V) was correlated to dTTP concentration (s). The K_m of dTTP determining form Lineweaver-Burk plot was 15.76±0.37 µM (*1/V* versus *1/S,* Y axis and X axis, respectively) and X co-ordinate showed $-1/K_m$, while Y co-ordinate showed $1/V_{max}$ (figure 30B). Our measured K_m value was in the range of previous report, for example, the wild type HIV-1 RT K_m for dTTP were 3.05-18.7 µM by the isotopic method, and 7.7±1.56 µM by the fluorometric assay with 4', 6'-diamidio-2-phenylindole. We also determined kinetic parameters by using Lineweaver-Burk plot for mutant RT, the kinetic parameters of mutant and wild type RT were shown in Table1. The K_m value indicated that substrate binding property was different among mutant RTs (figure 31, 32 and 33). The mutant K103N showed tight binding to dTTP with K_m of 8.73±1.58 µM, while Y181C and K103N/Y181C showed lower binding with K_m of 25.66±0.66 and 34.65±2.39 µM, respectively. The K_{cat} showed difference reaction processing property for wild type and mutant RT, the values were 0.032± 0.0006 s^{-1}, 0.020±0.001 s^{-1}, 0.0022 ± 0.0004 s^{-1} and 0.025±0.003 s^{-1} for wild type, K103N, Y181C and K103N/Y181C, respectively.

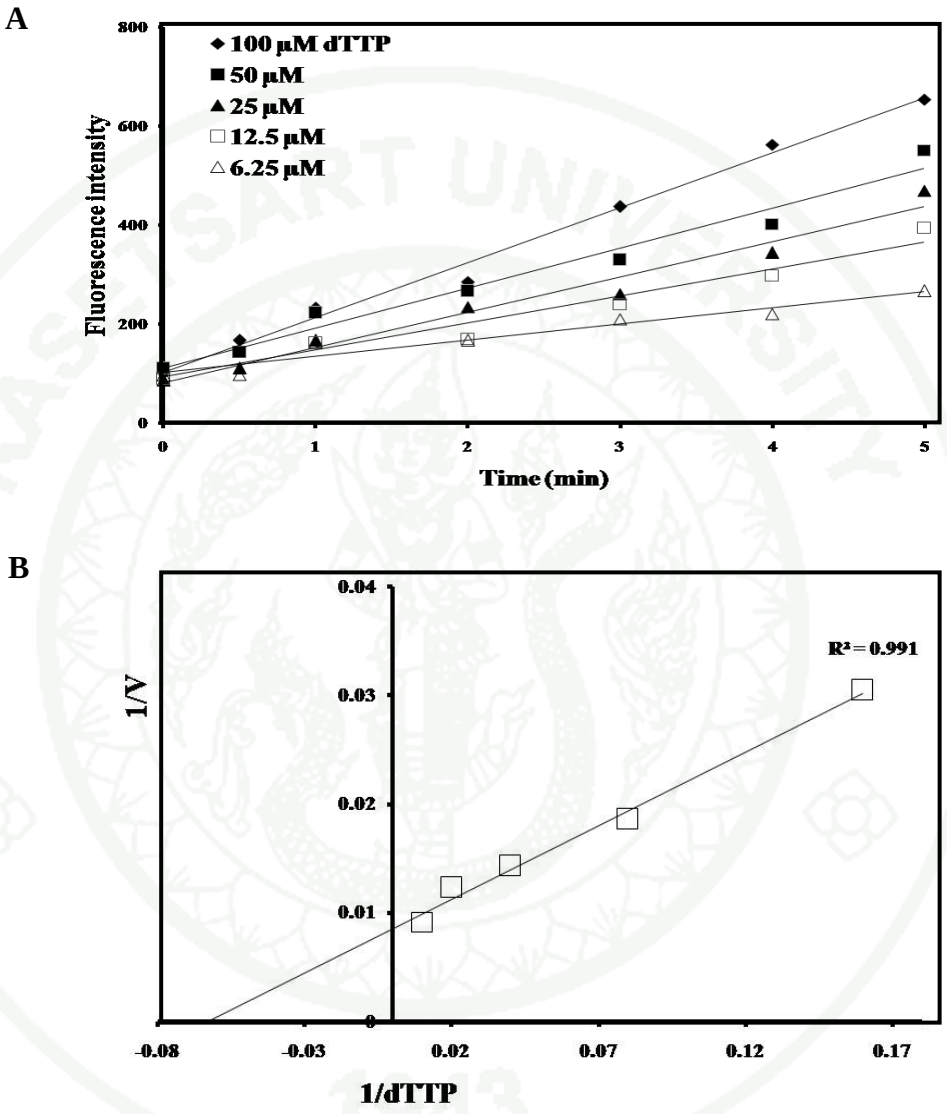

Figure 30 The fluorometric method measure the substrate dTTP dependent RT activity, showing the effect of varying the concentration of dTTP on the reaction rate of the RNA-dependent DNA polymerase activity of Wild type HIV-1 reverse transcriptase and determining plots (A) and the K_m for dTTP by using Lineweaver-Burk plot (B).

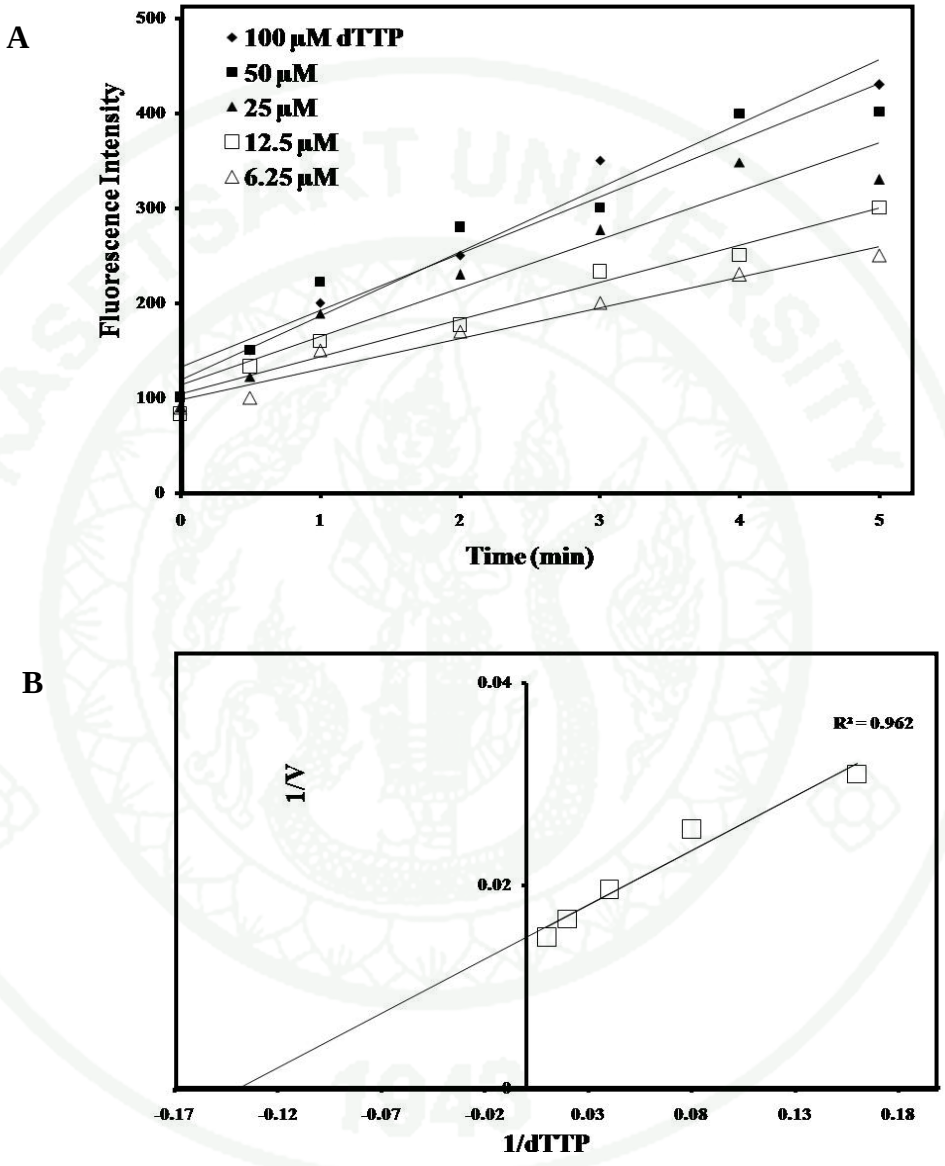

Figure 31 Substrate dTTP dependent activity of mutant K103N HIV-1 RT (A) and Lineweaver-Burk plot (B).

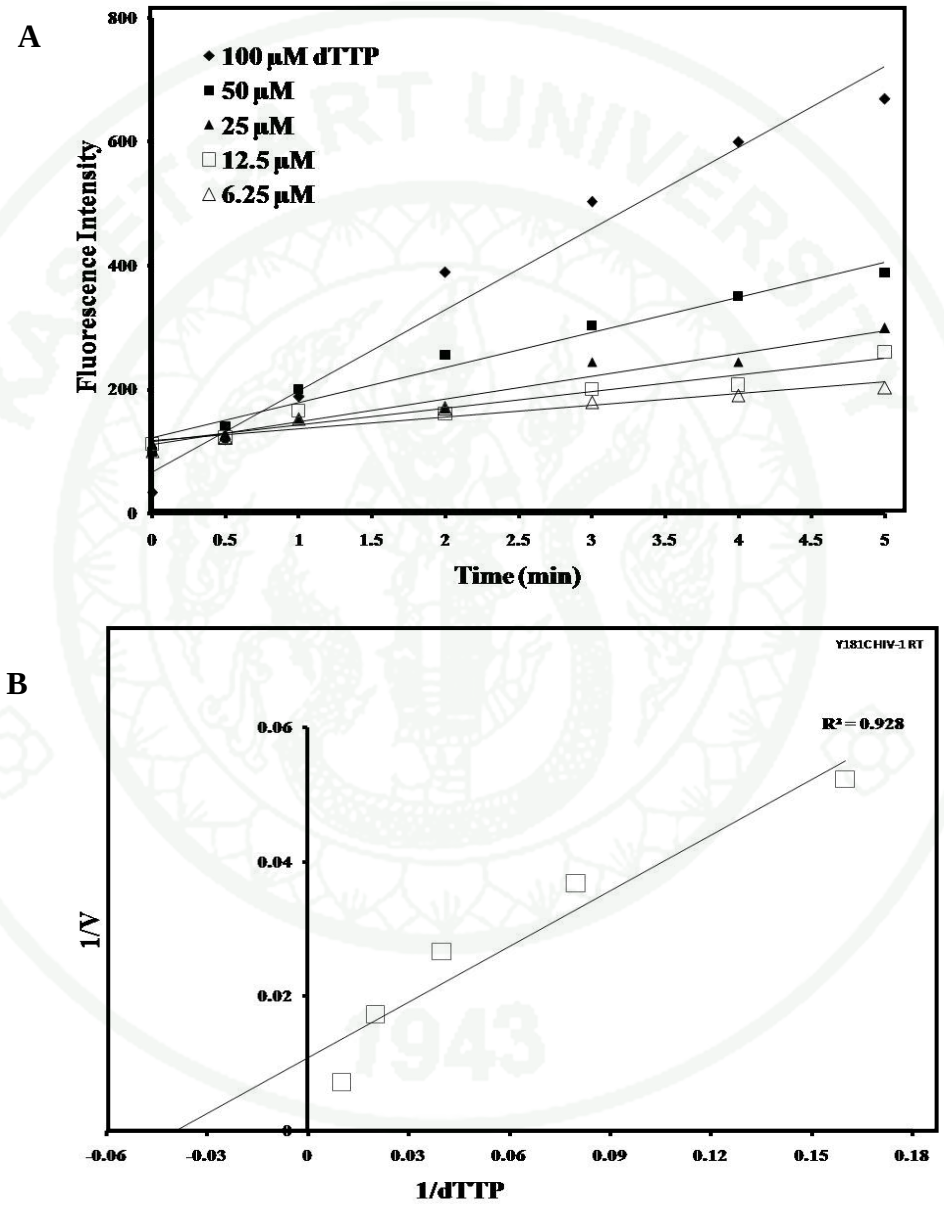

Figure 32 Substrate dTTP dependent activity of mutant Y181C HIV-1 RT (A) and Lineweaver-Burk plot (B).

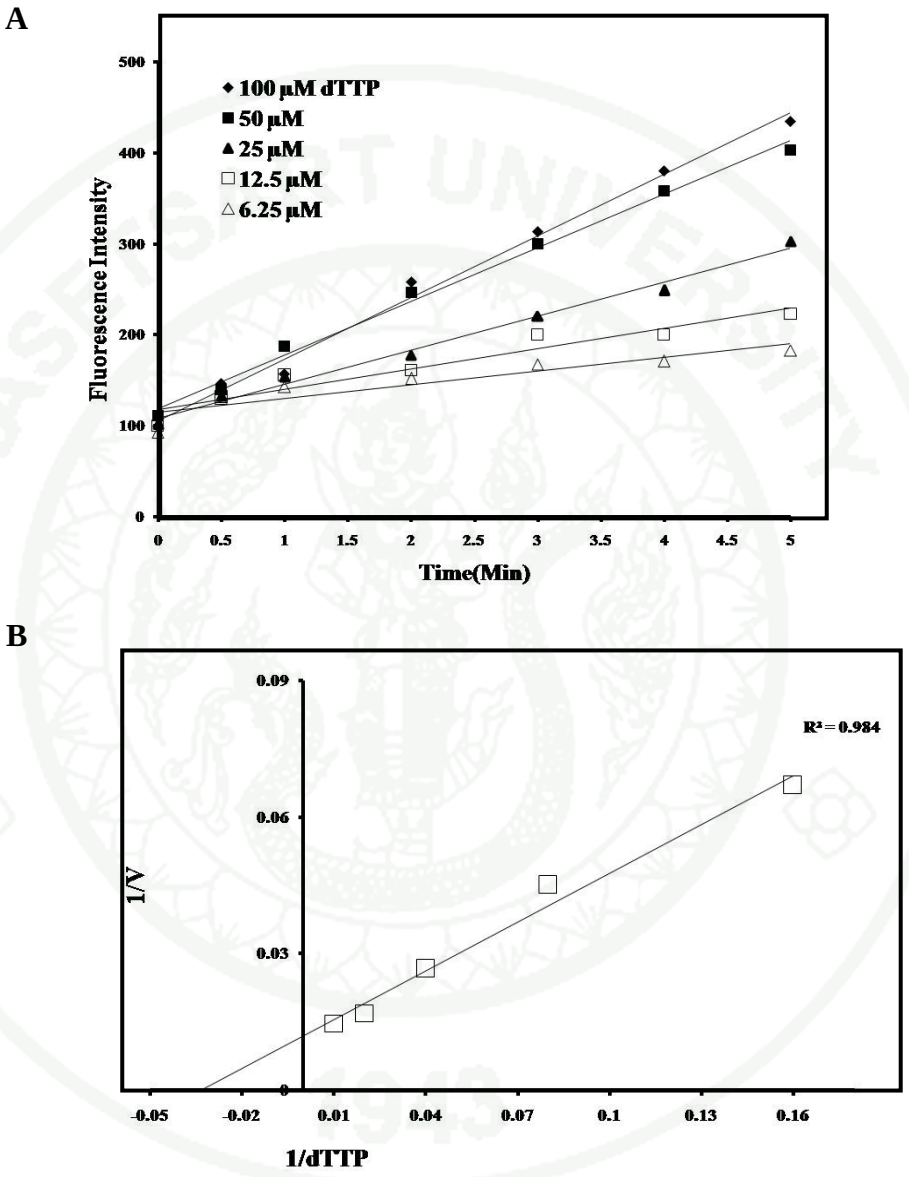

Figure 33 Substrate dTTP dependent activity of double mutant K103N/Y181C HIV- 1 RT (A) and Lineweaver-Burk plot (B).

Table 2 PicoGreen-Fluorescence determination kinetic parameter of HIV-1 RT

HIV-1 RT	K_m (μM)		V_{max} [1] (F min^{-1} ng^{-1})	K_{cat} [3] (s^{-1})	
	Fluorescence	Isotropic [2]	Fluorescence	Fluorescence	Isotropic [2]
Wild type	15.76±0.37	4.8	115.64 ±2.00	0.032±0.0006	1.9
K103N	8.73± 1.58	4.1	71.79± 5.13	0.020±0.001	1.7
Y181C	25.66±0.66	8.1	81.67±1.667	0.0022 ± 0.0004	1.5
K103N/ Y181C	34.65±2.39	6.6	88.46±11.53	0.025±0.003	1.8

[1] Unit of V_{max} was Fluorescence intensity min^{-1} ng^{-1}

[2] Carroll *et al.,* 1994, previous report using [α-^{32}P]dTTP by isotropic method

[3] K_{cat} = V_{max} / mg protein / time

Although, the values were deviated from previous report, the K_m indicated that tight binding and lower binding to dTTP by mutant HIV-1 RT caused decreasing of K_{cat} , while appropriate dTTP binding property of wild type HIV-1RT showed higher K_{cat}. These K_m and K_{cat} relationship was similar to previous reports (Carroll, *et al.,* 1994). Therefore, PicoGreen-fluorescence assay is able to measure kinetic parameter and determine kinetic properties both wild type and mutant RT. To descript Km-binding effect on Kcat- reaction processivity, the HIV-1RT reaction mechanism showed the 3′ end of the primer strand is bound at the priming site (P site), adjacent to the polymerase active site. The initial step in nucleotide incorporation is the binding of the incoming dNTP at the nucleotide binding site (N site) to form a ternary complex. The rate-limiting step in the polymerization reaction is a conformational change in which a portion of the p66 fingers subdomain closes down on the incoming dNTP, Because of polymerization process need incoming dNTP to elongate polymer,

tight-binding to earlier dNTP cause slow polymerization as descripted in " tigh-binding inhibition" (Stephen *et al.,* 1993). In addition, the binding of substrate at one site on the holoenzyme negatively affects the activity of the enzyme by inhibiting the rate of polymerization (West *et al.,* 1992). Therefore, tight binding to dTTP for K103N and dTTP lower binding for Y181C , loss in polymerization processivity.

8. Inhibition of HIV-1 reverse transcriptase activity by Dipyridodiazepinone derivatives PicoGreen-Fluorescence method for Screening of anti-HIV agents

To screen the inhibitors against wild type HIV-RT, ten of dipyridodiazepinone derivatives were selected to study the efficiency inhibition of HIV-1 RT activity. There dipyridodiazepinone derivatives were previously reported by our group with PCR-based assay. However it was not the direct determination of inhibitors against RT since crude protein from HIV-1 infected cell line was used for reverse transcription step and then follow by using *Taq* polymerase to amplify the RT products. Therefore, the RT activity was indicated by amount of PCR-amplified products, it involved in ability of *Taq* polymerase and many uncertain parameters from crude protein may reduce testing accuracy for PCR based assay. Therefore, the direct assay for determination of these inhibitors against RT was needed to be done. Since IC_{50} of nevirapine has been reported with approximate 1 μM, therefore, we adjusted all dipyridodiazepinone derivatives to 1 μM and compared inhibition efficiency of HIV-1 RT activity. By activity assay experiment showed that the relationship between the increasing of fluorometric intensity and time were in linear range in first 5 minute period, therefore we chose to incubate 5 minute for inhibitors assay.

The first screening was performed with wild type HIV-1 RT, the purified of 11 dipyridodiazepinone derivatives which designed by computational study, was used for HIV-1 RT inhibition screening. The inhibition activity was compared with nevirapine**.** The results showed 5 inhibitors contain high efficiency; NA14, NA15, NA16, NA17 and 68NV (figure 34). For further assay, 5 best compounds were test with mutant RT. The triplicate results were defining for average, we found that

inhibition efficiency was higher than nevirapine for wild type and mutant HIV-1 RT which represented by fold of relative inhibition (figure 35). Taken together, among 11 inhibitors, NA14, NA15, NA16, NA17 and 68NV were of interested and IC_{50} values will be obtained from following experiments.

The inhibition efficiency was measured by comparing fold of relative inhibition to nevirapine at 1 μM on the HIV-1 RT activity, five high effective of derivatives were tested with wild-type and mutant HIV-1RT.

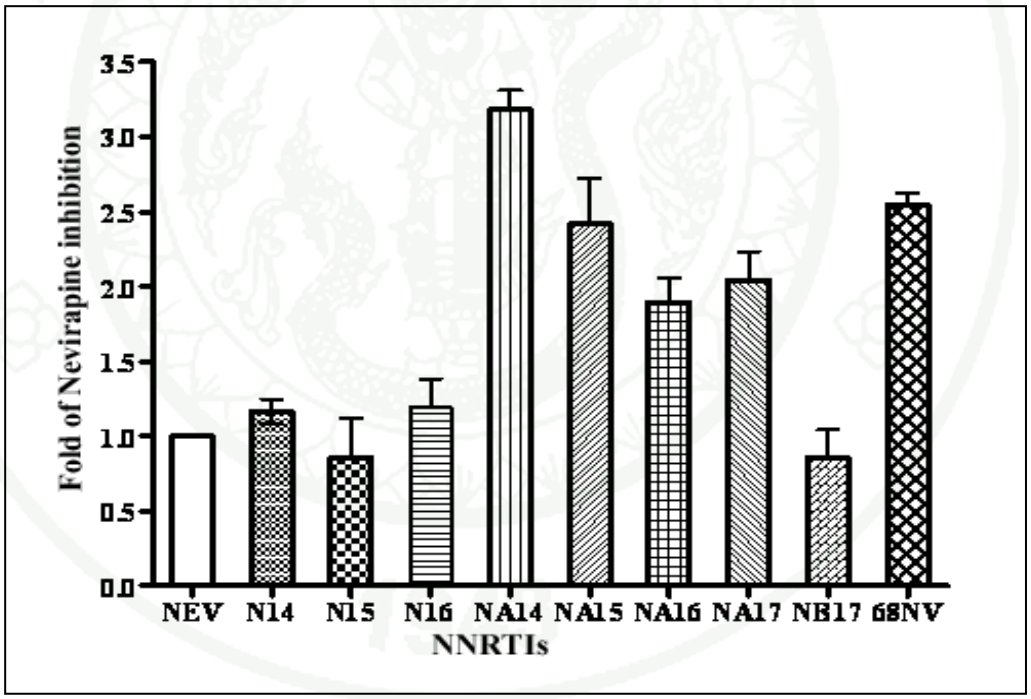

Figure 34 Screening of HIV-1 RT inhibitor from dipyridodiazepinone derivatives by PicoGreen-Fluoroscopic method.

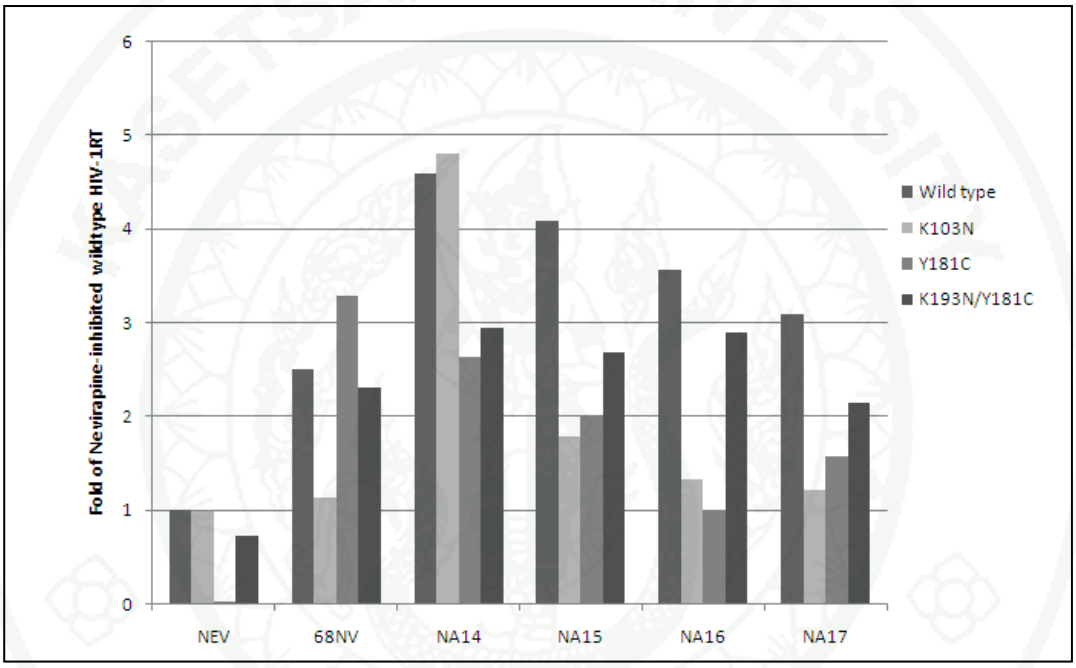

Figure 35 Screening of anti-HIV-1 RT activity. A, screening of 5 compounds with recombinant Wild type HIV-1 RT and its mutant.

9. Fifty percent inhibition value determination of anti- HIV agents

To determine the HIV-1 RT inhibition efficiency, nevirapine, 68NV and 4 dipyridodiazepinone derivatives were compared by IC_{50} values. The figure 45 showed Dose-response curves, this method have been used to determine inhibition efficiency and IC_{50} values were determined. The wild type HIV-1 RT activity was measured with different inhibitor concentrations which were two fold serial dilutions in 96 well plates. The Dose-response curves using Non-linear regressive were plotted with percent inhibition and log inhibitor concentration (figure 36). Five inhibitors were determined for IC_{50} and compared to nevirapine (figure 37). The results showed that nevirapine inhibited wild type HIV-1 RT activity with IC_{50} value of 15.67 ± 3.574 μM (R^2 = 0.7658). This IC_{50} result closed to previously fluorescence assay (13.1± 6.3 μM) (Chavan *et. al.,* 1995) and was within range of many publications from 0.084 - 23±11 μM by isotropic method (Merluzzi *et al.,* 1990, Balzarini *et al.,* 1992, Nissley *et al.,* 2007, Hang *et. al.,* 2007 and Herschhorn *et al.,* 2008). Moreover, the results showed that NA14 and NA15 were effective inhibitors which provide the IC_{50} values about 0.2138 μM and 0.5199 μM which were better than nevirapine 30-70 times, respectively. Previous experiment by using PCR based method showed similar results, high inhibition efficiency of NA14 and NA15, but IC_{50} value was better than our reported 10 fold times (Table 3). Since, RT activity was indicated by fluorescence intensity that depends on PicoGreen-RNA/DNA complex, these variations of IC_{50} values may cause by PicoGreen-RNA/DNA complex stability. However, efficiency ratio which indicated inhibition fold of nevirapine was similarity. Therefore, developed PicoGreen-fluorescence activity assay could be applied for anti HIV-RT agents screening and inhibition kinetic study.

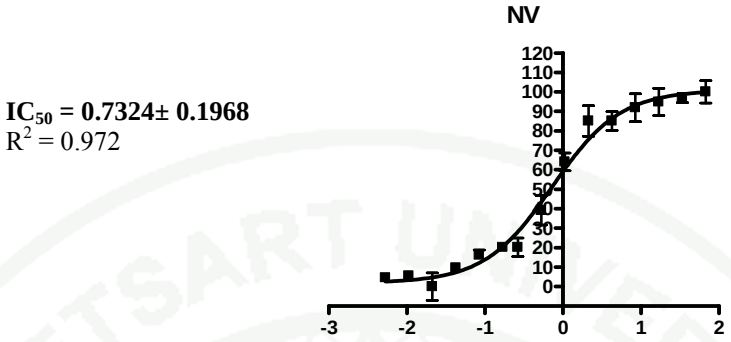

Sigmoidal dose-response	
Best-fit values	
BOTTOM	1.909
TOP	100.9
LOGEC50	-0.1352
EC50	0.7324
Std. Error	
BOTTOM	2.449
TOP	2.625
LOGEC50	0.06625
95% Confidence Intervals	
BOTTOM	-3.115 to 6.934
TOP	95.49 to 106.3
LOGEC50	-0.2712 to 0.0007238
EC50	0.5356 to 1.002
Goodness of Fit	
Degrees of Freedom	27
R?	0.972
Absolute Sum of Squares	1273
Sy.x	6.867
Data	
Number of X values	15
Number of Y replicates	2
Total number of values	30
Number of missing values	0

Figure 36. IC_{50} values determining with dose-response plot by using PISM software. The R^2 and error values were calculated and display for data analysis.

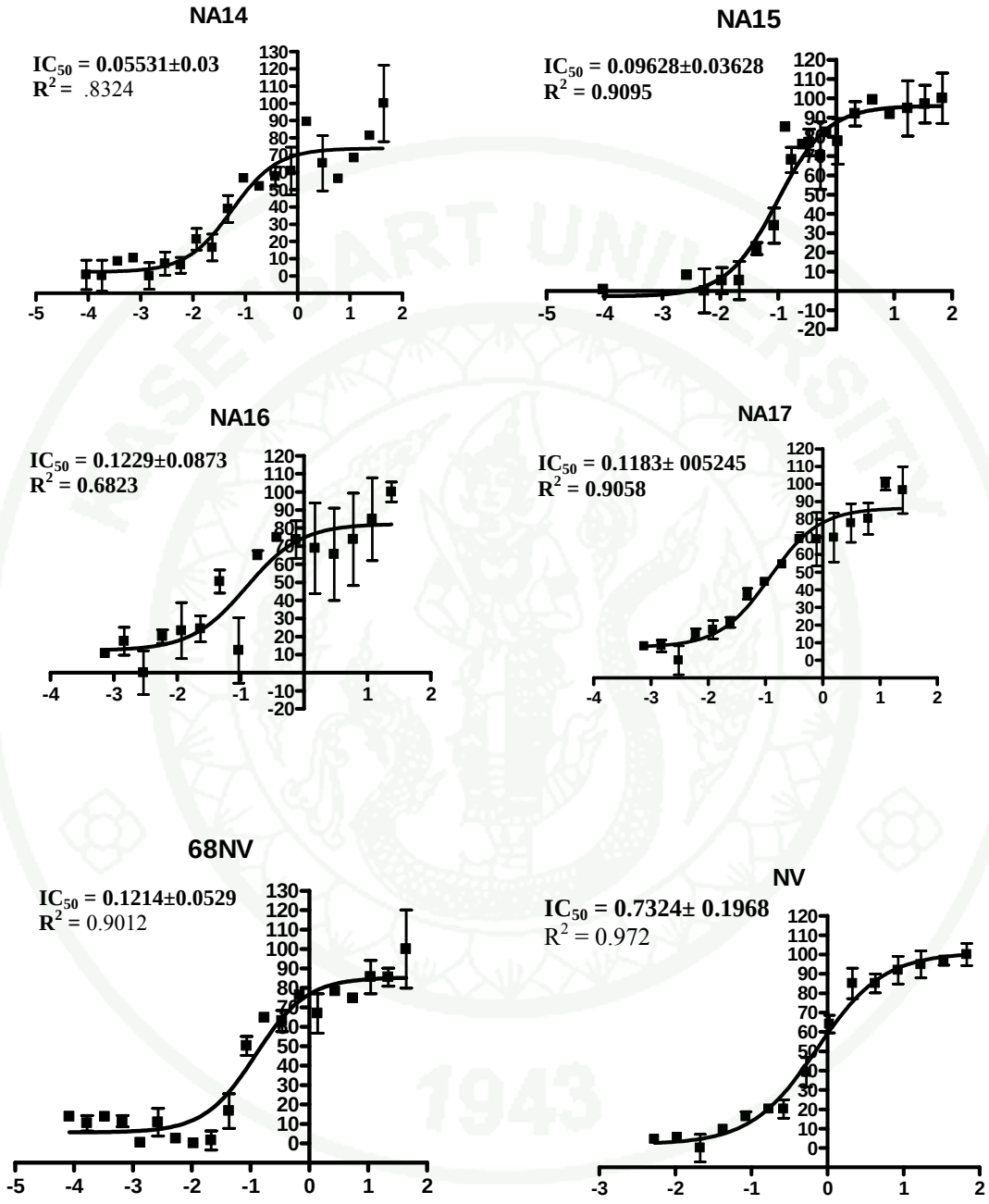

Figure 37 IC_{50} value determination of dipyridodiazepinone derivatives for Wild type HIV-1RT.

Table 3 Comparation of Inhibitory activity of the synthesized compounds against wild type HIV- 1 reverse transcriptase between PicoGreen-Fluorescence based assay and cell-based assay

Compounds	IC_{50} (μM)			
	PCR based method [1]	Efficiency ratio [2]	PicoGreen-Fluorometric Assay	Efficiency ratio [2]
Nevirapine [3]	1.070 ± 0.60	-	0.7324± 0.1968	-
68NV	0.0858 ± 0.00001	12.47	0.1214±0.0529	6.03
NA14	0.0186 ± 0.002	57.52	0.05531±0.03	13.24
NA15	0.0229 ± 0.01	46.72	0.09628±0.03628	7.61
NA16	0.0828 ± 0.03	12.92	0.1229±0.0873	5.96
NA17	0.124 ± 0.03	12.92	0.1183± 005245	6.19

[1]Khunnawutmanotham *et al*., 2009.

[2]Efficiency ratio = IC_{50} Nevirapine/IC_{50} NNRTIs.

[3]Isotropic method were 0.084-23±11 μM and 13.1± 6.3 μM by fluorescence method.

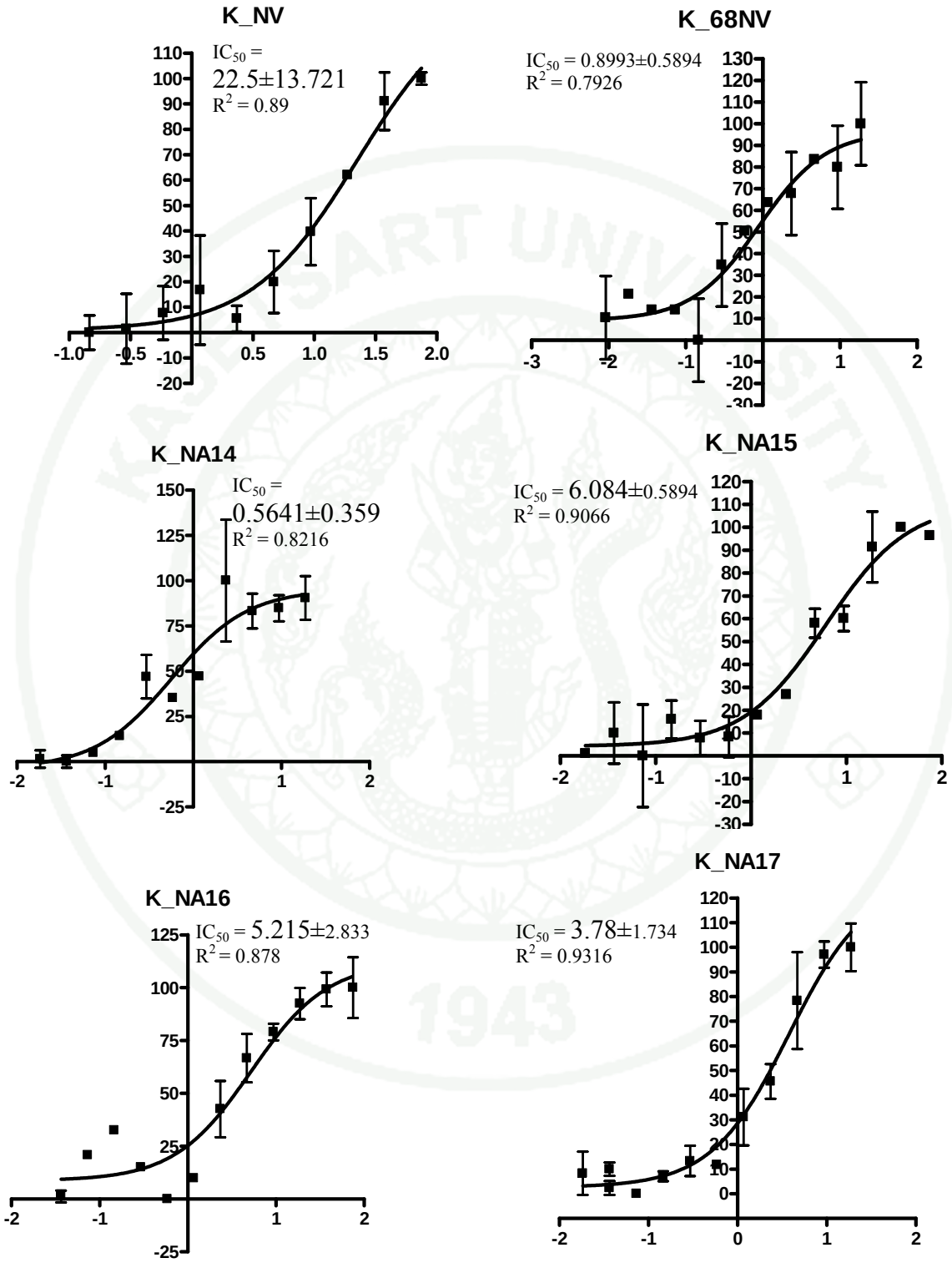

Figure 38 IC_{50} determination of dipyridodiazepinone derivatives for K103N HIV-1RT.

Table 4 Comparation of Inhibitory activity of the synthesized compounds against K103N HIV- 1 reverse transcriptase between PicoGreen-Fluorescence based assay and cell-based assay

Compounds	IC_{50} (μM)			
	PCR based method [1]	Efficiency ratio [2]	PicoGreen-Fluorometric Assay	Efficiency ratio [2]
Nevirapine	27.10 ± 5.20	-	22.5±13.721	-
68NV	0.39 ± 0.23	69.5	0.8993±0.5894	25.0
NA14	0.224 ± 0.14	120.9	0.5641±0.359	39.9
NA15	0.428 ± 0.39	63.32	6.084±0.5894	3.7
NA16	4.59 ± 2.23	5.90	5.215±2.833	4.3
NA17	4.31 ± 0.66	6.28	3.78±1.734	5.6

[1]Khunnawutmanotham *et al*., 2009.

[2]Efficiency ratio = IC_{50} Nevirapine/IC_{50} NNRTIs.

Dipyridodiazepinone nevirapine is a potent non-nucleoside inhibitor of human immunodeficiency virus type 1 reverse transcriptase (HIV-1 RT) and is approved as a therapeutic agent for the treatment of AIDS. However, nevirapine monotherapy results in relatively rapid drug resistance due to mutation of the RT enzyme. The second generation inhibitor with improved activity against the mutant RT enzyme has been focused on the synthesis of dipyridodiazepinone derivatives. On the basis of molecular modeling analysis on the wild-type (WT) and Y181C HIV-1 RT (Khunnawutmanotham *et al.,* 2009), it was found that the dipyridodiazepinone derivatives containing an unsubstituted lactam nitrogen and a 2-chloro-

arylthiomethyl moiety, are effective inhibitors of this mutant enzyme. Some dipyridodiazepinone derivatives containing an *N*-methylated of lactam also exhibited good potency against the WT enzyme. The 8-amino derivative of nevirapine and its hydrochloride salt also provided interesting potency. These compounds were synthesized and assay inhibition activity by using PCR based method (Table 3 and 4). Because of highly inhibition efficiency of these compounds, the molecular mechanism will be studied. Although, crystal structure has not been reported, the drugs mechanism was expanded by molecular docking study. The report showed that new hydrogen forming for these compounds in wild type, mutant K103N and Y181C binding pocket. The newly hydrogen formation may cause highly affinity to NNRTI binding pocket on HIV-1RT

Searching for novel inhibitors of the HIV –1 Reverse transcriptase is one of the main interesting; numerous lead compounds were both synthetic and natural. However, HIV-1 virus exhibits a high ability to develop resistance against therapeutic agents and therefore new promising substances have to be discovered. The screening of synthetic and natural substances is very useful method to find inhibitor. The early developed assays to screen for HIV-1 RT inhibitory activity were relatively complicated, time consuming and included work with radioactive material. We developed PicoGreen-fluorescence based assay, it was simple and rapid, reliable and safe screenings with a minimum amount of sample. Numerous natural inhibitors of HIV-1 reverse transcriptase have been described most of them obtained from plants.

The 24 Thai herbs (Thai common name were recorded in Appendix) were extracted by ethanol extraction method. To avoid RT activity inhibition by absolute ethanol, each extracts were two fold-diluted with 10 mM Tris-HCl pH7.4, 75 mM NaCl, and the extract was kept in 50% ethanol containing buffer. Control reaction was prepared by using 2 µl of buffer containing 50% ethanol instead of sample. The fluorometric method was determined. Percent inhibition and fold of relative inhibition were compared to nevirapine. The figure 39 showed five samples which contained high inhibition efficiency more than Nevirapine*, Rhinacanthus nasutus, Myristica fragrans, Ruellia tuberose, Curcuma longa* and *Peltophorum pterocarpum*

with inhibition of 3, 3.5, 2.5, 3 and 1.5 fold of 1 µl nevirapine, respectively. The lead compounds from these extract has to be study in the future.

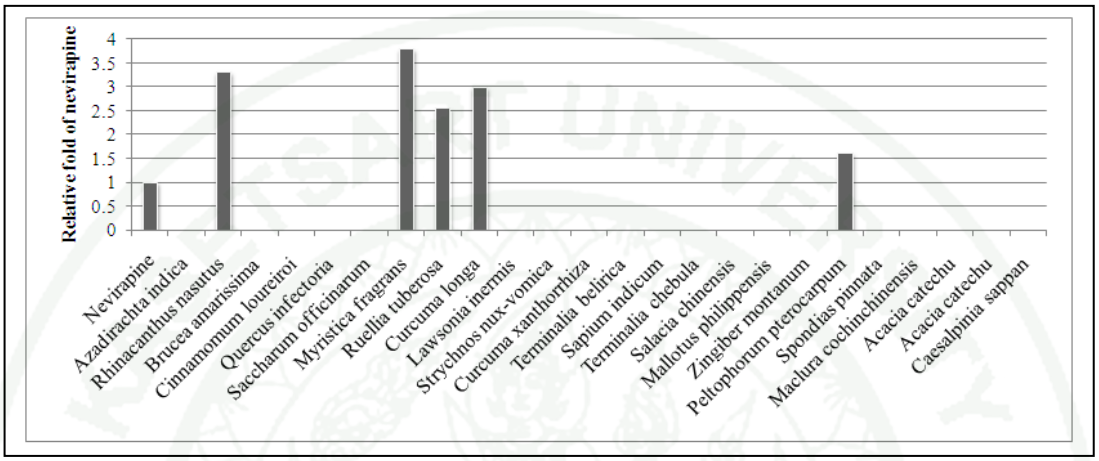

Figure 39 Inhibition of HIV-1 RT activity by 25 Thai herbs crude ethanol extraction comparing with Nevirapine.

The *Rhinacanthus nasutus* is Thai medicinal plant, the plant have been reported that contained antiviral activity (Send *et al.,* 1996) and its lignans, showed anti-HIV, anti-influenza and anti-hepatitis potencies (Jassim *et al.,* 2003). Altough, *Rhinacanthus nasutus* extract contained anti HIV viral, the mechanism and molecular targeting did not known. May be, HIV-1 RT is one target protein of this activity.

Curcuma longa crude extracts was reported anti-SAR (Itokawa *et al.,* 2008) and anti-HIV activity. The compounds, curumin and curcumin boron complexes, was reported anti-HIV-1 protease (Jayaprakasha *et al.,* 2005).

Although, anti-HIV viral was not reported for *Ruellia tuberose, Peltophorum pterocarpum* and *Myristica fragrans*. However, there are many compounds in medicinal plant contained anti-viral activity. Long time ago, medicinal plants have been widely used to treat a variety of infectious and non-infectious ailments. Several plants could offer a rich reserve for drug discovery of infectious diseases. The human immunodeficiency virus type 1 (HIV-1) and 2 (HIV-2) are one of infectious diseases

that was treatment with medicinal plats. For the anti-HIV activity of medicinal plants at molecular level, a recent study compared various plants and their individual parts (stem, leaves, roots, etc.) in inhibiting viral reverse transcriptase (RT) and integrase, (Bessong *et al.,* 2006). Since, RT plays a major role in controlling viral infectivity and replication, several reports have linked medicinal plants capability to inhibit RT activity (Woradulayapinij *et al.,* 2005). In addition, many experiments have been reported that anti HIV-1RT agent were located both organic solvents and aqueous extracted fractions.

Many organic compounds from natural products have been found to be inhibitors of HIV-1-RT such as coumarins, flavonoids, tannins, alkaloid, lignans, terpenes, quinines and protein e.g. (Asres *et al.,* 2005**)**. Especially, number of hydrolyzable tannins are known for their activity against HIV-1 RT (Nonaka *et al.,* 1990). In other hand, one of the most prominent compounds is calanolide A (Mahidol *et al.,* 2002). The calanolide A was called in different name depend on plant source, a coumarin isolated from the tropical rainforest tree, *Calophyllum lanigerum* (Guttiferae), Buchapine and a quinolone derivative were isolated from *Euodia roxburghiana* collected in Surat Thani, province of Thailand. (McCormick *et al.,* 1996).

For water soluble compounds from plant which contained anti-HIV-RT acivity, such as the water extracts of *Ipomoea carnea* subsp. *fistulosa* (aerial parts), *Vitex glabrata* (branch), *Vitex trifolia* (aerial part), *Vitex negundo* (aerial part), *C. indica* (rhizome), and *Justicia gendarussa* (aerial part) showed HIV-1 RT inhibition (Woradulayapinij *et al,*. 2005). The extracts of the leaves of C. hartmannianum completely inhibited the enzyme HIV-1 RT at a concentration of 66 mg/ml. The extract of the seeds of *Croton zambesicus* was weakly active against HIV-1 RT, the extracts of P. pamianthe and Z. spina -christi (seeds) against the HIV-RT enzyme were considered as weak and not significant. The extract of C. hartmannianum was found to be active against HIV1-RT, not selectively (Ali *et al.,* 2002**)**.

Moreover, the plant-biological molecules can inhibit HIV-RT activity. The

fruits of *Momordica charantia* have been shown to contain many proteins with varying molecular weights and these proteins exhibit a ribosomeinactivating property. MAP30, a ribosomal inactivating protein, was isolated from this fruit and found to inhibit HIV-1 reverse transcription, viral core protein synthesis and syncytium formation between the infected and the new white blood cells (Lee-Huang, *et. al.,* 1990-1994). From the ripe fruit and seed of Thai *Momordica charantia*, a protein (MRK29) of molecular weight 28.6 kD was isolated and purified. MRK29 was found to inhibit HIV-1 reverse transcriptase with 50% of inhibitory ratio (IR) at a concentration of 18 μg/ml (Jiratchariyaku *et al.,* 2001).

In summary, Thai herbs contained many potential molecules which can inhibit HIV-1 RT activity such as chemical and biological compounds, they located in both organic solvents and water soluble fraction. Therefore, these herbs are very interesting for potential source of HIV-1 inhibitors. In addition, we interested in anti-HIV-1RT activity by small peptide from plants.

The figure 40, we tested water soluble compounds by using water extraction of 2 herbs, *Maclura cochinchinensis* and *Sapium indicum*. The inhibition of these crude extracts were compared with nevirapine, the results showed that water extracts of *Sapium indicum* could inhbit HIV-1 RT by 1.2 fold of nevirapine (Figure 40), while *Maclura cochinchinensis* did not. The water soluble materials contained many biological molecules including polypeptide. Based on provisory publications, Clayette *et al.,* 2008 showed new class HIV-1 RT inhibitor, peptide-based Inhibitors of HIV-1RT. The water extraction of 2 herbs were digested, the crude extracts of small peptide (*Maclura cochinchinensis* hydrolystae and *Sapium indicum* hydrolystae) was used for anti-HIV-RT activity measurement.

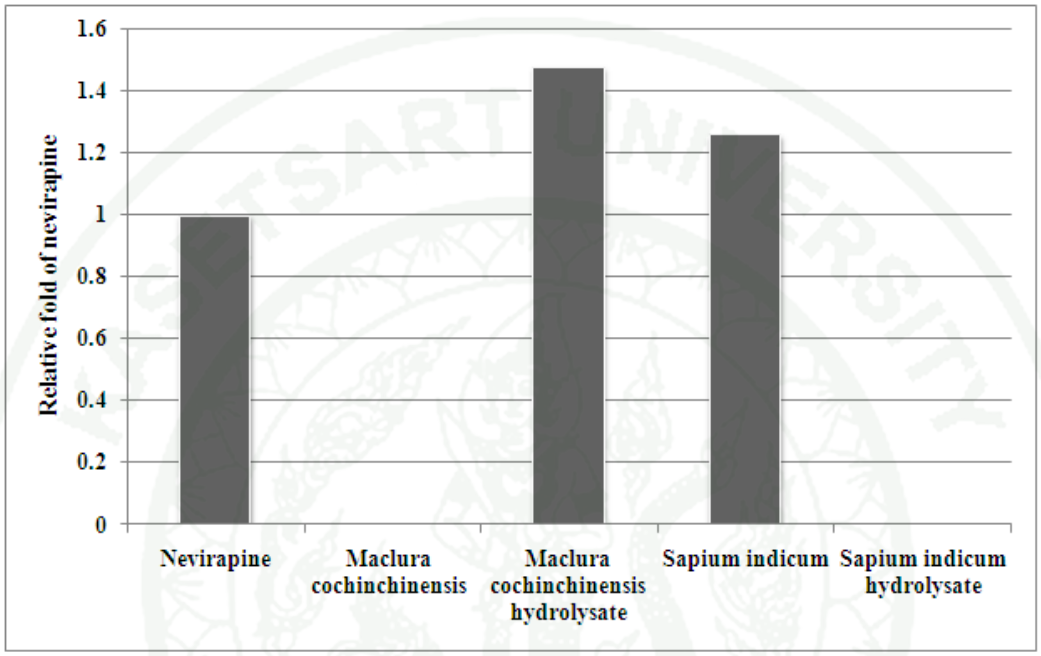

Figure 40 RT inhibitions activity of water soluble crude extracted from *Maclura cochinchinensis* and *Sapium indicum* (2 Thai herbs) comparing with Nevirapine.

The results showed that only *Maclura cochinchinensis* hydrolysates could inhibit HIV-1 RT activity, it was possible that RT activity was inhibited by small peptide from these extracts. Since, HIV-1 RT is heterodimeric enzyme, the active enzyme involves contacts between the thumb of p51 and the RNaseH of p66 as well as between the fingers of p51 with the palm of p66. The interfering of dimerization caused inactive enzyme, the mechanism of small peptide inhibitor involves protein/protein interaction (Agopian *et al.,* 2009). Previously reports shoed that the short 9-mer peptide (Pep-71) derived from the Trp-rich cluster of the connection subdomain, which blocked RT dimerization. Pep-71 interacted preferentially with the p51 subunit within heterodimeric RT, and destabilized the dimeric conformation, thereby triggering dissociation. The binding site of Pep-71 has been located to a cleft

between the connection and fingers domains of the small p51 subunit and found to involve contacts between the highly conserved residues Trp-24 and Phe-61 on the p51 subunits. The small peptide from plants may be new source for anti-HIV-1 RT agants.

Moreover, the figure 41 showed natural product, lamellrin K, form submarine animal, could inhibit HIV-1RT with 3 fold of nevirapine. The figure 42 showed molecular structure of lamellrin, over 38 lamellarins (A-Z and α-γ) have been described (Fan, 2008). Lamellarins is in a family of hexacyclic pyrrole alkaloids originally isolated from marine invertebrates and first isolated from a marine prosobranch mollusk of the genus lamellaria, display promising anti-tumor activity. They induce apoptotic cell death through multi-target mechanisms, including inhibition of topoisomerase I, interaction with DNA and direct effects on mitochondria. However, no one reported that lamirarins could inhibit HIV1-RT. Since lamellrins can inhibit topoisomerase I by weak interact with DNA that intercalates between base pairing of the double helix. (Michael *et al.,*2003). It is possible that lamellrin K interact with heteroduplex DNA/RNA, substrate of HIV-1 RT. The inhibition of HIV-1intregase by lamellrins was reported by Venkat *et al.,* 1999. The lamellrins a 20-sulfate showed selective inhibition of integrase and inhibited growth of the HIV-1 virus in cell culture (IC_{50} = 8 mM).

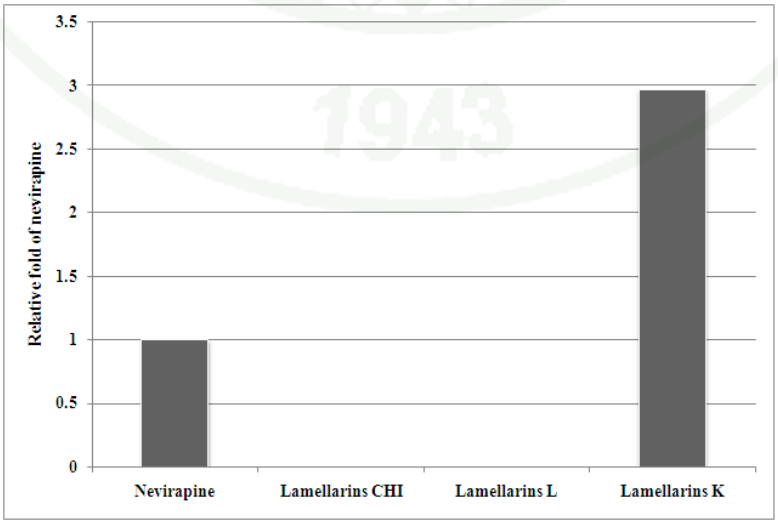

Figure 41 RT inhibition activity of Lamellarin comparing with Nevirapine.

In summary of anti HIV-1 RT agents screening from natural products, there were many compounds which showed anti HIV-1 RT activity, including organic solvents and water soluble fraction extraction of Thai herbs. The anti RT activities by small peptides were found from *Maclura cochinchinensis* hydrolystaes. Inaddition, Lamellarin K, the compounds from submarine animal showed anti HIV-1 RT activity. Therefore, these materials are very interesting for potential source of HIV-1 inhibitors. Further study will identify some potential compounds and study its inhibition efficiency.

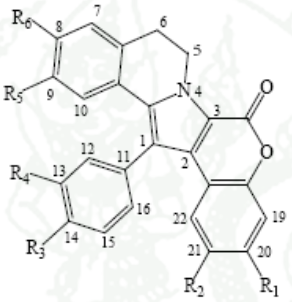

#	Lamellarin	R1	R2	R3	R4	R5	R6	5-6
1	lamellarin D	OH	OMe	OH	OMe	OMe	OH	═
2	lamellarin α	OH	OMe	OH	OMe	OMe	OMe	═
3	di-H-lamellarin D	OH	OMe	OH	OMe	OMe	OH	—
4	lamellarin H	OH	OH	OH	OH	OH	OH	═
5	di-H-lamellarin H	OH	OH	OH	OH	OH	OH	—
6	lamellarin N	OH	OMe	OMe	OH	OMe	OH	═
7	lamellarin L	OH	OMe	OMe	OH	OMe	OH	—
8	lamellarin G tri-OMe	OMe	OMe	OMe	OMe	OMe	OMe	—
9	lamellarin 3	OH	H	OH	OMe	OMe	OH	═
10	lamellarin 4	H	OMe	OH	OMe	OMe	OH	═
16	lamellarin 11	H	H	OMe	OMe	OMe	OMe	═
17	lamellarin 12	O-CH_2-O		OMe	OMe	OMe	OMe	═
18	lamellarin 33	O*i*-Pr	OMe	O*i*-Pr	OMe	OMe	O*i*-Pr	═
19	lamellarin 31	O*i*-Pr	OMe	O*i*-Pr	OMe	OMe	O*i*-Pr	—
20	lamellarin 34	O*i*-Pr	OMe	OMe	O*i*-Pr	OMe	O*i*-Pr	═
21	lamellarin 32	O*i*-Pr	OMe	OMe	O*i*-Pr	OMe	O*i*-Pr	—
22	lamellarin K	OH	OMe	OH	OMe	OMe	OMe	—

Figure 42 Lamellarins structure.

Source: Baunbek *et al.* (2008)

11. **RT crystallization**

Purified recombinant HIV-1 RT was concentrated into 10 mM Tris-HCl pH 8.0, 75 mM NaCl by using Centricon C-100. Recombinant HIV-1 RT was confirmed heterodimeric protein purity and its activity by previously experiment. For crystallization experiment, 10 mg/ml protein was used crystallization. The first experiment, we tried to crystallizes untag HIV-1RT (no his-tag RT was purified by following protocol figure 24). Following previously reported solution (Hsiou *et al*., 1998), a chosen solution composed of 50 mM Bis-tris Propane pH 6.8, 100 mM Ammonium sulfate, 10% glycerol, 10% PEG8000, by using microbacth method at 16 ^{o}C. Clear solution was observed for first 2 weeks, and then needle crystal appeared in 2 months.

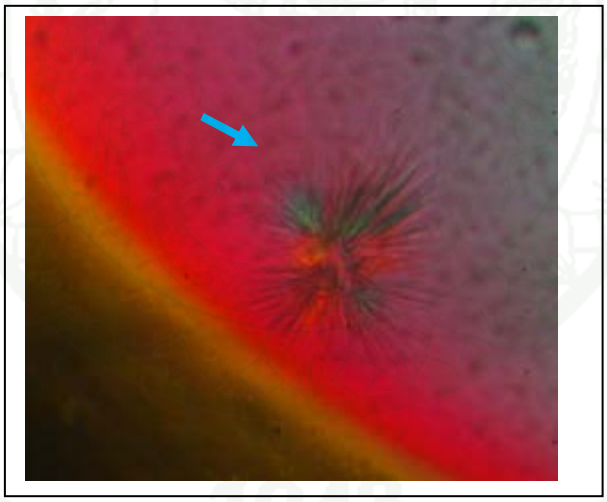

Figure 43 The untag HIV-1RT crystallization, needle crystal which was observed under poralized light, grown by using 50 mM Bis-tris Propane pH 6.8, 100 mM Ammonium sulfate, 10%glycerol, 10% PEG8000.

The figure 43 showed needle cluster crystal which was observed under polarized stereo microscope. The crystal showed birefringent properties, and then we optimized condition by varying pH 6.2-8 and 6-12 % PEG 8000 concentration. The crystallization conditions were observed every 3 days for first 2 weeks, and then it was observed every week for a month. Some conditions showed light and heavy

precipitate within one month. The experiments were incubated in 16 ^{o}C refrigerator until 3 months. The crystal and needle crystal was observed after 3 months, the results were shown in figure 44.

PEG pH	A 6% PEG8000	B 8 % PEG8000	C 10 % PEG8000	D 12 % PEG8000	E	F
1 pH 6.2	crystal	L	s	L		
2 pH 6.4	L	s	L	needle		
3 pH 6.6	crystal	L	L	L		
4 pH 6.8	L	needle	L	L		
5 pH 7	H	S	L	L		
6 pH 7.2	L	needle	L	L		
7 pH 8	L	needle	L	L		
8						
9						
10 Buffer	Buffer C	Buffer C	Buffer C	Buffer C		

Figure 44 The crystallization work sheet, 3 months observations were recorded**.**

S : salt (no polarize and no fragile)

L : light precipitate

H : Heavy precipitate

C : clear solution

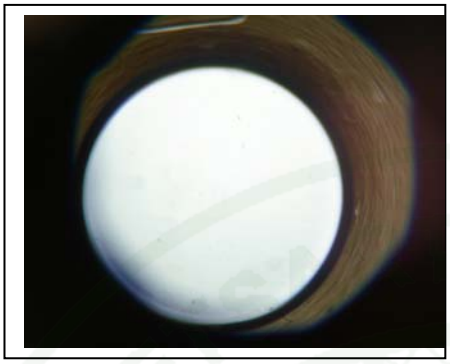

A. The Clear drop

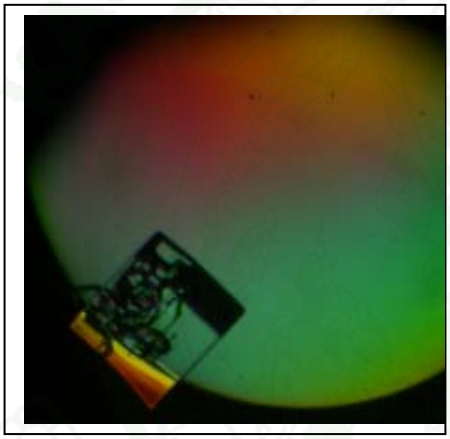

B. Salt crystal showed no polarizes and no fragile

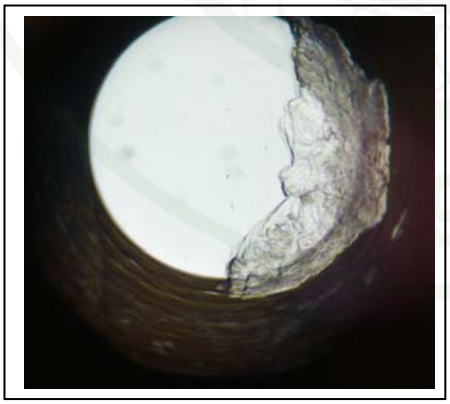

C. Dry out drop was observed when left the crystal plate more than 4 months at 16 ^{o}C

Figure 45 Clear and salt crystal containing drop, crystallization was performed by using microbatch at 16 ^{o}C.

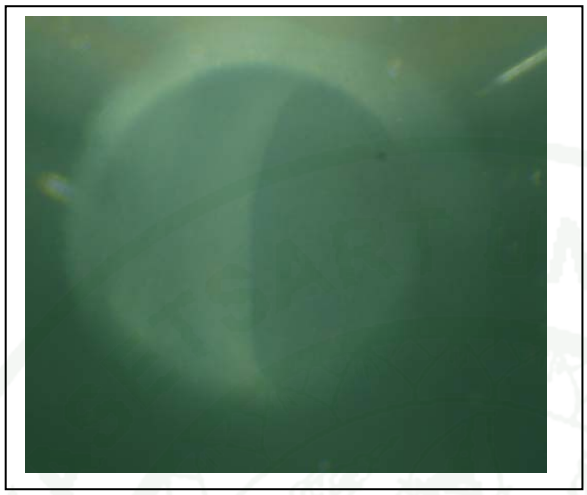

A. Light precipitate containing drop

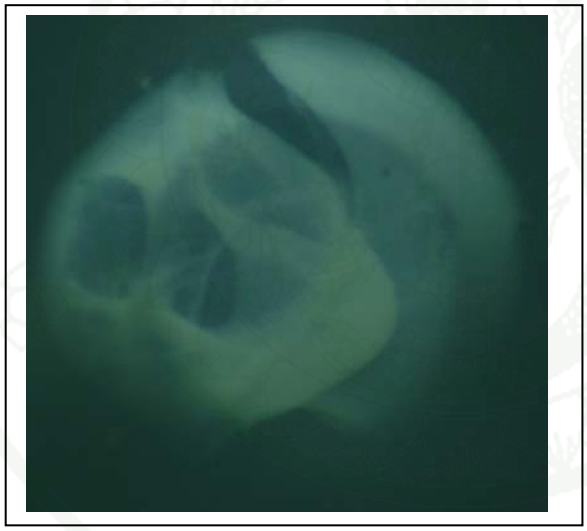

B. Heavy precipitate containing drop

Figure 46 Heavy and light precipitate containing drop, crystallization was performed by using microbatch at 16 ^{o}C.

Following figure 44, the drop was interpreted as showed in figure 45 -46. The heavy and light precipitation was observed within first 2 weeks, while the salt and dry out drop was observed after 3 months observation. The precipitation of protein indicated that high concentration of precipitant or protein were used, therefore PEG or ammonium sulfate concentration should be reduced for further crystallizing experiment.

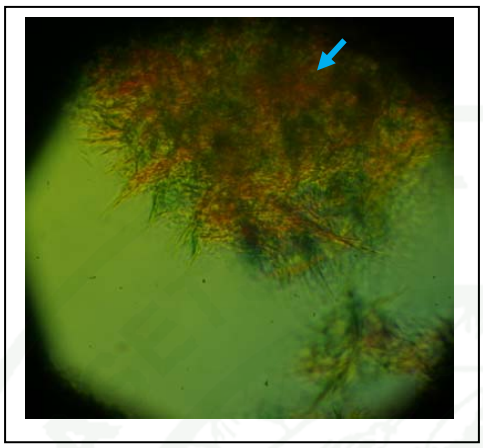

A. Needle crystal was observed by using 50 mM Bis-tris Propane pH 6.8 ammonium sulfate, 10% glycerol, 8-12 % PEG8000.

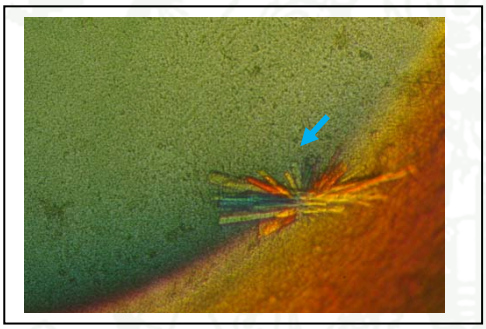

B. Rod cluster crystal was observed by using 50 mM Bis-tris propane pH 6.2 ammonium sulfate, 10% glycerol, 6% PEG8000.

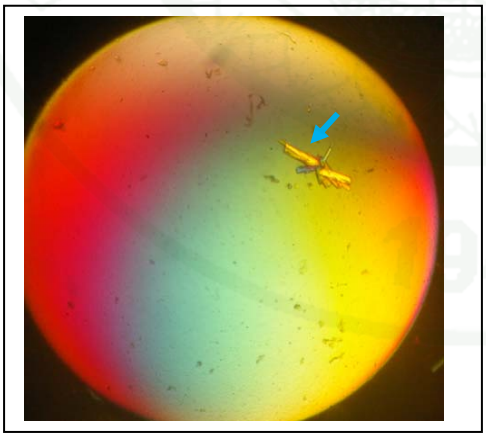

C. Rod cluster crystal was observed by using 50 mM Bis-tris propane pH 6.6 ammonium sulfate, 10 % glycerol, 6% PEG8000.

Figure 47 The HIV-1 RT crystal occurring with optimization condition. The crystal was observed after 3 months, the rod cluster crystal appeared by using 6% PEG 8000 containing solutions.

In addition, we tried to use other condition to crystallize untag HIV-1RT, the additional condition with 50 mM HEPES pH 7.5, 1 M ammonium sulfate, 5 mM $MgCl_2$ (figure 47). The results showed the thick plate crystal was observed after 2 months.

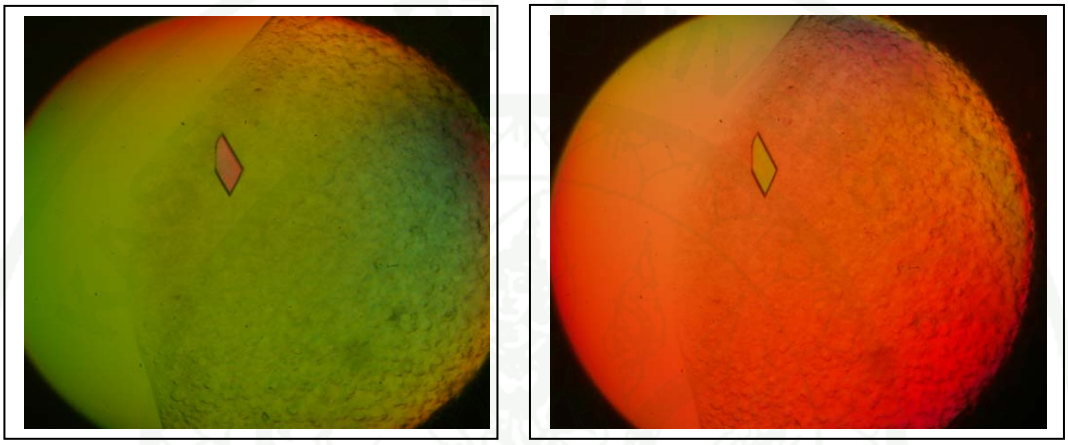

Figure 48 HIV-1 RT crystallization by using micro batch method at 16 ^{o}C, the thick plate crystal was observed under different polarized light.

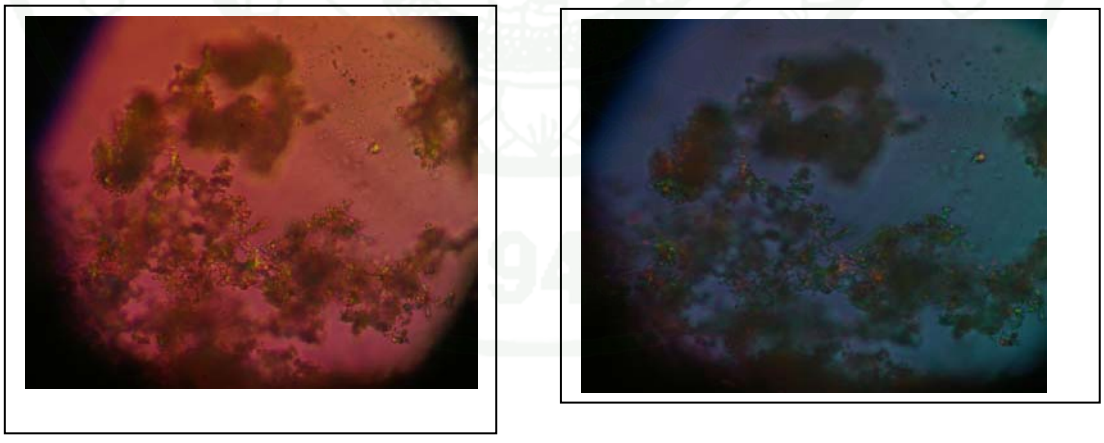

Figure 49 Microcrystal containing drop. The microcrystal which showed birefringent properties under poralized light source, was grown by using 100 mM sodiumcadodylate pH6.5, 1.4M sodiumacetate, 30% ammonium sulfate.

For untag HIV-1 RT crystallization, the needle crystal was observed after 2 months by using microbatch method at 16 ^{o}C, the crystallizing solution composed of 50 mM Bis-tris Propane pH 6.8, 100 mM ammonium sulfate, 10% glycerol, 10% PEG8000. We optimized by ad justify pH and PEG 8000 concentration, the cluster rod crystals was observed after 2 months with using solution composed of 50 mM Bis-tris Propane pH 6.6 Ammonium sulfate, 10 % Glycerol, 6% PEG8000. The crystal was not good enough for x-ray diffraction testing, because single crystal did not appeared by our experiment. We tried to use other reported condition, solution 1; 50 mM HEPES pH 7.5, 1 M $(NH_4)_2SO_4$, 5 mM $MgCl_2$ and solution 2; 100 mMsodiumcadodylate pH6.5, 1.4M sodiumacetate, 30% ammonium sulfate. The microcrystal was observed for solution 2 while the best crystal appeared for solution 1, the thick plate crystal was observed after 3 months with microbatch method at 16 ^{o}C. Unfortunately, we tried to mount crystal with microloops, the crystallizing solution was very sticky which caused difficult to mount this crystal. The increasing of force for crystal mounting caused crystal was cracked and broken.

However, the growth of crystal spent long incubation time (2-3 months) which indicated that crystal hardly grown by using our experiment. It was possible that unstable conformation of HIV-1 RT. The HIV-1 RT composed of 2 subunits, the heterodimeric formation need for active HIV-1 RT. Since, the untag purification protocol used ion exchange chromatography, the heterodimeric enzyme was not confirmed by gel filtration. May be mixing population of monomeric (p51 and p66), homodimeric (p51/p51, p66/p66), and heterodimeric protein (p66/p51) of HIV-1 RT interfered protein crystallization.

Since our new plasmids were constructed and confirmed for heterodimeric HIV-1 RT purification, we used his tag HIV-1RT for further crystallizing experiment. For co-crystallization with inhibitor (2:1 molar ratio inhibitor: protein solution). The 19 solutions from many previously publications were used for condition screening. The crystallization was performed by 3 methods, microbacth, hanging drop and hanging drop at 4 ^{o}C. We found that light precipitate was appeared all condition for microbacth with in 2 day, and crystal did not developed until 3 months. Maybe rapid

vaporization by this method was not suitable for our protein, we had to reduce protein or salt concentration for next condition screening with this method. However, the star shape of small cluster crystal was appeared in 1 week from NA15/WRT complex by using hanging drop with solution A1 (50 mM Bis-tris Propane pH 6.8, 100 mM ammonium sulfate, 10% glycerol, 4% PEG8000), figure 50, and this solution had to optimize for getting better crystal. The figure 49 showed larger single crystals appeared after 2 week from 68NV/WRT complex by using sitting drop method with solution D1 (50 mM Imidazole pH 6.4, 100 mM ammonium sulfate, 15 mM MgSO4, 10% PEG8000), this crystal size was large enough for x-ray diffraction study.

Table 5 Nineteen crystal solutions screening by using 3 crystallization methods

	Methods		
Inhibitors	Microbacth	Hanging Drop	Sitting Drop
NV	Precipitate	Precipitate	Precipitate
68NV	Precipitate	Precipitate	Cupid shape -single crystal (~0.2 mm) , Sol. D1
NA14	Precipitate	Precipitate	Precipitate
NA15	Precipitate	Small star shape-cluster ,Sol. A1	Precipitate
NA16	Precipitate	Precipitate	Precipitate
NA17	Precipitate	Precipitate	Precipitate

Solution A1 = 50 mM Bis-tris propane pH 6.8, 100 mM ammonium sulfate, 10%glycerol, 4%PEG8000.

Solution D1 = 50 mM Imidazole pH 6.4, 100 mM ammonium sulfate, 15 mM MgSO4, 10% PEG8000.

A

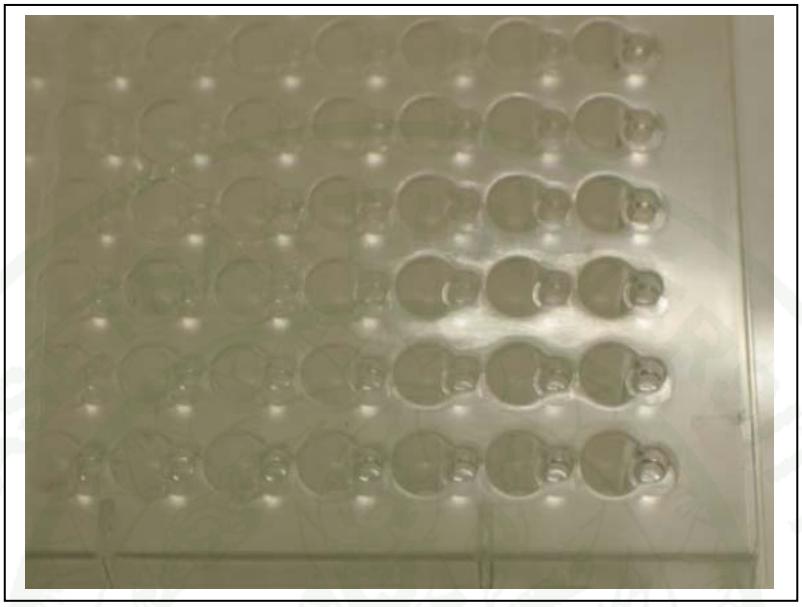

B

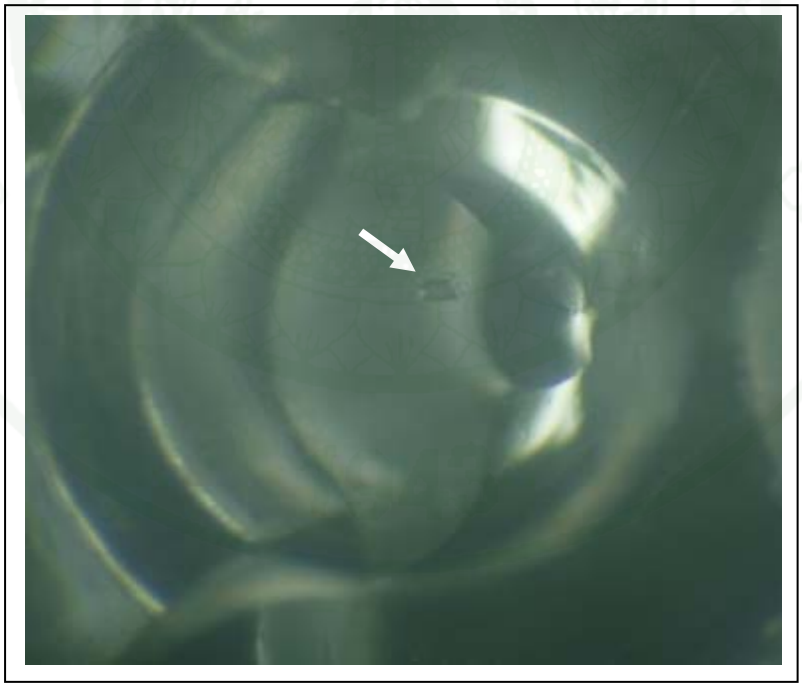

Figure 50 Inhibitor/Wild type HIV-1 RT complex crystal. The 68NV/WRT crystal with sitting drop. (A) sitting drop plate and (B) single crystal was observed.

A

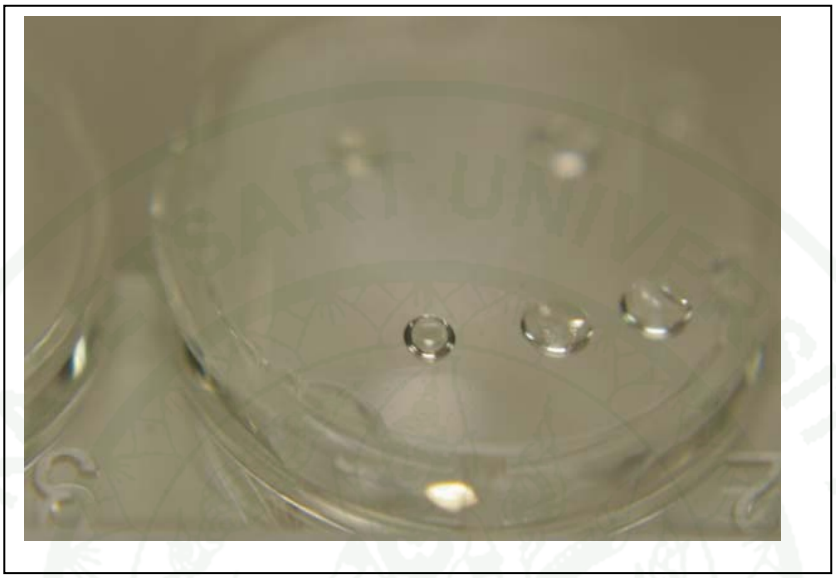

B

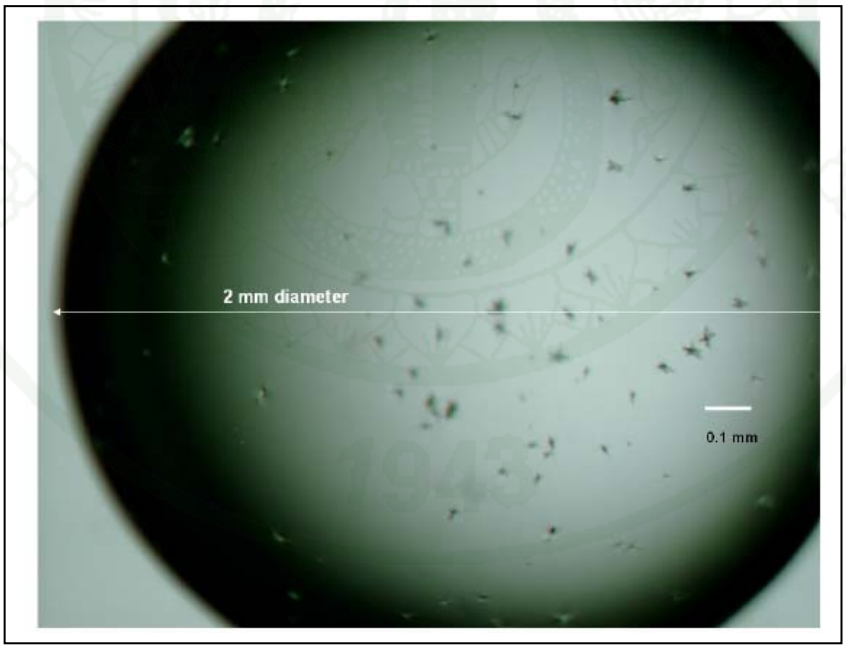

Figure 51 Inhibitor/K103N HIV-1 RT complex crystal. The NA15/K03N RT crystal with hanging drop. (A) hanging drop on cover slip and (B) star crystal was observed.

CONCLUSIONS

The HIV-1RT p66 and p51 gene was successful separately cloned into the pGEX3X expression plasmid after amplification by PCR using specific primers with restriction recognition sites. The cloned gene was identical to the known DNA sequence of HIV-1 RT gene. By the small-scale expression from *E. coli* strains – BL21 (DE3), the highest expression of two proteins was observed.

The drug resistant strain of HIV-1RT, K103N, Y181C and double mutant K103N/Y181C were successfully created on p66 gene by using site directed mutagenesis PCR based method with wild type plasmid, pGEXp66. The DNA sequence confirmed that all the mutagenesis lived on right position. The small-scale expression of these mutant plasmid form *E. coli* strains – BL21 (DE3), was confirmed by SDS PAGE.

The large scale expression of wild type recombinant p51 and p66 were observed after 0.4 mM IPTG induction, 20 ^{o}C 18 h. The 2 mg/l of purified heterdimeric protein was recovered form 35 % ammonium sulfate precipitation, anion exchange P11 cellulose phosphate and DEAE cellulose column chromatography. The purified wild type -recombinant HIV-1 RT showed 97.37 purify fold form cell lysate with 100 A.U. (fluorescence intensity)/mg of specificity determining by PicoGreen-fluorometric method.

The new plasmid construction of HIV-1RT was performed for the high expression and large amount of purified HIV-1 RT. The HIV-1RT p51 gene was successfully cloned into the pET33b expression plasmid after amplification by PCR using specific primers with restriction recognition sites and 6 histidines tag coding sequence were add to 3' of p51 gene. Comparing of recombinant expression plasmid by small scale expression, the 6 his-tagged p51 by pETp51H expression was higher than untag p51 by pGEXp51 expression.

The large scale expression of wild type and mutant recombinant HIV-1 RT, p51 and p66, were observed after 0.4 mM IPTG induction, 20 ^{o}C 18 h. The untag p66 and his-tag p51 by pGEXp66 and pETp51H plasmid expression, respectively, were mixed together for HIV-1 RT purification. The 15-20 mg/l of purified heterdimeric protein was recovered form DEAE cellulose column, P11 cellulose phosphate and Ni^{2+} - NTA column. Heterdimeric pure protein was confirmed, since untag p66/histag p51 was eluted together form Ni^{2+} - NTA column. The purified protein was at a satisfactory purity level and suitable for further experiment including protein crystallization.

The PicoGreen-fluorometric method was developed for rapidly determining of enzyme activity and kinetics study. The 1/2,000 dye dilution can use to extend amount of assay reaction. This method could detect the HIV-1 RT activity with using of small amount of RNA template and oligo dT primer, 10 and 0.0625 - 0.5 ng in 5-20 µl total reaction volume. The increasing of fluorescence signals corresponds to enzyme amount, substrate and time dependent RT activity. The RT activities of wild-type and all mutant RTs were also linearly increased by the longer reaction time and reached maximum after 5 min.

The PicoGreen-fluorescence assay is able to measure kinetic parameter and determine kinetic properties both wild type and mutant RT, The kinetic parameters determined by our method was within range of previously reported (15.76±0.37 µM, 8.73±1.58 µM, 25.66±0.66 and 34.65±2.39 µM, Km of wild-type, K103N, Y181C and K103N/Y181C HIV-1RT) and Km-Kcat relation can expand substrate binding properties effect on enzyme reaction rate for wild type and mutant RT.

The PicoGreen-fluorescence assay was applied for screening of dipyridodiazepinone derivatives anti HIV-1 RT agents. Five inhibitors (NA14, NA15, NA16, NA17 and 68NV) contained higher inhibition efficiency than nevirapine. The NA 14 compounds inhibitor shown high inhibition efficiency which can inhibit recombinant wild type HIV-1 RT and its K103N mutant with IC50 values were better than nevirapine 30-70 fold.

The PicoGreen-fluorescence assay was applied for screening of anti-HIV-1 RT agents form herbs , this method was simple and rapid, reliable and safe screenings with a minimum amount of sample. The ethanol extracted samples of 24 Thai herbs were used for anti-HIV-1 RT screening. The four samples of ethanol extraction that contained high inhibition efficiency more than Nevirapine, *Rhinacanthus nasutus, Myristica fragrans, Ruellia tuberose, Curcuma longa* and *Peltophorum pterocarpum* with inhibition of 3, 3.5, 2.5, 3 and 1.5 fold of 1ul nevirapine, respectively. While 2 sample of water extraction *Sapium indicum* sample and *Maclura cochinchinensis* hydrolysates. Show 1.2 and 1.4 fold of nevirapine inhibition, respectively. Lamellarins K, the compound from submarine invertebrate, showed highly inhibition with 3 fold of 1µl nevirapine.

Since, some dipyridodiazepinone derivatives can inhibit HIV-1 RT with high efficiency, the molecular structure of theseenzyme /inhibitors complex was very interested. The co-crystallization experiment was performed with wildtype HIV-1 RT and 19 reported solutions were used for crystallization. The star shape-small cluster crystal of NA15/WRT was appeared by using hanging drop with solution A1 (50 mM Bis-tris propane pH 6.8, 100 mM ammonium sulfate, 10% glycerol, 4% PEG8000). The larger single crystal of 68NV/WRT was appeared by using sitting drop method with solution D1 (50 mM Imidazole pH 6.4, 100 mM ammonium sulfate, 15 mM $MgSO_4$, 10% PEG8000).

LITERATURE CITED

Abram, M. E. and M. A. Parniak. 2005. Virion Instability of Human Immunodeficiency Virus Type 1 Reverse Transcriptase (RT) Mutated in the Protease Cleavage Site between RT p51 and the RT RNase H Domain. **J. Virol.** 79(18)**:**11952-11961.

Agopian, A., E. Gros, G. Aldrian-Herrada, N. Bosquet, P. Clayette, and G. Divita. 2009. New Generation of Peptide-based Inhibitors Targeting HIV-1 Reverse Transcriptase Conformational Flexibility. **J. Biol. Chem**. 284: 254-264.

Ali, H., G. M. König, S. A. Khalid, A. D. Wright and R. Kaminsky. 2002. Evaluation of selected Sudanese medicinal plants for their in vitro activity against hemoflagellates, selected bacteria, HIV-1-RT and tyrosine kinase inhibitory, and for cytotoxicity. **J. Ethnopharmacol**. 83(3): 219-228.

Asres K , A. Seyoum, C. Veeresham, F. Bucar and S. Gibbons. 2005. Naturally Derived Anti-HIV Agents. **Phytother Res.** 19*:* 557-581.

Baneyx, F. and M. Mujacic. 2004. Recombinant protein folding and misfolding in Escherichia coli. **Nat Biotechnol**. 22(11):1399-1408.

Balzarini, J., M.J. Perez-Perez, A. San-Felix, M.J. Camarasa, I.C. Bathurst, P.J. Barr and E. De Clercq. 1992. Kinetics of inhibition of human immunodeficiency virus type 1 (HIV-1) reverse transcriptase by the novel HIV-1-specific nucleoside analogue [2',5'-bis-O-(tert-butyldimethylsilyl)-beta-D-ribofuranosyl]-3'-spiro-5"-(4"-amino-1",2"-oxathiole-2",2"-dioxide)thymine (TSAO-T). **J. Biol. Chem.** 267(17): 11831-11838.

Baunbek, D., N. Trinkler, Y. Ferandin, O. Lozach, P. Ploypradith, S. Rucirawat , F. Ishibashi, M. Iwao and L. Meijer. 2008. Anticancer Alkaloid Lamellarins Inhibit Protein Kinases, **Mar. Drugs**. 6:514-527.

Benas, P., G. Bec, G. Keith, R. Marquet, C. Ehresmann, B. Ehresmann, and P. Dumas. 2000. The crystal structure of HIV reverse-transcription primer $tRNA^{Lys,3}$ shows a canonical anticodon loop. **RNA.** 6:1347-1355.

Bergfors, T.M. 1999. Protein Crystallization, Techniques, Strategies, and Tips. International University Line, La Jolla.

Bessong, P. O. , L. B. Rojas, L. C. Obi, P. M. Tshisikawe and E. O. Igunbor. 2006. Further screening of Venda medicinal plants for activity against HIV type 1 reverse transcriptase and integrase. **Afr. J. Biotechnol**. 5(6):526-528.

Blotta, I., F. Prestinaci, S. Mirante and A. Cantafora. 2005. Quantitative assay of total dsDNA with PicoGreen reagent and real-time fluorescent detection. **Ann Ist Super Sanita**. 41(1):119-123.

Boyer, P., H. Q. Gao, and S. Hughes. 1998. A Mutation at Position 190 of Human Immunodeficiency Virus Type 1 Reverse Transcriptase Interacts with Mutations at Positions 74 and 75 via the Template Primer. **Antimicrob Agents Chemother.** 42:447-452.

Boyer, P. L., S. G. Sarafianos, E. Arnold,. and Hughes, S. H. 2000. Analysis of mutations at positions 115 and 116 in the dNTP binding site of HIV-1 reverse transcriptase. **Proc. Natl. Acad. Sci**. 97(7): 3056-3061.

Boyle, B.A. 2002. Guide to management of Non-Nucleotide Reverse Transcriptase Inhibitor (NNRTI): Toxicities & Side Effects. **HIV and Hepatitis.com™.**

Buckle, M., R. M. Williams, M. Negroni and H. Buc. 1996. Real time measurements of elongation by a reverse transcriptase using surface plasmon resonance. **Proc. Natl. Acad. Sci**. 93:889-894.

Campbell, E. A., O. Pavlova, N. Zenkin, F. Leon, H. Irschik, R. Jansen, K. Severinov,

and S. A. Darst. 2005. Structural, functional, and genetic analysis of sorangicin inhibition of bacterial RNA polymerase. **EMBO J.** 24**:**674-682.

Carroll, S. S., J. Geib, D. B. Olsen, M. Stahlhut, J. A. Shafer, and L. C. Kuo. 1994. Sensitivity of HIV-1 reverse transcriptase and its mutants to inhibition by azidothymidine triphosphate. **Biochemistry**. 33:2113-2120.

Chavan, S.J. and H.J. Prochaska. 1995. Fluorometric measurement of reverse transcriptase activity with 4',6-Diamidino-2-phenylindole. **Anal. Biochem.** 225: 54-59.

Choi, S.J and F. C. Szoka,. 2000. Fluorometric determination of deoxyribonuclease I activity with PicoGreen. **Anal. Biochem**. 281, 95-97.

Clayette, P., A Agopian, N. Dereuddre- Bosquet, C. Goffinet, R Yousfi, J Depollier, K Storck, E Gros , O Keppler, G Divita, 2008. Peptide-based Inhibitors of HIV-1RT Dimerization and Polpolyprotein Maturation. **Antiviral Research** 78(2):A27.

Cosa, G., K. S. Focsaneanu, J. R. N. McLean, J. P. McNamee and J. C. Scaiano. 2001. Photophysical properties of fluorescent DNA-dyes bound to single- and double-stranded DNA in aqueous buffered solution. **Photochem. Photobiol.** 73:585-599.

Crespan, E. , G. A. Locatelli, R. Cancio, U. Hubscher, S. Spadari, and G. Maga. 2005 Drug Resistance Mutations in the Nucleotide Binding Pocket of Human Immunodeficiency Virus Type 1 Reverse TranscriptaseDifferentially Affect the Phosphorolysis Dependent Primer Unblocking Activity in the Presence of Stavudine and Zidovudine and Its Inhibition by Efavirenz. **Antimicrob. Agents Chemother**. 49: 342-349.

Das, K., J. D. Bauman, A. D. Clark, Jr. Y. V. Frenkel, P. J. Lewi, A. J.

Shatkin, S. H. Hughes and E. Arnold. 2008. High-resolution structures of HIV-1 reverse transcriptase/TMC278 complexes: Strategic flexibility explains potency against resistance mutations. **Proc. Natl. Acad. Sci**. 105(5):1466-1471.

Das, K., A. D. Clark, P. J Lewi, J Heeres, M. R De Jonge , L. M Koymans, H. M Vinkers, F Daeyaert, D. W Ludovici, M. J Kukla, B De Corte , R. W Kavash, C. Y Ho, H Ye, M.A Lichtenstein, K Andries, R Pauwels, M.P De Béthune, P.L Boyer, P Clark., S.H Hughes, P.A Janssen, E. Arnold. 2004. Roles of conformational and positional adaptability in structure-based design of TMC125-R165335 (etravirine) and related non-nucleoside reverse transcriptase inhibitors that are highly potent and effective against wild-type and drug-resistant HIV-1 variants. **J. Med Chem**. 47(10):2550-2560.

Das, K., J. Ding, Y. Hsiou, A. D. Clark, H. Jr., Moereels, L. Koymans, K Andries, R. Pauwels, P. A. J. Janssen, P. L. Boyer, P. Clark, R. H Smith , M. B. K. Jr. Smith, , C. J. Michejda, S. H. Hughes and, E. Arnold. 1996. Crystal Structures of 8-Cl and 9-Cl TIBO Complexed with Wild-type HIV-1 RT and 8-Cl TIBO Complexed with the Tyr181Cys HIV-1 RT Drug-resistant Mutant. **J**. **Mol. Biol**. 264:1085-1100.

Delarue, M., O. Poch, N. Tordo, D. Moras and P. Argos. 1990. An attempt to unify the structure of polymerases. **Protein Eng**. 3:461-467.

Di, L and E. H. Kerns. 2006. Biological assay challenges from compound solubility: strategies for bioassay optimization. **Drug Discovery Today**. 11: 446-451

Ding, J., K. Das, Y. Hsiou, S. G. Sarafianos, A. D. Clark Jr., A. Jacobo-Molina, C. Tantillo, S. H. Hughes, and E. Arnold. 1998. Structure and functional implications of the polymerase active site region in a complex of HIV-1 RT with a double-stranded DNA template-primer and an antibody Fab fragment at 2.8 A resolution. **J. Mol. Biol**. 284:1095-1111.

Facompre, M., C. Tardy, C. Bal-Mayeu, P. Colson, C. Perez and I. Manzanares C. Cuevas, and C. Bailly. 2003. Lamellarin D : A Novel Potent Inhibitor of Topoisomerase I. **Cancer Res.** 63:7392-7399.

Fan H, J Peng, M. T Hamann and H Jin-Feng. 2008. Lamellarins and Related Pyrrole-Derived Alkaloids from Marine Organisms. **Chem. Rev**. 108(1):264–287.

Gao, G, M. Orlova, M. M. Georgiadis, W. A Hendrickson. and, S. P Goff. 1997. Conferring RNA polymerase activity to a DNA polymerase: a single residue in reverse transcriptase controls substrate selection. **Proc. Natl. Acad. Sci**. 94:407-411.

Hammarstro, M., E. A. Woestenenk, N. Hellgren, T. Härd and H. Berglund. 2006. Effect of N-terminal solubility enhancing fusion proteins on yield of purified target protein, **J. Struct. Funct. Genomics 7:**1-14.

Hang J. Q., Y. Li, Y. Yang, N. Cammack, T. Mirzadegan and K. Klumpp. 2007. Substrate-dependent inhibition or stimulation of HIV RNase H activity by non-nucleoside reverse transcriptase inhibitors (NNRTIs). **Biochem. Biophys. Res. Commun.** 352: 341-350.

Hengen, P.N., 1995. Purification of His-tag fusion proteins from *Escherichia coli*. **TIBS** 20:285-286.

Herschhorn, A. and A Hizi. 2008. Virtual screening, identification, and biochemical characterization of novel inhibitors of the reverse transcriptase of humanimmunodeficienc virus type-1. **J. Med. Chem**. 51:5702-5713.

Hsiou, Y., K. Das, J. Ding, A. D. Clark, J. P. Jr. Kleim, M. Rosner, I. Winkler, G. Riess, S. H. Hughes, and E. Arnold. 1998 Structures of Tyr188Leu mutant and wild-type HIV-1 reverse transcriptase complexed with the non-nucleoside

inhibitor HBY 097: inhibitor flexibility is a useful design feature for reducing drug resistance. **J. Mol Biol.** 284**:**313-323.

Huang, H., R. Chopra, G. L Verdine and, S. C Harrison. 1998. Structure of a covalently trapped catalytic complex of HIV-1 reverse transcriptase: implications for drug resistance. **Science**. 282, 1669-1675.

Ismall, R. 1999. Sexually Transmitted Disease (STD) and Acquired Immunodeficiency Syndrome (AIDS) in South East Asia. **Clin Dermatol**. 7(2):127-135.

Itokawa, H, Q Shi, T. Akiyama, S. L Morris-Natschke and K. H. Lee. 2008 Recent advances in the investigation of curcuminoids. **Chin Med**. 3:11.

Jacobo-Molina, A. and E. Arnold. 1991HIV Reverse Transcriptase Structure-Function Relationships ?, **Biochemistry.** 30(26):6351-6356.

Jacobo-Molina, A., J. Ding, R. G. Nanni, A. D. Clark, Jr., X. Lu, C. Tantillo, R. L. Williams, G. Kamer, A. L. Ferris, P. Clark, A. Hizi, S. H. Hughes and E. Arnold. 1993. Crystal structure of human immunodeficiency virus type 1 reverse transcriptase complexed with double-stranded DNA at 3.0 A resolution shows bent DNA. **Proc. Natl. Acad. Sci**. 90:6320-6324.

Jaeger, J., T. Restle and T. A. Steitz. 1998. The structure of HIV-1 reverse transcriptase complexed with an RNA pseudoknot inhibitor. **EMBO J**. 17(15):4535-4542.

Jassim S. A. A. and M. A Naji. 2003. Novel antiviral agents: a medicinal plant perspective . **J.** A**ppl Microbiol**. 95(3):412-427.

Jayaprakasha, G. K., L. Jagan Mohan Rao and K. K. Sakariah. 2005.

Chemistry and biological activities of C. longa . **Trends Food Sci. Tech.** 16(12):533-548.

Jewel, N. A., R. Chen, R. Raice and L. M. Mansky. 2003. Nucleoside reverse transcriptase inhibitors and HIV mutagenesis. **J Antimicrob Chemother**. 52:547-550.

Jiratchariyakul, W. , C. Wiwat, M. Vongsakul, A. Somanabandhu, W. Leelamanit, I. Fujii, N. Suwannaroj, Y. Ebizuka. 2001. HIV inhibitor from Thai bitter gourd. **Planta-Med**. 67(4):350-353.

Johnson, M. S., M. A. McClure, D. F. Feng, J. Gray And R. F. Doolittle. 1986. Computer analysis of retroviral pol genes: assignment of enzymatic functions to specific sequences and homologies with nonviral enzymes. **Proc. Natl. Acad. Sci**. 83:7648-7652.

Kati, W. M, K. A. Johnson, L. F Jerva. and K. Anderson. 1992. Mechanism and fidelity of HIV reverse transcriptase. **J. Biol. Chem**. 267. 25988-25997.

Kernan, MR, A Send, J. L. Chen, S. D. Jolad, P. Blanc, J. T. Murphy, C. A. Stoddart, W. Nanakorn, M. J. Balick and E. J. Rozhon. 1997. Two New Lignans with Activity against Influenza Virus from the Medicinal Plant Rhinacanthus nasutus. **J. Nat. Prod**. 60(6):635-637

Khunnawutmanotham, N., N. Chimnoi, P. Saparpakorn, P. Pungpo, S Louisirirotchanakul, S. Hannongbua and S. Techasakul. 2007. Novel 2-Chloro-8-arylthiomethyldiazepinone Derivatives with Activity against HIV-1 Reverse Transcriptase. **Molecules.** 12: 218-230.

Kim, B. and, L. A. Loeb.1995. A screen in *Escherichia coli* for nucleoside analogs that target Human Immunodeficiency Virus (HIV) reverse transcriptase: Co-

expression of HIV reverse transcriptase and herpes simplex virus thymidine kinase. **J. Virol.** 69(10): 6563-6566.

Larder, B. A., D. J. Purifoy, K. L Powell and G Darby. 1997Site-specific mutagenesis of AIDS virus reverse transcriptase. **Nature**. 327:716-717.

Lee-Huang S., A. Bourinbaiar, H. C. Chen, P. Huang, P. L. Huang, H. F. Kung. 1994. The anti-HIV activity of recombinant MAP 30 from bitter melon. **Int Conf AIDS**. 10:35.

Lee-Huang S., H. C. Chen, H. F. Kung, P. L. Huang, P. L. Huang. 1993. MAP30, an anti-HIV protein, inhibits both ribosomal RNA function and DNA topological interconversions. **Int Conf AIDS**. 9:467.

Lee-Huang S., P. L. Huang, P. L. Nara, H. C. Chen, H. F. Kung, P. Huang, H. I. Huang, P. L. Huang. 1990 MAP 30: a new inhibitor of HIV-1 infection and replication. **FEBS Lett**. 272(1-2):12-18.

Mahidol C., H. Prawat, V. Prachyawarakorn and S. Ruchirawat. 2002. Investigation of some bioactive Thai medicinal plants. **Phytochemistry Reviews**. 1: 287-297.

Marchand, B. and Gotte, M. 2003. Site-specific footprinting reveals differences in the translocation status of HIV-1 reverse transcriptase. Implications for polymerase translocation and drug resistance. **J. Biol. Chem.** 278:35362-35372.

Marchand, B., Tchesnokov, E. P. and Gotte, M. 2007. The pyrophosphate analogue foscarnet traps the pretranslocational state of HIV-1 reverse transcriptase in a Brownian ratchet model of polymerase translocation. **J. Biol. Chem**. 282: 3337-3346.

Martin-Hernandez, A. M., E. Domingo and L M. Arias. 1996. Human

immunodeficiency virus type 1 reverse transcriptase: role of Tyr115 in deoxynucleotide binding and misinsertion fidelity of DNA synthesis. **EMBO J**. 15: 4434-4442.

Merluzzi,V. J., KD Hargrave, M Labadia, K Grozinger, M Skoog, JC Wu, CK Shih, K Eckner, S Hattox, J Adams. 1990. Inhibition of HIV-1 replication by a non-nucleotide reverse transcriptase inhibitor. **Science**. 250:1411-1413.

Mikelsons, L., C. Carra, M. Shaw, S. Claude and J. C. Scaiano. 2005. Experimental and theoretical study of the interaction ofsingle-stranded DNA homopolymers and a monomethine cyaninedye: nature of specific binding. **Photo chem. Photobiol. Sci**. 4:798-802.

Munshi, V., M. Lu, P. Felock, R. J. O. Barnard, D. J. Hazuda, M. D. Miller, M.T. Lai. 2008. Monitoring the development of non-nucleoside reverse transcriptase inhibitor-associated resistant HIV-1 using an electrochemiluminescence based reverse transcriptase polymerase assay. **Anal. Biochem**. 374(1):121-32.

Nissley, D.V., J. Radzio, Z. Ambrose, C.W. Sheen, N. Hamamouch, K.L. Moore, G. Tachedjian and N. Sluis-Cremer. 2007. Characterization of novel non-nucleoside reverse transcriptase (RT) inhibitor resistance mutations at residues 132 and 135 in the 51 kDa subunit of HIV-1 RT. **Biochem. J.** 404: 151-157.

Nonaka, G-I, I. Nishioka, M. Nishizawa, T. Y. amagishi, Y. Kashiwada, G. E. Dutschman, A. J. Bodner, R. E. Kilkuskie, Y.-C. Cheng, K.-H. Lee. 1990. Anti-AIDS agents 2: Inhibitory effects of tannins on HIV reverse transcriptase and HIV replication in H9 lymphocyte cells. **J. Nat Prod**. 53:587-595.

Odawara, F., H. Abe, T. Kohno, Y. Nagai-Fujii, K. Arai, S. Imamura, H. Misaki. H Azuma, K. Ikebuchi, H. Ikeda, S. Mohan and K. Sano. 2002. A highly sensitive chemiluminescent reverse transcriptase assay for human immunodeficiency virus, **J. Virol. Methods.** 106 :115-124.

Olivares, I., M. Gutierrez-Rivas, C. Lopez-Galindez and L. Menendez-Arias. 2004 Tryptophan scanning mutagenesis of aromatic residues within the polymerase domain of HIV-1 reverse transcriptase: critical role of Phe-130 for p51 function and second-site revertant restoring viral replication capacity. **Virology**. 324(2):400-411.

Palaniappan, C., M. Wisniewski and P. S. Jacques. 1997. Mutations within the Primer Grip Region of HIV-1 Reverse Transcriptase Result in Loss of RNase H Function. **J. Biol. Chem.** 72(17):11157–11164.

Palmer, S., V Boltz and N. Martinson. 2006. Persistence of nevirapine-resistant HIV-1 in women after single-dose nevirapine therapy for prevention of maternal-to-fetal HIV-1 transmission. **Proc. Natl. Acad. Sci**. 103(18): 7094-7099.

Pata, J. D., B. R. King and T. A. Steitz. 2002. Assembly, purification and crystallization of an active HIV-1 reverse transcriptase initiation complex. **Nucleic Acids Res** 30(22):4855-4863.

Pata, J. D., W. G. Stirtan, S. W. Goldstein and T. A. Steitz. 2004. Structure of HIV-1 reverse transcriptase bound to an inhibitor active against mutant reverse transcriptases resistant to other nonnucleoside inhibitors. **Proc. Natl. Acad. Sci**. 10548-10553.

Poch, O., I. Sauvaget, M. Delarue And N. Tordo. 1989. Identification of four conserved motifs among the RNA-dependent polymerase encoding elements. **EMBO J**. 8:3867-3874.

Reddy, M, V, M. R. Rao; D. Rhodes; M. S. Hansen; K. Rubins; F. D. Bushman; Y. Venkateswarlu*;* D. J. Faulkner. 1999. Lamellarin α 20-Sulfate, an Inhibitor of HIV-1 Integrase Active against HIV-1 Virus in Cell Culture**. J. Med. Chem**. 42(11):1901-1907.

Reardon, J. E. 1992 Human immunodeficiency virus reverse transcriptase: steady-state and presteady- state kinetics of nucleotide incorporation. **Biochemistry.** 31:4473-4479.

Ren, J. and D. K. Stammers. 2005. HIV reverse transcriptase structures: designing new inhibitors and understanding mechanisms of drug resistance. **Trends Pharmacol Sci.** 26(1):4-7.

Ren, J., L. E. Bird, P. P. Chamberlain, G. B. Stewart-Jones, D. I. Stuart and D. K. Stammers. 2002. Structure of HIV-2 reverse transcriptase at 2.35-Å resolution and the mechanism of resistance to non-nucleoside inhibitors**. Proc. Natl. Acad. Sci**. 99**:**14410-14415.

Ren, J., R. M. Esnouf, A. L. Hopkins, E. Y. Jones, I. Kirby, J. Keeling, C. K. Ross, B. A. Larder, D. I. Stuart, and D. K. Stammers. 1998. 3'-Azido-3'-deoxythymidine drug resistance mutations in HIV-1 reverse transcriptase can induce long range conformational changes. **Proc. Natl. Acad. Sci**. 95:9518-9523.

Ren, J., C. E. Nichols, A. Stamp., P. P. Chamberlain., R. Ferris., K. L. Weaver, S. A. Short, D. K Stammers. 2006 Structural insights into mechanisms of non-nucleoside drug resistance for HIV-1 reverse transcriptases mutated at codons 101 or 138. **FEBS J**. 273:3850-3860.

Rittinger, K., G. Divita and R. S. Goody. 1995. Human immunodeficiency virus reverse transcriptase substrate- induced conformational changes and the mechanism of inhibition by nonnucleoside inhibitors. **Proc. Natl. Acad. Sci**. 92:8046-8049.

Rodgers, D. W., S. J. Gamblin and B. A. Harris. 1995. The structure of unliganded reverse transcriptase from the human immunodeficiency virus type 1. **Proc. Natl. Acad. Sci**. 92:1222-1226.

Sarafianos, S. G., K. Das, C. Tantillo, A. D. Clark Jr, J. Ding, J. M. Whitcomb, P.L. Boyer, S. H. Hughes and E. Arnold. 2001. Crystal structure of HIV-1 reverse transcriptase in complex with a polypurine tract RNA:DNA. **EMBO J.** 20(6):1449-1461.

Sarafianos S. G., B. Marchand, K. Das. D. M. Himmel, M. A. Parniak, S. H. Hughes and E. Arnold. 2009. Structure and Function of HIV-1 Reverse Transcriptase: Molecular Mechanisms of Polymerization and Inhibition. **J. Mol Biol**. 385(3):693-713.

Send, A., J. L. Chen, S. D. Jolad, C. Stoddart, E. Rozhon and M. Kernan. 1996. Two New Naphthoquinones with Antiviral Activity from Rhinacanthus nasutus. **J. Nat. Prod.** 59(8):808-811.

Seville, M., A. B. West, M. G. Cull and C. S. McHenry. 1996. Fluorometric assay for DNA polymerases and reverse transcriptase. **BioTechniques**. 21:664-672.

Schweitzer, C and J. C Scaiano. 2003. Selective, binding and local photophysics of the fluorescent cyanine dye PicoGreen in double-stranded and single-stranded DNA. **Phys. Chem. Chem. Phys.** 5:4911-4917.

Singer, V. L., L. J. Jones, S. T. Yue and R. P. Haugland. 1997. Characterization of PicoGreen Reagent and Development of a Fluorescence-Based Solution Assay for Double-Stranded DNA Quantitation. **Anal. Biochem.** 249: 228-238.

Singh, I. P., S.B. Bharate and K. K. Bhutani. 2005. Anti-HIV natural products. **Curr Sci**. 89(2): 269-290.

Silprasit, K., R. Thammaporn., S. Hannongbua and K. Choowongkomon.2008. Cloning, expression, purification, determining activity of recombinant HIV-1 reverse transcriptase, **Kasetsart J. (Nat. Sci.)**. 42:231-239.

Sluis-Cremer, N., E. Kempner and M. A. Parniak. 2003 Structure–activity relationships in HIV-1 reverse transcriptase revealed by radiation target analysis. **Protein Sci**. 12:2081-2086.

Sobbi, R. A., A. Y Abramov., C. Diao, M. E. Kargacin, G. J Kargacin, R. J. French and E Pavlov. 2008. High Sensitivity, Quantitative Measurements of Polyphosphate Using a New DAPI-Based Approach. **J. Fluoresc**. 18(5): 859-866.

Steitz, T.A.1998. A mechanism for all polymerases. **Nature.** 391:231-232.

Stephen G.1993. The kinetics of slow-binding and slow, tight-binding inhibition: the effects of substrate depletion. **Biochem. J**. 294:195-200.

Strandberg, L. and S. O. Enfors. 1991. Factors Influencing Inclusion Body Formation in the Production of a Fused Protein in Escherichia coli. **Appl Environ Microbiol** 57:1669-1674.

Studier, F.W. and B. A. Moffatt. 1986. Use of bacteriophage T7 RNA polymerase to direct selective high-level expression of cloned genes. **J. Mol Biol**. 189(1):113-130.

Tolun, G and, R. S. Myers. 2003. A real-time DNase assay (ReDA) based on PicoGreen® fluorescence. **Nucleic Acids Res**. 31(18): e111.

Tong, W., C. D. Lu, S. K. Sharma, S. Matsuura, A. G. So and W. A Scott. 1997. Nucleotide-induced stable complex formation by HIV-1 reverse transcriptase. **Biochemistry.** 36: 5749-5757.

Turner, B. G. and M. F. Summers. 1999. Structural Biology of HIV. **J. Mol biol.** 285:1-32.

Wakefield, J. K., S. A. Jablonski and C. D. Morrow. 1992. In Vitro Enzymatic

Activity of Human Immunodeficiency Virus Type 1 Reverse Transcriptase Mutants in the Highly Conserved YMDD Amino Acid Motif Correlates with the Infectious Potential of the Proviral Genome. **J. Virol**. 66(11):6806-6812.

Wensing, A. M, D. A. van de Vijver, G. Angarano. 2005. Prevalence of Drug-Resistant HIV-1 Variants in Untreated Individuals in Europe: Implications for Clinical Management. Transmission of HIV Drug Resistance in Europe **. J. Infect Dis**. 192: 958-967.

West, A. B., T. M. Roberts, and R. Kolodner. 1992. Regulation of the reverse transcriptase of human immunodeficiency virus type 1 by dNTPs (DNA polymerase/noncompetitive inhibition/substrate inhibiton/allostenc regulation/AIDS). **Proc. Natl. Acad. Sci**. 89:9720-9724.

Woradulayapinij, W., N. Soonthornchareonnon and C. Wiwat. 2005. In vitro HIV type 1 reverse transcriptase inhibitory activities of Thai medicinal plants and Canna indica L. rhizomes**. J. Ethnopharmacol**. 101(1-3): 84-89.

Wulfing, C., J. Lombardero, A. Pluckthun. 1994. An Escherichia coli protein consisting of a domain homologous to FK506- binding proteins (FKBP) and a new metal binding motif. **J. Biol. Chem.** 269(4):2895-2901.

Yamamot, S., T. M. Folks, W. Heneine. 1996. Highly sensitive qualitative and quantitative detection of reverse transcriptase activity: optimization, validation, and comparative analysis with other detection systems. **J Virol Methods**. 61:135-143.

APPENDICES

Apendix A

Recombinant plasmids DNA sequencing

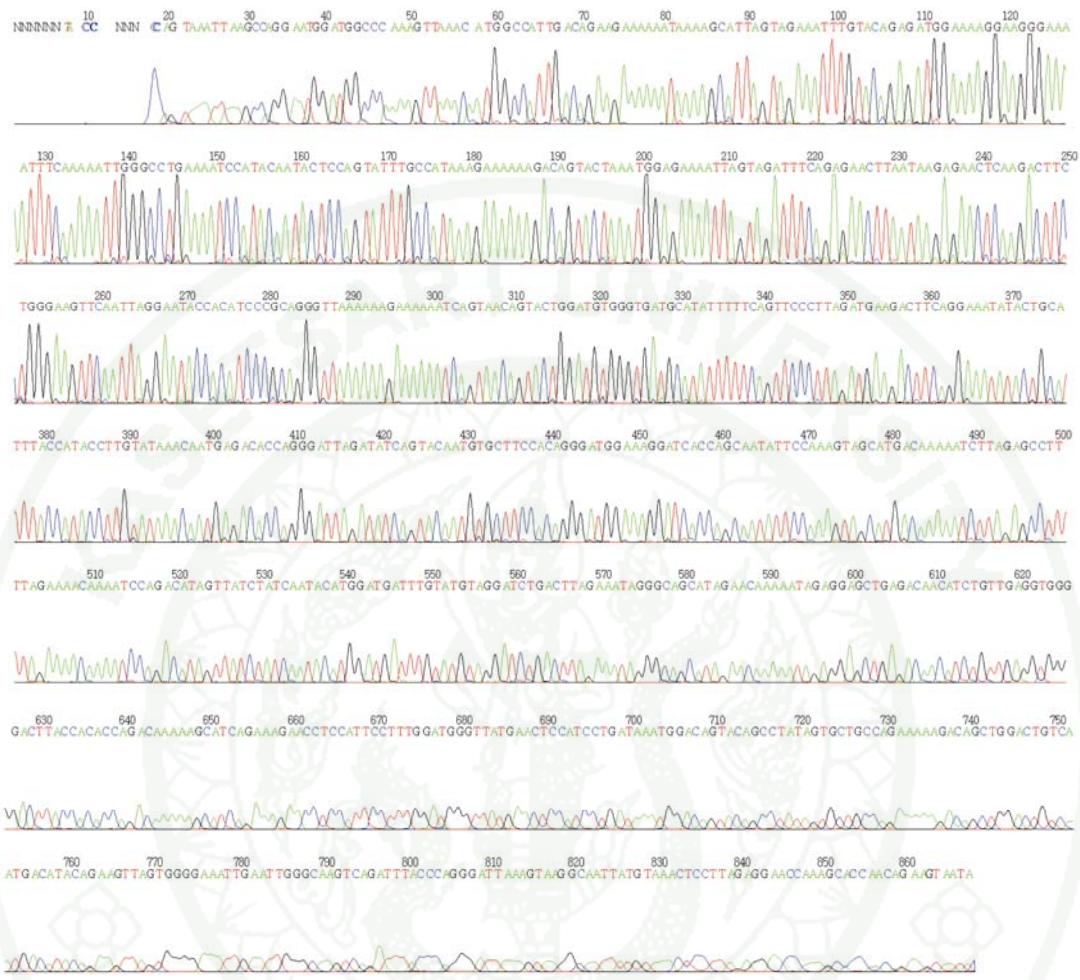

Appendix Figure 1 The recombinant plasmids DNA sequencing of pGEXp66.

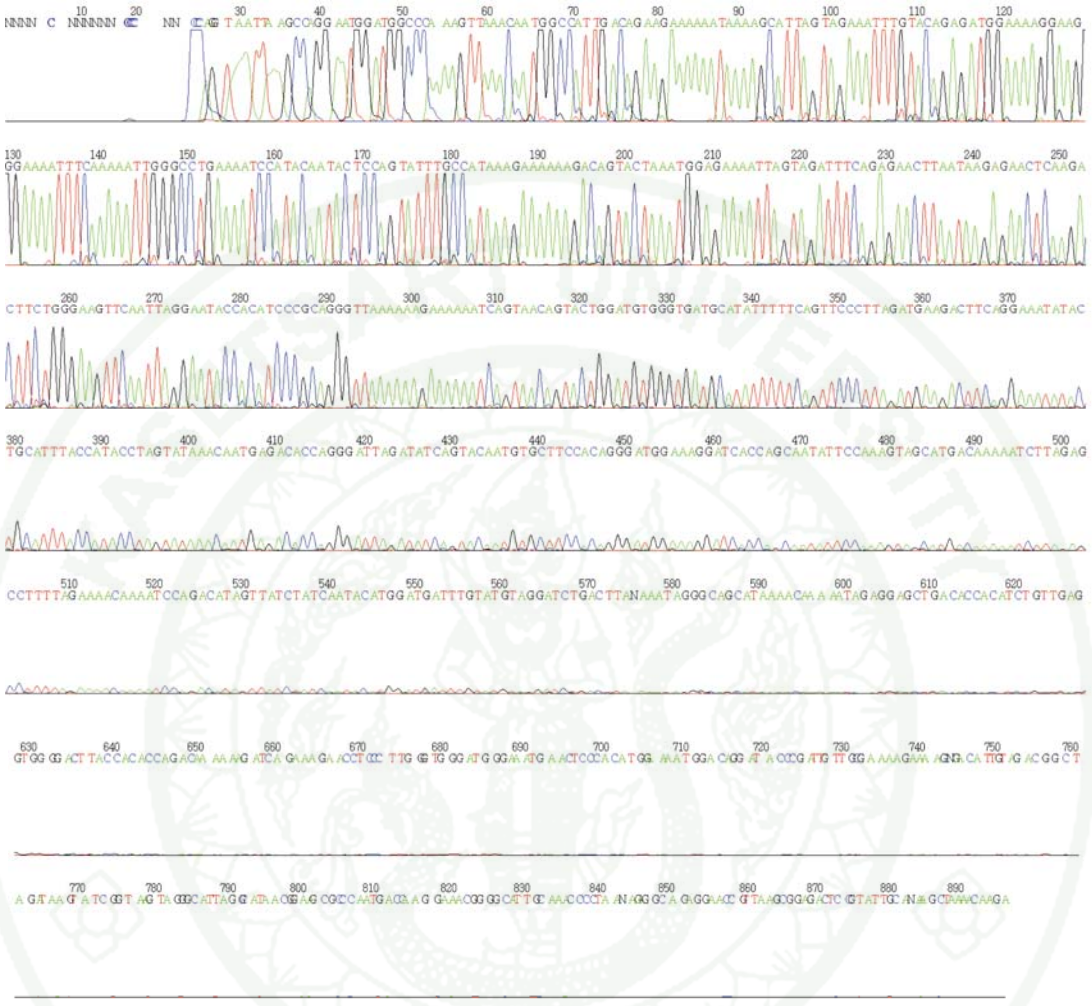

Appendix Figure 2 The recombinant plasmids DNA sequencing of pGEXp51.

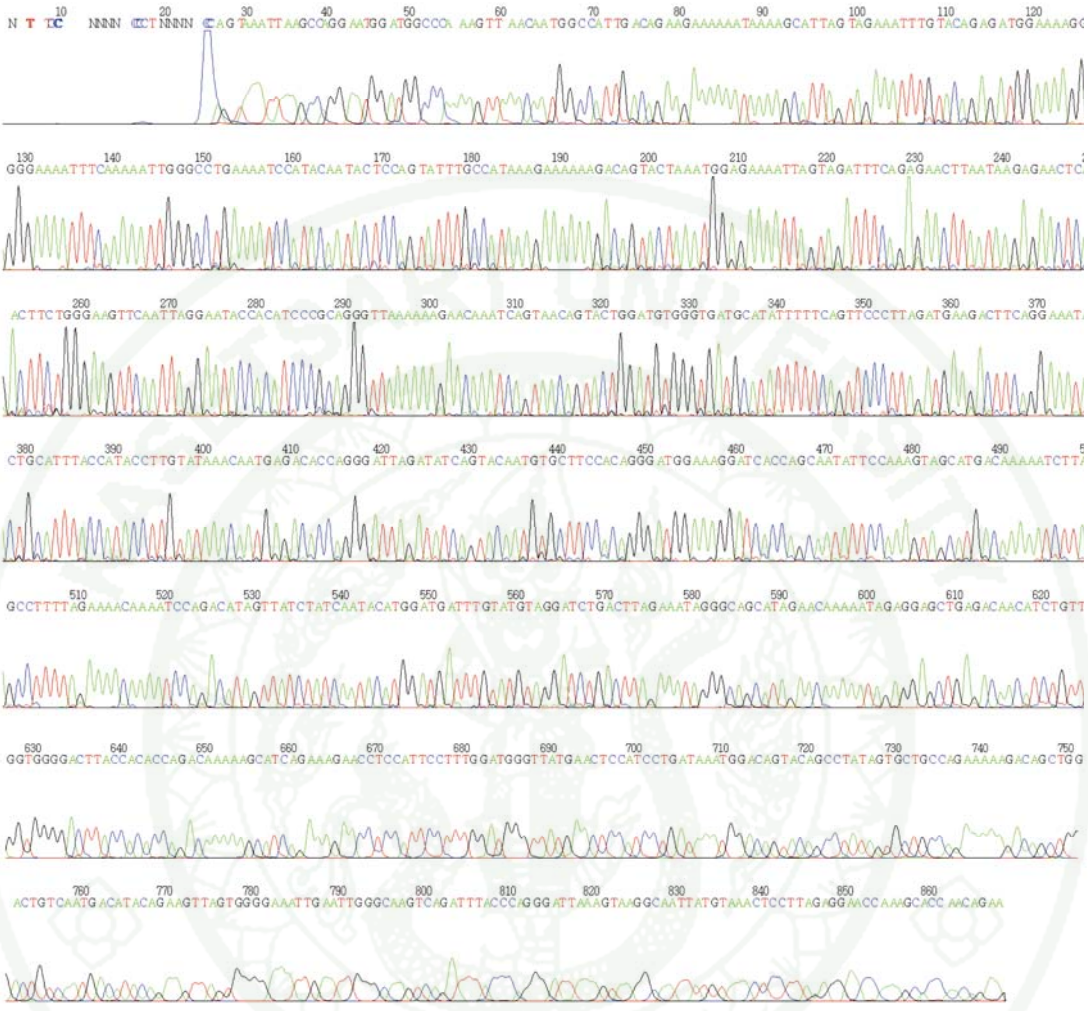

Appendix Figure 3 The recombinant plasmids DNA sequencing of pGEXp66 K103N.

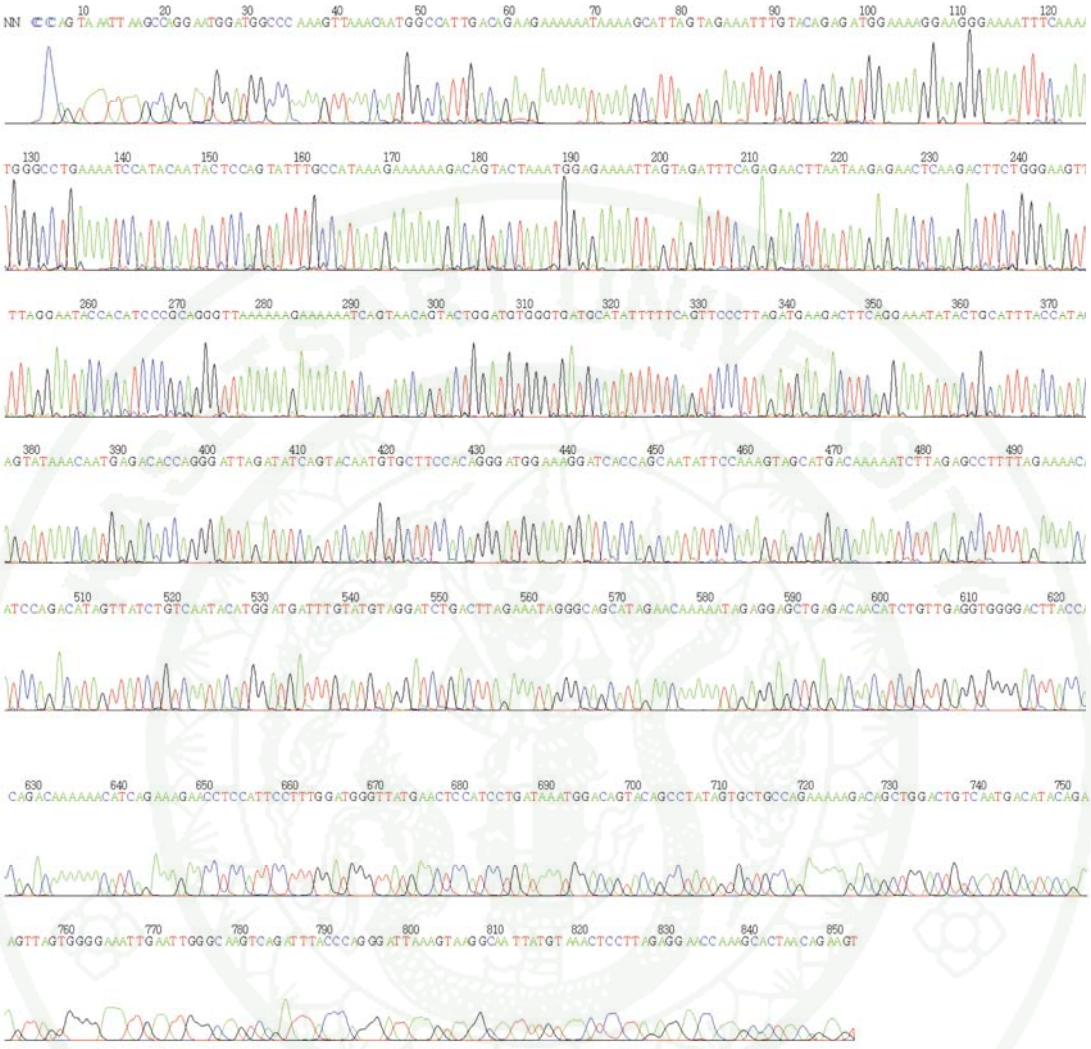

Appendix Figure 4 The recombinant plasmids DNA sequencing of pGEXp66 Y181C.

Appendix Figure 5 The recombinant plasmids DNA sequencing of pGEXK103N/Y181C.

Appendix B

HIV-1 reverse transcriptase inhibitor and Thai herbs

The Structure of Dipyridodiazepinone derivatives

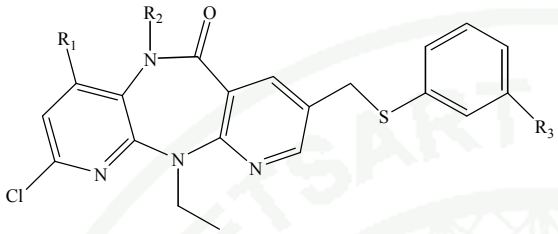

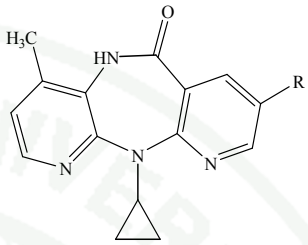

Appendix Table B1 The dipyridodiazepinone derivatives

Compounds	R_1	R_2	R_3
68NV	H	CH_3	H
N14	H	H	H
N15	H	H	OCH_3
N16	H	H	F
NA14	CH_3	H	H
NA15	CH_3	H	OCH_3
NA17	CH_3	CH_3	H
NA16	CH_3	CH_3	OCH_3

Compounds	R
Nevirapine	H
NB17	$NH_3^+Cl^-$
NB18	NH_2

Appendix Table B2 The concentration of stock solution of dipyridodiazepinone derivatives

Compounds	Mw (g/mole)	Concentration (mM)
Nevirapine	266.30	25
68NV	410.92	44
N14	396.89	25
N15	426.92	25
N16	414.88	12.5
NA14	410.92	12.5
NA15	440.95	25
NA16	454.97	10
NA17	424.95	20
NB17	317.77	50
NB18	281.31	-

Appendix Table B3 The list of Thai herbs

Thai herbs	Common Name (in Thai)	Scientific Name
1	สะเดา	*Azadirachta indica*
2	ทองพันชั่ง	*Rhinacanthus nasutus*
3	ราชดัด	*Brucea amarissima*
4	อบเชยญวน	*Cinnamomum loureiroi*
5	เบญกานี	*Quercus infectoria*
6	อ้อยแดง	*Saccharum officinarum*
7	จันทน์เทศ	*Myristica fragrans*
8	ต้อยติ่ง	*Ruellia tuberosa*
9	ขมิ้นชัน	*Curcuma longa*
10	เทียนกิ่ง	*Lawsonia inermis*
11	โกฐกะกลิ้ง	*Strychnos nux-vomica*
12	ว่านชักมดลูก	*Curcuma xanthorrhiza*
13	สมอพิเภก	*Terminalia belirica*
14	สมอทะเล	*Sapium indicum*
15	สมอไทย	*Terminalia chebula*
16	กำแพงเจ็ดชั้น	*Salacia chinensis*
17	ดอกคำแสด	*Mallotus philippensis*
18	ไพล	*Zingiber montanum*
19	เปลือกนนทรี	*Peltophorum pterocarpum*
20	มะกอก	*Spondias pinnata*
21	แกแล	*Maclura cochinchinensis*
22	สีเสียดเปลือก	*Acacia catechu*
23	สีเสียดยางก้อน	*Acacia catechu*
24	ฝาง	*Caesalpinia sappan*

Appendix C

Recombinant HIV-1 reverse transcriptase purity analysis based on coomasieblue stained

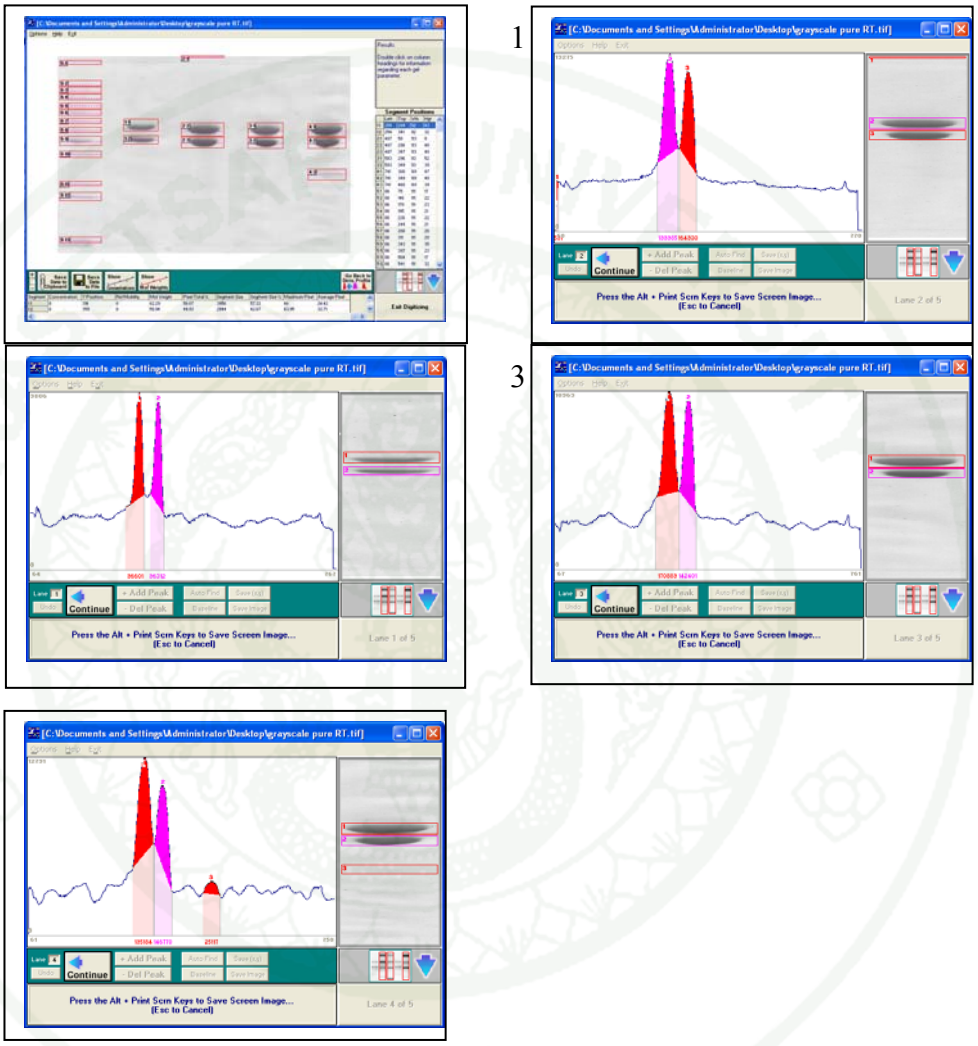

Protein purity calculation based Pixel

	Pixel	%Pixel	% Purity	
1.1	96601.08	50.07	> 95	P66/P51 wild-type
1.2	96312.61	49.93		
2.2	199985.6	55.04	> 90	P66/P51 K103N
2.3	164930.6	45.39		
3.1	170889.3	54.55	> 90	P66/P51 Y181C
3.2	142401.4	45.45		
4.1	195184.8	53.17	> 80	P66/P51 KY
4.2	146770.7	39.98		

Appendix D

Solutions and reagents preparation

1. Phosphocellulose (Whatman P-11) Washing procedure

1.1 Place ~300 ml of dry resin in a 2 liter flask. Fill flask with deionized water and suspend the resin by swirling and/or inverting the flask. Allow resin to settle fines (any unsettled material) as possible. Repeat washing 8-10 times, discarding the fines each 20 time. It is very important to remove the fines from phosphocellulose! If the fines are not removed, the column will run very slowly.

1.2 Suspend resin in 1 liter of 0.2 N NaOH. Allow to stand for at least 20 min. Decant NaOH, add another liter of 0.2 N NaOH and check pH of supernatant with indicator paper. The pH should be above 10; if not, wash with more NaOH.

1.3 Suspend resin in deionized water and wash with deionized water until the pH of the wash is below 8.

1.4 Suspend resin in 1 liter of 0.2 N HCl. Allow to stand for at least 20min. Decant HCl, add another liter of 0.2 N HCl and check pH of supernatant with indicator paper. The pH should be below 3; if not, wash with more HCl.

1.5 Suspend resin in deionized water and wash with deionized water until pH of wash is about 5 (or pH of water).

2. Reagents for bacterial culture

2.1 LB broth containing antibiotic

Dissolve 10 g Bacto Tryptone, 5 g Bacto Yeast Extract and 5 g NaCl in 950 ml distilled water. Stir until the solutes have been dissolved. Adjust the volume of the solution to 1 litre with distilled water. Sterilize by autoclaving the solution at 121oC for 15 min. Allow the medium to cool to 50oC before adding antibiotics, ampicillin to a final concentration 100 μg/ml and store at 4^{o}C.

2.2 LB plate containing anti biotic (1 L), dissolve 10 g Bacto Tryptone, 5 g Bacto Yeast Extract, 5 g NaCl and 15 g Bacto agar in 950 ml distilled water. Stir until the solutes have been dissolved. Adjust the volume of the solution to 1 liter with distilled water. Sterilize by autoclaving the solution at 121^{o}C for 15 min. Allow the medium to cool to 50^{o}C before adding antibiotics, ampicillin to a final concentration 100 µg/ml. Pour medium into Petridishes. Allow the agar to harden, and keep at 4^{o}C.

2.3 Ampicillin stock solution (100 mg/ml), dissolve 1 g ampicillin in 10 ml sterile distilled water, then aliquot and store at -30^{o}C.

2.4 IPTG stock solution (1.0 M), dissolve 2.38 g IPTG (isopropyl thio-β-D-galactoside) in distilled water and make to 10 ml final volume. Sterilize by filter sterilize, aliquot and store at -30^{o}C.

3. Reagents for protein determination

3.1 SDS-gel loading buffer (3× stock) (0.15 M Tris pH 6.8, 6% SDS, 0.1% bromophenol blue, 30% glycerol), dissolve 6 g SDS, 0.1 g bromophenol blue, 30 ml glycerol and add 0.15 M Tris pH 6.8 to bring a volume up to 100 ml. Store the solution at -30^{o}C. Before use add 20 µl of 2-mercapthoethanol to 40 µl of solution mixture.

3.2 0.5 M Tris pH 8.8 (100 ml), dissolve 18.17 g Tris Base in 80 ml distilled water. Adjust pH to 8.8 with 6 M HCl and bring the volume up to 100 ml with distilled water. Store at 4^{o}C.

3.3 0.5 M Tris pH 6.8 (100 ml), dissolve 6.05 g Tris Base in 80 ml distilled water. Adjust pH to 6.8 with 6 M HCl and bring the volume up to 100 ml with distilled water. Store at 4^{o}C.

3.4 30% Acrylamide solution (100 ml), dissolve 29 g acrylamide and 1 g *N, N′*-methylene-bis-acrylamide in distilled water to a volume 100 ml. Mix the solution

by stirring for 1 h to be homogeneous and filter through Whatman membrane No. 1. Store in the dark bottle at 4^{o}C.

3.5 Tris-Glycine electrode buffer (5× stock) (1 l), dissolve 30.29 g Tris Base, 144 g glycine, 5 g SDS in distilled water. Adjust pH to 8.3 with HCl and bring the volume up to 1 l with distilled water.

3.6 Staining solution with coomassie brillant blue for protein (1l), mix 1 g Coomassie brilliant blue R-250, 400 ml methanol, 500 ml distilled water and 100 ml glacial acetic acid and filter through a Whatman No. 1.189

3.7 Destaining solution for coomassie Stain (1l), mix 400 ml methanol, 100 ml glacial acetic acid, and add distilled water to a final volume of 1000 ml.

3.8 10% (w/v) Ammonium persulfate (1 ml), dissolve 100 mg ammonium persulfate in 1 ml distilled water. Store at -30 ^{o}C.

Appendix Table D1 Solution for preparation SDS-PAGE

Reagent	12% Separating Gel (ml)	5% Stacking Gel (ml)
30 % Bis-Acrylamide	2.0	0.33
Separating buffer	1.3	-
Stacking buffer	-	0.25
10% Amonium persulfate	0.05	0.02
10% SDS	0.05	0.02
TEMED	0.002	0.002
Water	1.6	1.4
total	5.0	2.0

4. Buffers and reagents for enzymatic studies

4.2 PicoGreen dsDNA quantitation reagent (Component A), 0.55 ml of 400X dye in DMSO.

4.3 20X TE buffer (Component B), 12 ml of 200 mM Tris. HCl, 20 mM EDTA, pH 7.5.

4.4 Lambda DNA standard (Component C), 0.55 ml of 100 µg/ml DNA in TE Buffer.

4.5 Poly(A) ribonucleotide template (Component D), 55 µl of 1 mg/ml template in 100 mM Tris.HCl, 0.5 mM EDTA, pH 8.1. The template is approximately 350 bases long.

4.5 Oligo d(T)16 primer (Component E), 55 µl of 50 µg/ml primer in 100 mM Tris.HCl, 0.5 mM EDTA, pH 8.1.

4.6 Polymerization buffer (Component F), 22.5 ml of 60 mM Tris.HCl, 60 mM KCl, 8 mM MgCl2, 13 mM DTT, 100 µM dTTP, pH 8.1.

4.7 EDTA (Component G), 2.5 mL of a 200 mM solution in water.

5. Running the Reverse Transcriptase Reactions

5.1 Anneal the template and the primer. For every 100 reactions, mix together 5 µl of poly(A) ribonucleotide template (Component D) and 5 µl of oligo d(T)16 primer (Component E) in a nuclease-free microfuge tube. Incubate the mixture at room temperature for one hour to allow the primer to anneal to the template.

5.2 Prepare the reaction mixture. Dilute the template/primer solution (prepared in step 1.1) 200-fold into polymerization buffer (Component F). For 100 reactions, dilute 10 µl of template/ primer solution into 2.0 ml of polymerization buffer.

5.3 Aliquot the reaction mixture. For each sample to be assayed, aliquot 20 µl of this reaction mixture into microplate wells or microfuge tubes.

5.4 Prepare the samples of reverse transcriptase activity test. Add 5 µl sample into each reaction mixture containing well, incubate 37 ^{o}C and then measure fluorescence signal by using 503 nm and 523 nm for excitation and emission wave length, respectively.

6. Buffers and reagents for protein crystallization studies

The stock solutions of polyethylene glycol (PEG) with a range of molecular weight (PEG6000, PEG4000 and PEG8000), were prepared by dissolving 25 g of PEG in ~20 ml of distilled ultra-pure water, then heat and the volume was brought to 50 ml with a final concentration of 50% (w/v). All of these solutions were filtered using 0.45 µm MF-Millipore Membrane Filters with a vacuum pump. Various types of salts and buffers were prepared as 1M stock solution for the crystallization solutions. The pH of each buffer was titrated using HCl (conc) or 5 M NaOH to obtain the desire pH ranging from 6.6 to 8.0 for initial screening and optimizing.

CURRICULUM VITAE

NAME : Mr. Kun Silprasit

BIRTH DATE : December 30, 1978

BIRTH PLACE : Nhongkai, Thailand

NATIONALITY : Thai

EDUCATION

YEAR	INSTITUTION	DEGREE/DIPLOMA
1997-2001	Khonkean University	B.Sc. (Biochemistry)
2001-2005	Chulalongkorn University	M.Sc. (Biochemistry)
2005-2010	Kasetsart University	Ph.D. (Genetic Engineering)

SCHOLARSHIPS :
1) Graduate Scholarship, Synchrotron Light Research Institute (GS50-D02) (2006-2009).
2) Research Scholarship, Synchrotron Light Research Institute (2550/08) (2006-2008).
3) Thailand Research Fund (2009- 2010).

PRESENTATION AND PUBLICATIONS

Silprasit K., Thammaporn R., Choowongkomon K., Hannongbua S., Cloning, Expression, Purification and Activity Assay of Recombinant HIV-1 Reverse Transcriptase in Escherichia coli. The Proceeding of 45th, Kasetsart University Annual Conference, Kasetsart University, Bangkok, Thailand. January 29 – February 1 , 2008 (Oral presentation).

Silprasit K., Thammaporn R., Tecchasakul S., Hannongbua S., Choowongkomon K Fluorometric determination of the enzyme kinetic properties of HIV-1 reverses

transcriptases and their inhibitors. the 2nd Annual Symposium of Protein Society of Thailand, Chulabhorn Research Institute Conference Center, Bangkok, Thailand, September 20-21, 2007. (Poster presentation).

Silprasit K., Thammaporn R., Choowongkomon K., Hannongbua S., Cloning, Expression, Purification and Activity Assay of Recombinant HIV-1 Reverse Transcriptase in Escherichia coli , Kasetsart J. (Nat. Sci.) 42: 231-239.